2012

Rhodium mediated bond activation: from synthesis to catalysis

Hung-An Ho
Iowa State University

Rhodium mediated bond activation: from synthesis to catalysis

by

Hung-An Ho

A dissertation submitted to the graduate faculty

in partial fulfillment of the requirements for the degree of

DOCTOR OF PHILOSOPHY

Major: Chemistry (Organic Chemistry)

Program of Study Committee:
Aaron D. Sadow, Major Professor
Marek Pruski
Gordon Miller
Malika Jeffries-EL
Javier Vela

Iowa State University

Ames, Iowa

2012

Dedicated to my Family

TABLE OF CONTENTS

Acknowledgements

This is a journey lasting for six years and finally I have conquered the “activation energy” to reach the destination. I need to thank a lot of people throughout the past six years. I could not accomplish anything without their company and assistance. Herein, I would like to sincerely express my full gratitude to these people.

First and foremost I want to thank my research advisor, Prof. Aaron Sadow, who has been extremely supportive for what I have been doing experimentally. I could always feel his unlimited passion in his heart toward the research as a synthetic chemist. The contagious passion has spread to everyone in the lab since the first day I joined the group. The continuous encouragement and patience have made me more confident of my ability. Under his guidance, besides the academic training, I have gained energy to move forward.

I would also like to thank my committee members, Prof. Marek Pruski, Prof. Gordon Miller, Prof. Malika Jeffries-EL and Prof. Javier Vela. Additionally, I want to thank the two previous committee members, Prof. Richard Larock and Prof. Victor Lin as well. All of your valuable suggestions and helpful critiques lead me to the right direction. Moreover, I have to thank the CIF staff, the BB&B scientist and the glassblower, Steve Veysey, Kamel Harrata, Arkady Ellern, Shu Xu, Sarah Cady, Bruce Fulton and Trond Forre because I could not get my work done without running these instruments (GC, LC, X-ray and NMR) or having my glasswares fixed.

Equally importantly, I want to thank all the Sadow group members for both constructive opinions for my research and great tolerance over my bad temper on occasion. Please forgive me if I ever yelled at any of you. Especially I would like to acknowledge Dr. Andy Pawlikowski for teaching me lots of useful slangs and being able to share my dirty jokes. I also want to acknowledge my senior colleagues, James Dunne, for running most of my EA samples and talking about all the madness. For the two members in my year, Kaking Yan and Steven Neal, I want to thank for their precious comments and suggestions of golfing. Moreover, I want thank Kaking again for joining the drinking party over weekends and overnights (when he was still single). I also want to thank Steven again for keeping all the instruments in good shape in the lab.

Outside of the lab, I want to thank Mr. Fu for coaching me how to play tennis for the two crazy summers. Regarding to winter time, Dr. Jack Su and Cologne Chen were the two who introduced me snowboarding-the most fun sport ever and it has become one of my favorite. Of course I would not forget Prof. Sung and Mrs. Sung, who have been constantly showing concern and hospitality. Thanks to my previous roommate, Ben Tang, who has been trash-talking with me even after he moved out. With no doubt, my current roommate, Steven Tsai took over this job with his wife, Irene Fu. I want to thank them for all the things that we have been through. I want to thank and congratulate my previous roommate back in college, Dr. Vic Chien, for inviting me to Florida and being a married man now. For the man who also just got married, Pin-Nan Cheng, I feel so sorry for not being able to be his best man in the wedding in California. I want to thank Vic and Pin-Nan for chatting with me on the phone

regularly in my Ph.D. student life. Lastly, I want to thank my family with all my heart for full support.

This work was performed at the Ames Laboratory under contract number DE-AC02-07CH11358 with the U.S. Department of Energy. The document number assigned to this thesis/dissertation is IS-T 3046.

Abstract

Recently, our lab has developed monoanionic tridentate ligand, To^R, showing the corresponding coordination chemistry and catalyst reactivity of magnesium, zirconium, zinc and iridium complexes. This thesis details synthetic chemistry, structural study and catalytic reactivity of the To^R-supported rhodium compounds.

$Tl[To^R]$ has been proved to be a superior ligand transfer agent for synthesizing rhodium complexes. The salt metathesis route of $Tl[To^M]$ with $[Rh(\mu\text{-}Cl)(CO)]_2$ and $[Rh(\mu\text{-}Cl)(COE)]_2$ gives $To^MRh(CO)_2$ (**2.2**) and $To^MRhH(\eta^3\text{-}C_8H_{13})$ (**3.1**) respectively while $Tl[To^P]$ with $[Rh(\mu\text{-}Cl)(CO)]_2$ affords $To^PRh(CO)_2$ (**2.3**). **2.2** reacts with both strong and weak electrophiles, resulting in the oxazoline N-attacked and the metal center-attacked compounds correspondingly. Using one of the metal center-attacked electrophiles, **2.3** was demonstrated to give high diastereoselectivity. Parallel to COE allylic C–H activation complex **3.1**, the propene and allylbenzene allylic C–H activation products have also been synthesized. The subsequent functionalization attempts have been examined by treating with Brønsted acids, Lewis acids, electrophiles, nucleophiles, 1,3-dipolar reagents and reagents containing multiple bonds able to be inserted. Various related complexes have been obtained under these conditions, in which one of the azide insertion compounds reductively eliminates to give an allylic functionalization product stoichiometrically.

3.1 reacts with various primary alcohols to give the decarbonylation dihydride complex $To^MRh(H)_2CO$ (**4.1**). **4.1** shows catalytic reactivity for primary alcohol decarbonylation under a photolytic condition. Meanwhile, **2.2** has been found to be more reactive than **4.1** for

catalytic alcohol decarbonylation under the same condition. Various complexes and primary alcohols have been investigated as well. The proposed mechanism is based on the stochiometric reactions of the possible metal and organic intermediates. Primary amines, hypothesized to undergo a similar reaction pathway, have been verified to give dehydrogenative coupling product, imines.

In the end, the well-developed neutral tridentate Tpm coordinates to the rhodium bis(ethylene) dimer in the presence of $TlPF_6$ to give the cationic complex, $[TpmRh(C_2H_4)_2][PF_6]$ (**5.1**). **5.1** serves as the first example of explicit determination of the solid state hapticity, evidenced by X–ray structure, among all the cationic $Tpm^RM(C_2H_4)_2^+$ (Tpm^R = Tpm, Tpm^*, M = Rh, Ir) derivatives. The substitution chemistry of this compound has been studied by treating with soft and hard donors. The trimethylphosphine-sbustituted complex activates molecular hydrogen to give the dihydride compound.

Chapter 1. Introduction of ligand supported metal complexes for investigation of bond activation

Bond Activation *via* Oxidative Addition

This thesis describes oxidative addition of H–H, C–X, C–H, O–H and N–H bonds to rhodium complexes to provide insight into these reactions and possible catalyses. The related investigation of the first two types of bond activation (H–H, C–X) will be addressed in Chapters 5 and 2, where we have studied oxidative addition reactions en route to C–H, O–H and N–H bond activation in chapters 3 and 4.

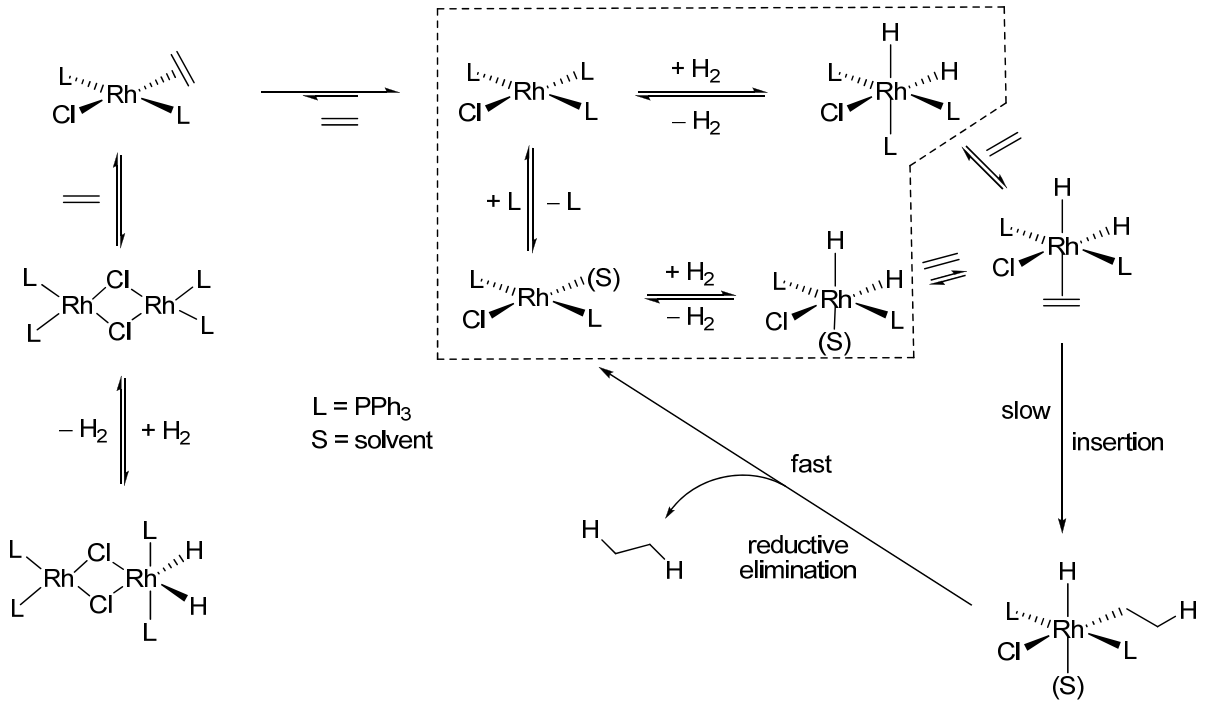

Scheme 1.1. The mechanism of catalytic olefin hydrogenation using Wilkinson reagent as the catalyst. The step of oxidative addition of H_2 to the metal center is highlighted by the dashed box.

Rhodium has the greatest role versus all transition metals in catalysis in terms of practicability and utility.[1] The well-known Wilkinson catalyst, $RhCl(PPh_3)_3$, catalyzes the homogeneous alkene hydrogenation (Scheme 1.1).[2,3] Another important application is the industrial procedure to prepare acetic acid that employs Monsanto process. The process involves the carbonylation of methanol to form the product and this reaction is catalyzed by the complex *cis*-$[RhI_2(CO)_2]^-$ (Scheme 1.2).[4–6]

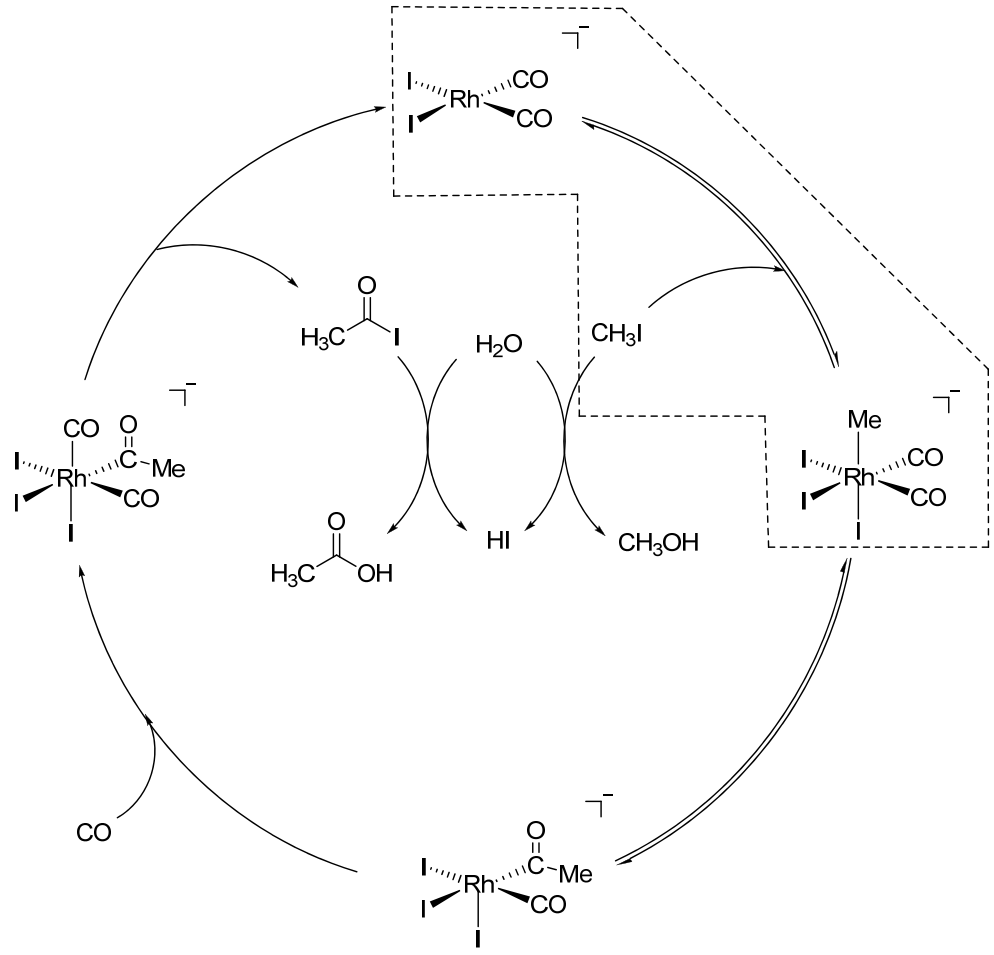

Scheme 1.2. Catalytic cycle for the Monsanto acetic acid synthesis. The key step circled by the dashed line represents the oxidative addition of MeI to the rhodium metal center.

These two well-studied catalytic reactions demonstrate the influential power of rhodium complexes facilitating transformations in which the common and critical feature of the processes is that the metal center inserts into the relatively unreactive H–H and C–I bonds under the reaction conditions to generate M–H and M–C bonds respectively (M = Rh).

This type of metal insertion is typically called oxidative addition. The newly formed M–H or M–C bonds provide reaction pathways that are not available to the H–H and C–I bonds. That is, the bond activation of H–H and C–I bonds provides a reaction pathway with lower energy barrier and allows the cycle to proceed to give the desire products. Oxidative addition is ubiquitous in organometallic chemistry and plays a critical role in numerous catalysis processes in addition to the hydrogenation and the acetic acid synthesis described above.[7,8]

One could consider a bidirectional reaction pathway that contains C–H functionalization to form carbon-heteroatom bonds as well as the reverse C–E (E = OH, NH_2) bond cleavage (Defunctionalization) to give simple hydrocarbons (Scheme 1.3). In fact, the activation (of O–H or N–H bonds) of the hydrogen containing unit, E, is the initial and consequential step during the process of C–E bond cleavage. The development of a general method for in-depth exploration of such bidirectional reaction mechanisms is critical due to the following justification.

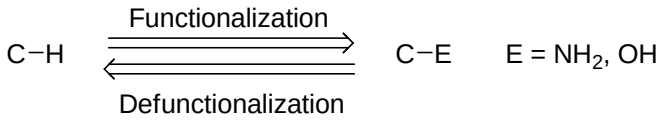

Scheme 1.3. The concept of bidirectional C–H bond functionalization and C–E bond defunctionalization.

The ubiquitous C–H bonds constitute the most basic framework of organic molecules. The inert nature of C–H bonds leads to the difficulty for metals to oxidatively insert to give simultaneously the M–H and M–C intermediates for further functionalizations. Therefore, the direct conversion of C–H bonds into C–E (E = N, O) bonds, providing versatile functionalized molecules, remains a great challenge.[9,10] Thus far, chemists have been pursuing various methods for converting unreactive C–H bond to synthetically useful functionalities under mild and selective conditions.

Meanwhile, the vast majority of these simple hydrocarbons are derived from crude oil or reserved in a natural gas. The public have realized the impending crisis of running short of the oil resources. Moreover, the demand for renewable feedstocks for producing chemicals has recently increased. One of the solutions is the transformation biomass into selected chemical products.[11] However, the highly oxygen and nitrogen containing materials in biomass could tremendously reduce the burning efficiency.[12] Therefore, we have an immediate demand to develop an efficient deoxygenating process (defunctionalization) to convert biomass to fuels and commercial chemicals.[12,13]

To cover this bidirectional reaction pathway, Chapter 3 entails the study of rhodium mediated C–H bond activation and functionalization while Chapter 4 deals with catalytic photon promoted O–H and N–H bond activation to give hydrocarbons.

Development of Ancillary Ligands

To explore the process of C–X, C–H, O–H, N–H and H–H activation chemistry, a suitable and robust ancillary ligand has to be used for the ease of the observation of the reaction intermediates. Cp (Cp = cyclopentadienyl) and its derivatives have long been utilized for bond activation chemistry of group 9 transition metals.[14] Tp (Tp = hydrotrispyrazolylborate) and its derivatives, on the other hand, are viewed as the analogues of Cp, sharing some common features: 1) Monoanionic L_2X type ligand. 2) 5-e donors for electron counting purpose. 3) Three coordination sites occupied on a metal.[15] Despite these similarities, the nature of hard N-donors on a Tp pyrazole motif is quite different from a relatively soft Cp ancillary ligand. The biting angle of a Tp (262°) ligand is significantly greater than that of a Cp (150°), making Tp a sterically bulkier and better-protected ligand for coordinated metal center. More importantly, based on the coordination environment, the Tp complex could render several informative NMR splitting patterns including C_{3v}, C_s and C_1 symmetry of the overall complex whereas the rotational property of a Cp ligand obviates the possibility of giving various symmetries.[16]

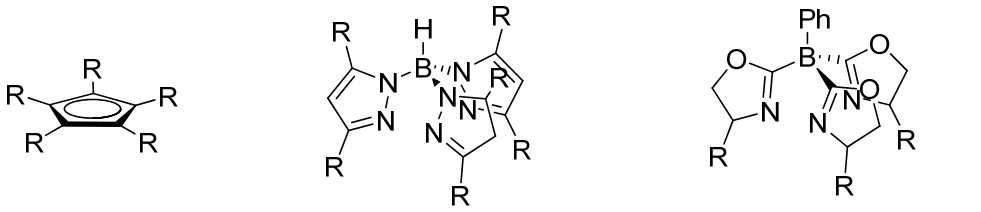

Figure 1.1. Comparison of Cp, Tp and To^R ligands.

However, some disadvantages of using Tp as the supporting lignad have been reported that the isomerization process and B–N bond cleavage could lead to complex

decomposition.[17] These downsides would hinder the investigation toward mechanistic study. Therefore, we have developed the Tp analogue, tris(oxazolinyl)phenylborate scorpionate ligand, to circumvent such possible problems while keeping the all the characteristics (hard N donors, bulk, informative NMR) of Tp.[18] We envision that the ease of tuning the steric bulk of To^R ligand by varying the substituent on oxazolines would result in diverse reaction behaviors.[19] In fact, oxazolines are derived from readily available amino acids which are belonged to a collection of an easily accessible chiral pool. The installation of chiral motifs to the ancillary ligand might be beneficially applied to asymmetric synthesis and catalysis. Here in this thesis, we study the bond activation chemistry by employing the rhodium metal supported by the newly-developed To^R ligand, spanning from synthesis and characterization to catalysis and mechanistic study.

Thesis Organization

The thesis contains six chapters. Chapter 1 gives a brief general introduction of the topic. Chapters 2 through 5 are journal articles of which 2 and 3 have been already published. The thesis ends in Chapter 6 with a general conclusion. All the published journal articles are modified to some degree to have a coherent description.

Chapter 2 describes the synthesis of the rhodium dicarbonyl complexes as well as the regioselectivity and stereoselectivity of these complexes toward various electrophiles, giving the C–X activation complexes in certain cases. One of the starting ligand transferring agent, $Tl[To^M]$ was synthesized by James Dunne that the compound description and the X-ray diagram are removed from the original published paper. Chapter 3 reports the synthesis of several allylic C–H activation rhodium complexes and numerous attempts to functionalize

these compounds with stepwise process. The related iridium complexes synthesized by Tristan Gray are removed from the original published paper.

Chapter 4 illustrates the photocatalytic acceptorless alcohol decarbonylation and amine coupling. Both transformations include dehydrogenation in the initial step, in which the O–H or N–H bonds are activated by the rhodium followed by β-elimination to give dehydrogenated and decarbonylated products. Chapter 5 describes the substitution chemistry of the first example of Tpm-supported rhodium bis(ethylene) complex. The phosphine-substituted complex could activate the H_2 molecule to give the dihydride complex.

References

(1) Evans, P. A. Ed. *Modern Rhodium-Catalyzed Organic Reactions*; Wiley-VCH Verlag GmbH & Co. KGaA, Weinheim, FRG., 2005.

(2) Osborn, J. A.; Jardine, F. H.; Young, J. F.; Wilkinson, G. *J. Chem. Soc. A*, **1966**, 1711-1732.

(3) (a) Halpern, J.; Wong, C. S. *J. Chem. Soc., Chem. Commun.* **1973**, 629. (b) Halpern, J.; Okamoto, T.; Zakhariev, A. *J. Mol. Catal.* **1976**, *2*, 65-69. (c) Halpern, J. *Inorg. Chim. Acta.* **1981**, *50*, 11-19.

(4) D. Forster, *Adv. Organomet. Chem.* **1979**, *17*, 255-268.

(5) (a) Kent, A. G.; Mann, B. E.; Manuel, C. P. *J. Chem. Soc., Chem. Commun.* **1985**, 728-729. (b) Kent, A. G.; Mann, B. E.; Manuel, C. P. *J. Chem. Soc., Dalton Trans.* **1987**, 489-496.

(6) (a) Haynes, A.; Mann, B. E.; Gulliver, D. J.; Morris, G. E.; Maitlis, P. M. *J. Am. Chem. Soc.* **1991**, *112*, 8567-8569. (b) Haynes, A.; Mann, B. E.; Morris, G. E.; Maitlis, P. M. *J. Am. Chem. Soc.* **1993**, *115*, 4093-4100.

(7) Crabtree, R. Ed. *The Organometallic Chemistry of the Transition Metals,* 3rd ed.; Wiley-Interscience John Wiley & Sons, INC., 2001; pp152-161.

(8) Miessler, G. L.; Tarr, D. A. Eds. *Inorganic Chemistry*, 2nd ed.; Prentice-Hall Inc., NJ, 1998.

(9) (a) Bergman, R. G. *Nature* **2007**, *466*, 391-394. (b) Hartwig, J. F. *Nature* **2008**, *455*, 314-322. (c) Labinger, J. A.; Bercaw, J. E. *Nature* **2002**, *417*, 507-514.

(10) (a) Shilov, A. E.; Shul'pin, G. B. *Chem. Rev.* **1997**, *97*, 2879-2932. (b) Arndtsen, B. A.; Bergman, R. G.; Mobley, T. A.; Peterson, T. H. *Acc. Chem. Res.* **1995**, *28*, 154-162.

(11) (a) Corma, A.; Iborra, S.; Velty, A. *Chem. Rev.* **2007**, *107*, 2411-2502. (b) Gallezot, P. *Chem. Soc. Rev.* **2012**, *41*, 1538-1558.

(12) (a) Lin, Y.; Zhang, C.; Zhang, M.; Zhang, J. *Energy Fuels* **2010**, *24*, 5686-5695. (b) Jiang, X.; Ellis, N. *Energy Fuels* **2010**, *24*, 1358-1364.

(13) (a) Tong, X.; Li, M.; Yan, N.; Ma, Y.; Dyson, P. J.; Li, Y. *Catal. Today* **2011**, *175*, 524-527. (b) Miranda, M. O.; Pietrangelo, A.; Hillmyer, M. A.; Tolman, W. B. *Green Chem.* **2012**, *14*, 490-494.

(14) (a) Janowicz, A. H.; Bergman, R. G. *J. Am. Chem. Soc.* **1982**, *104*, 352-354. (b) Periana, R. A.; Bergman, R. G. *J. Am. Chem. Soc.* **1984**, *106*, 7272-7273. (c) Hoyano, J. K.; McMaster, A.; Graham, W. A. G. **1983**, *105*, 7190-7191. (d) Jones, W. D.; Feher, F. *J. Am. Chem. Soc.* **1982**, *104*, 4240-4242.

(15) (a) Trofimenko S. *Chem. Rev.* **1993**, *93*, 943-980. (b) Trofimenko, S. *J. Am. Chem. Soc.* **1966**, *88*, 1842-1844.

(16) Slugovc, C.; Padilla-Martínez, I.; Sirol, S.; Carmona, E. *Coord. Chem. Rev.* **2001**, *213*, 129-157.

(17) (a) Murtuza, S.; Casagrande, O. L.; Jordan, R. F. *Organometallics* **2002**, *21*, 1882-1890. (b) Michiue, K.; Jordan, R. F. *Organometallics* **2004**, *23*, 460-470. (c) Reger, D. L.; Tarquini, M. E. *Inorg. Chem.* **1982**, *21*, 840-842. (d) Reger, D. L.; Tarquini, M. E. *Inorg. Chem.* **1983**, *22*, 1064-1068. (e) Reger, D. L.; Tarquini, M. E.; Lebioda, L. *Organometallics* **1983**, *2*, 1763-1769.

(18) (a) Dunne, J. F.; Su, J. C.; Ellern, A.; Sadow, A. D. *Organometallics* **2008**, *27*, 2399-2401.

(19) (a) Baird, B.; Pawlikowski, A. V.; Su, J.; Wiench, J. W.; Pruski, M.; Sadow, A. D. *Inorg. Chem.* **2008**, *47*, 10208-10210. (b) Neal, S. R.; Ellern, A.; Sadow, A. D. *J. Organomet. Chem.* **2011**, *696*, 228-234.

Chapter 2. Reactions of tris(oxazolinyl)phenylborate rhodium(I) with C–X (X = Cl, Br, OTf) bonds: Stereoselective intermolecular oxidative addition

Modified from a paper published in *Organometallics*[†]

Hung-An Ho,[‡] James F. Dunne,[¶] Arkady Ellern, Aaron D. Sadow[*]

Abstract

The achiral and enantiopure chiral compounds $To^{M}Rh(CO)_2$ (**2.2**) (To^{M} = tris(4,4-dimethyl-2-oxazolinyl)phenylborate) and $To^{P}Rh(CO)_2$ (**2.3**) (To^{P} = tris(4S-isopropyl-2-oxazolinyl)phenylborate) were prepared to investigate stereoselective oxidative addition reactions and develop new catalytic enantioselective bond functionalization and cross-coupling chemistry. Reactivity at the rhodium center is first shown by the substitution of the carbonyl ligands in **2.2** and **2.3** in the presence of the appropriate ligand; thus treatment of $To^{M}Rh(CO)_2$ with $P(OMe)_3$ provides $To^{M}Rh(CO)[P(OMe)_3]$ (**2.4**). However, reaction of $To^{M}Rh(CO)_2$ and MeOTf affords the complex [{*N*-Me-κ^2-To^{M}}$Rh(CO)_2$]OTf (**2.5**) resulting from *N*-oxazoline methylation rather than oxidative addition to rhodium(I). In contrast, $To^{M}Rh(CO)_2$ reacts with allyl bromide and chloroform forming the rhodium (III) species (κ^3-To^{M})Rh(η^1-C_3H_5)Br(CO) (**2.6**) and (κ^3-To^{M})Rh($CHCl_2$)Cl(CO) (**2.7**), respectively. Interestingly, the chiral $To^{P}Rh(CO)_2$ and $CHCl_3$ react to give one diastereomer of (κ^3-

[†] *Organometallics* **2010**, *29*, 4105-4114.

[‡] Primary researcher and author

[¶] Contributed synthesis of $Tl[To^{M}]$

[*] Author for correspondence

To^P)Rh($CHCl_2$)Cl(CO) (**2.8**; 100:3 d.r.) almost exclusively. To evaluate the reactivity of these rhodium(I) compounds, the carbonyl stretching frequencies have been examined. The data for the mono- and trivalent rhodium oxazolinylborate compounds indicate that the electron donating abilities of To^M is slightly greater than To^P, and both ligands provide electronic environments that can be compared to the tris(pyrazolyl)borate ligand family.

Introduction

Transition metal mediated bond activation *via* oxidative addition plays crucial roles in various catalytic processes.[1] The oxidative addition of C–X bond could involve concerted pathway, S_N2 type, radical mechanism and ionic mechanism.[2] All possible mechanisms could affect the stereochemistry and the catalytic reactivity. A representative example is the oxidative addition of MeI to the planar $[RhI_2(CO)_2]^-$ metal center that undergoes S_N2 mechanism to give the *trans*-Me[Rh]I intermediate in Monsanto process.[3] Along the line, Eisenberg and his co-workers have reported the first example of highly diastereoselective oxidative addition of MeI to the square planar chiral complex, IrI(CO)(duphos).[4] Other examples of highly diastereoselective oxidative addition of MeI include non-square-planar chiral Cp complexes [Rh(η^5-C_5H_4-$CH_2CH(R)PPh_2$)(η^2-Olefin)] (R = Ph or Cy, Olefin = ethylene or COE (COE = cyclooctadiene))[5] while even a stronger electrophiles, [Me_3O][BF_4] (Meerwein reagent) has also been reported to give the oxidative addition metal complex with high diastereoselectivity.[6] The diastereoselective oxidative addition chemistry has not only been restricted to methylating reagent but investigated for inert C–H bond. For example, irradiation of $Tp^{menth}Rh(CO)_2$ pentane solution yields a stereoselective ligand cyclometalation product forming carbon-metal bond along with metal-hydride bond.[7]

Another photolytic example involves oxidative addition of benzene and cyclohexane C–H bond to a racemic planar-chiral iridium dihydride complex to generate both Ir–C and Ir–H bonds as well.[8]

On the other hand, regioselective reaction pathways provide fundamental consequences among synthesis, catalysis and mechanistic understanding. For a metal complex, the reaction site could be situated either on the ligand or metal or both such as the process of protonation of Cp_2Ru with acids.[9] Meanwhile, protonation of the complex $Tp^*Rh(CO)_2$ (Tp^* = hydrotris(3,5-dimethylpyrazolyl)borate) with $HBF_4 \cdot Et_2O$ occurs at 2-position of pyrazole nitrogen, whereas the iridium analogue, $Tp^*Ir(CO)_2$, undergoes a metal-based protonation.[10] In contrast, $Tp^*Rh(CO)L$ (L = CO or phosphines) reacts with MeI to generate a metal-methylation intermediate followed by alkyl migration to give the product, $[Tp^*RhI(COMe)L]$.[11]

Along this context, we are interested in the stereoselectivity as well as regioselectivity of the achiral and chiral metal complexes toward several organic electrophiles containing C–X bonds. Recently, we synthesized achiral tridentate To^M supporting ligand with dimethyl group on the oxazoline ring as well as chiral tridentate ligand To^P, equipping with chiral (*S*-configured) isopropyl group on the 4- position.[12] Both To^M and To^P are isoelectronic with well-studied Cp and Tp analogues, viewed as anionic 5 electron donor ligands. The nature of the metal center and the property of κ^2-κ^3 equilibrium of the tris(oxazolinyl)phenylborate ancillary ligands to give bi- or tridentate coordination mode greatly affect the reaction pathway that either oxazoline nitrogen or metal center could be the reactive site. Therefore, the diastereoselectivity determination of the product is feasible once the electrophiles

selectively react with the prochiral metal center (coordinated by To^P). We have discovered that the selective N-protonation and N-methylation of both To^M and To^P iridium complexes with HOTf and MeOTf previously.[12b,c] Herein, we further expand the varieties of the electrophiles and focus on the To^M and To^P-supported rhodium complexes. We found that metal-centered oxidative additions are thermally accessible, N-oxazoline- versus metal-based selectivity is governed by the nature of the electrophile (Scheme 2.1), and the enantiopure oxazolinylborato rhodium(I) complex reacts with high diastereoselectivity.

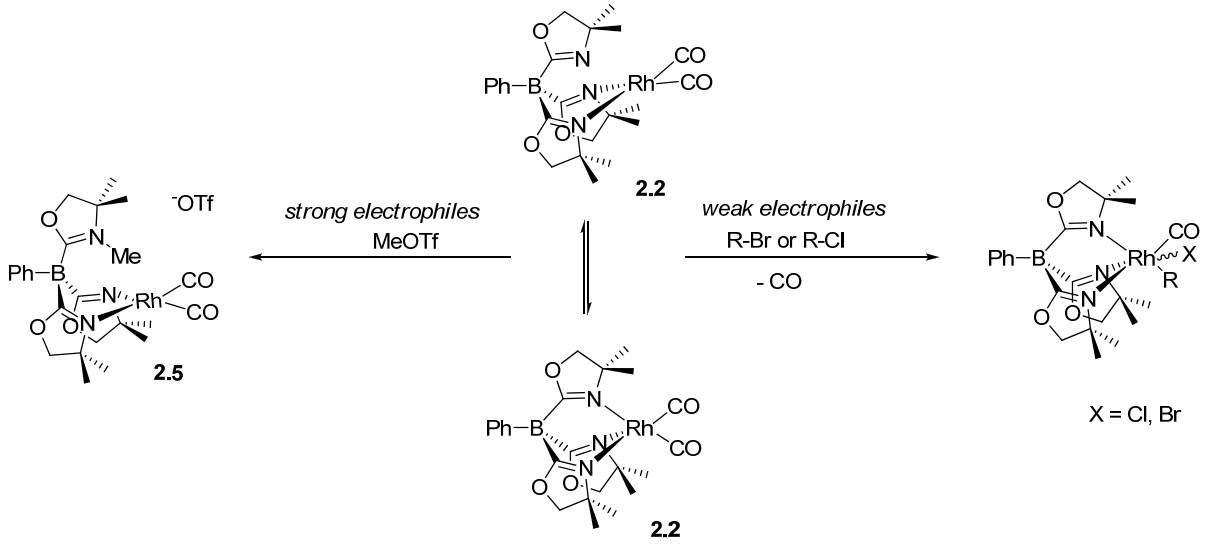

Scheme 2.1. Reaction pathways for the interaction of $To^MRh(CO)_2$ (**2.2**) with strong and weak electrophiles.

Results and Discussion

Synthesis and characterization of Tl[To^P], To^{M}Rh(CO)$_2$ and ToPRh(CO)$_2$

Previously, we obtained LiCl containing adduct, $(LiCl)_2[(\kappa^2\text{-}To^MIr(COD)]_2$ (COD = 1,5-cyclooctadiene), *via* salt metathesis of $Li[To^M]$ and $[Ir(\mu\text{-}Cl)(COD)]_2$, showing that the oxazoline-based ancillary ligand appears to be lithiophilic.[12c] Although **2.2** could be obtained

by following the similar metathesis route, impurities were also observed. Thus, we decided to use an alternative ligand transfer agent Tl[To^{M}][13] to attain the goal of synthesizing **2.2**. Analogously, attempts to prepare Tl[To^{P}] (**2.1**) by treating Li[To^{P}] with $TlNO_3$ were ineffective and neither were Li[To^{P}] or K[To^{P}] with $TlPF_6$. Fortunately, **2.1** could be prepared by the reaction of Li[To^{P}] and TlOAc in methylene chloride suspension (eq 2.1). After filtration and recrystallization, **2.1** could be isolated with moderate yield. Despite the absence of X-ray structure of **2.1**, ^{11}B NMR showed one single resonance at −16.0 ppm which implies the existence of only one boron-containing species as well as two sets of diastereotopic dimethyl group in the ^{1}H NMR spectrum, meaning that the three chiral centers on the oxazolines remained enantiopure. Moreover, the IR stretching frequency of oxazoline C=N bond appeared at 1590 cm^{-1} solely, indicating a κ^3coordinaiton mode of **2.1**.

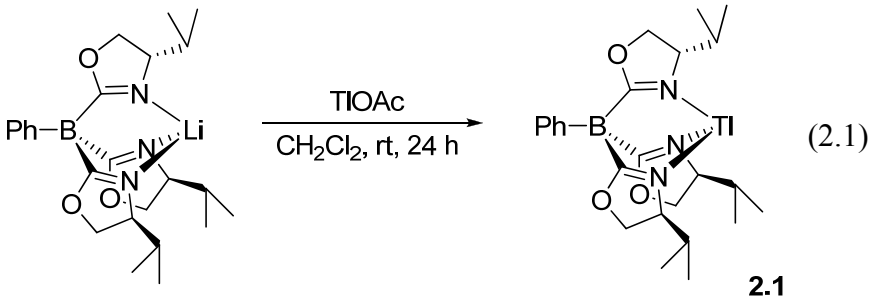

(2.1)

2.1

Treating Tl[To^{M}] with half equivalent of [Rh(μ-Cl)(CO)]$_2$ affords To^{M}Rh(CO)$_2$ (**2.2)** in decent yield (eq 2.2). All the methylene groups (3.50 ppm) and dimethyl groups (1.07 ppm) appeared to be equivalent in the ^{1}H NMR spectrum. **2.2** also provided one signal (−163.1 ppm) in the ^{1}H–^{15}N HMBC NMR spectrum. These two observations imply the equivalence of the three oxazolines of To^{M}. The carbonyl signal exhibited at 188.42 ppm ($^{1}J_{RhC}$ = 66.6 Hz) in the ^{13}C{^{1}H} NMR spectrum and five CO absorption peaks were observed at the region

between 1968 to 2070 cm^{-1} in the IR spectrum. These IR absorption peaks could be assigned and divided into two classes correlated to two coordination modes (κ^2 or κ^3). Additionally, two C=N IR absorption signals were observed in the IR spectrum, which provides further evidence to support the presence of κ^2 and κ^3 isomers.

Table 2.1. Infrared and NMR spectroscopic data for tris(oxazolinyl)phenylborato rhodium and related tris(pyrazolyl)borato rhodium carbonyls.

Compound	**ν_{CO} (KBr, cm^{-1})**	**ν_{CN} (KBr, cm^{-1})**
$To^MRh(CO)_2$ (**2.2**)	κ^2: 2070, 2010, 1997 κ^3: 2048, 1968	non-coordinated: 1616 Rh-coordinated: 1571
$To^PRh(CO)_2$ (**2.3**)	κ^2: 2072, 2002	Rh coordinated: 1575
$To^MRh(CO)[P(OMe)_3]$ (**2.4**)	κ^2: 1995 κ^3: 1965	non-coordinated: 1610 Rh coordinated: 1576
$Tp^*Rh(CO)_2$[14]	κ^2: 2108, 2073[14c] κ^2: 2083, 2012[14c] κ^3: 2051, 1972[14c] κ^3: 2052, 1974[14c]	n.a.
$Tp^{Me}Rh(CO)_2$[14]	κ^3: 2061, 1981[14a]	n.a.
$Tp^{Me2Cl}Rh(CO)_2$[15a]	κ^2: 2083, 2017 κ^3: 2059, 1984	n.a.
[{*N*-Me-κ^2-To^M}$Rh(CO)_2$]OTf (**2.5**)	2083, 2012	1580, 1551
(κ^3-To^M)Rh(η^1-C_3H_5)Cl(CO) (**2.6**)	2058	1582
(κ^3-To^M)Rh($CHCl_2$)Cl(CO) (**2.7**)	2088	1575
(κ^3-To^P)Rh($CHCl_2$)Cl(CO) (**2.8**)	2092	1590
$Tp^{Me2Cl}Rh(CHCl_2)Cl(CO)$[15b]	2100[15b]	n.a.

Comparing to the well explored $Tp^*Rh(CO)_2$ complex, the CO stretching frequencies of **2.2** are lower than those of $Tp^*Rh(CO)_2$ for both κ^2 and κ^3 coordination modes, suggesting that the ancillary To^M is more electron donating than Tp^*(Table 2.1). Furthermore, in general, it is not uncommon to observe the κ^2-κ^3 equilibrium issue for the Tp^* supported group 9 family.[16]

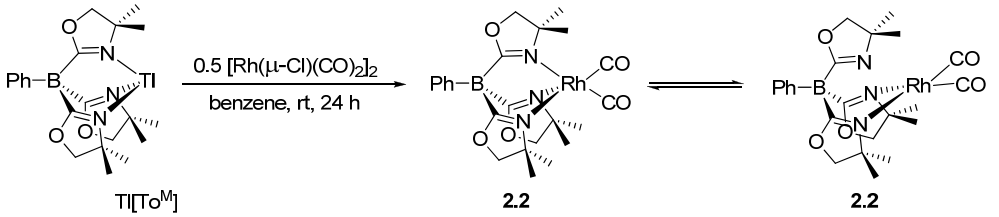

(2.2)

Solid state structure of **2.2** revealed the κ^2 coordination connectivity exclusively (Fig 2.1) even though both κ^2 and κ^3 configurations are observed in solid state and form the equilibrium in solution phase. The X-ray crystallography shows that the complex **2.2** displays SP geometry formed by the two coordinated oxazolines and two carbonyls along with the rhodium center while the face of the third uncoordinated oxazoline is oriented nearly parallel to the SP plane. In addition, the six-membered ring formed by B1–C5–N1–Rh1–N2–C10 atoms adopts a boat conformation.

Similarly, the reaction of **2.1** and $[Rh(\mu\text{-}Cl)(CO)_2]_2$ gives the compound $To^PRh(CO)_2$ (**2.3)**. The reaction proceeds to completion within 6 h and **2.3** was isolated with excellent yield (95%). Like **2.2**, **2.3** appeared to give a single resonance in the $^1H–^{15}N$ HMBC NMR spectrum (–182.8 ppm) and the three isopropyl group are equivalent, showing two sets of diastereotopic dimethyl signals (0.72 and 0.66 ppm) in the ^1H NMR spectrum. The distinct carbonyl peak exhibited a doublet at 186.11 ppm ($^1J_{RhC}$ = 65.0 Hz) in the $^{13}C\{^1H\}$ NMR

spectrum. In comparison, the ^{15}N chemical shift of the iridium analogue, $To^{P}Ir(CO)_2$, showed a single cross-peak which was slightly more upfield (–183.9 ppm) than the one of **2.3** as well as the more upfield ^{13}C chemical shift of the carbonyl peak (174.5 ppm).[12b]

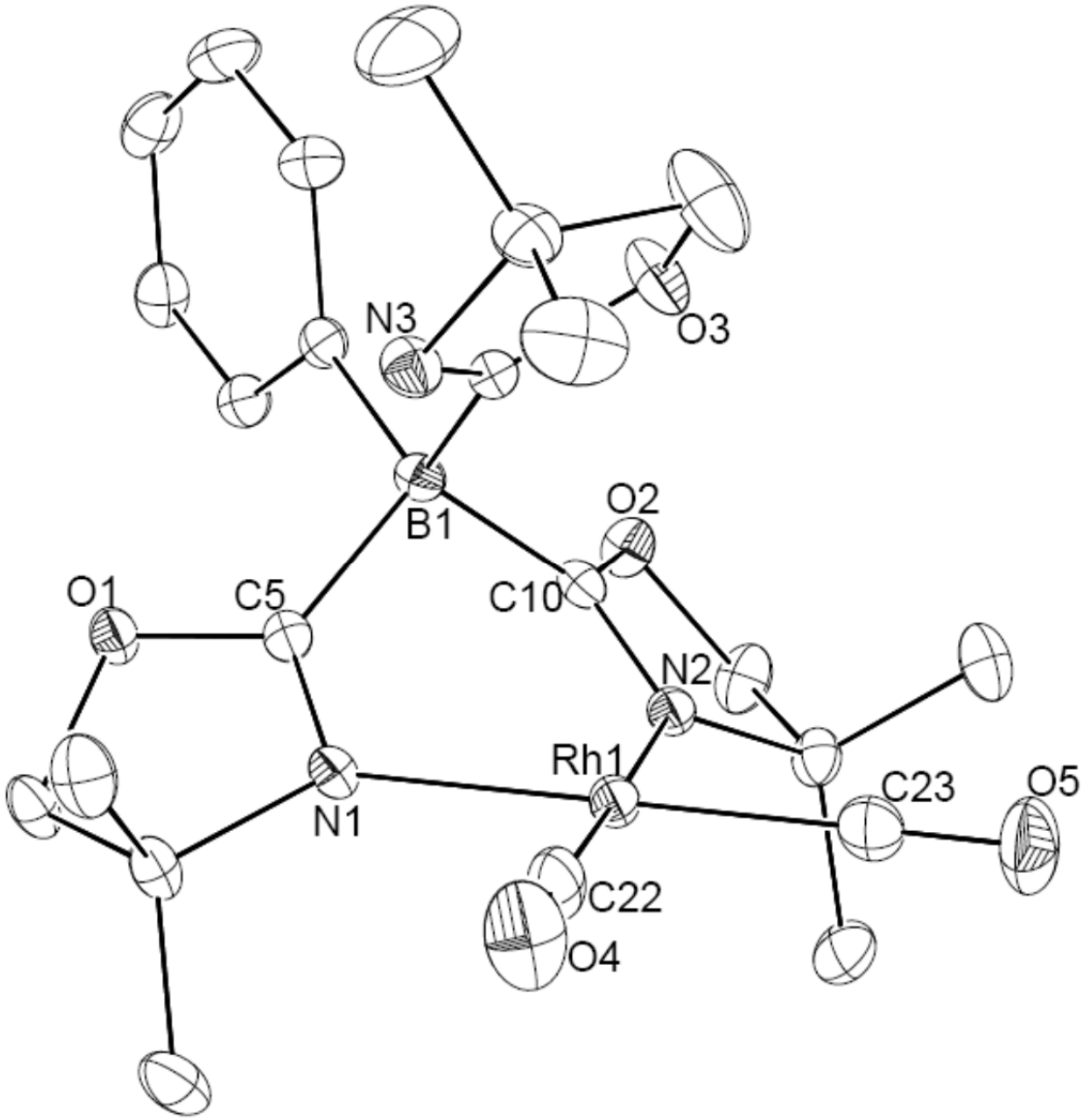

Figure 2.1. ORTEP diagram of **2.2** drawn at 50% probability. Hydrogens are omitted for clarity. Bond distances (Å): Rh1–C22, 1.851(2); Rh1–C23, 1.854(2); Rh1–N1, 2.087(1); Rh1–N2, 2.096(2). Bond angles (°): C22–Rh1–C23, 86.14(8); N1–Rh1–N2, 92.28(7);

N1–Rh1–C23, 178.37(7); N2–Rh1–C22, 178.52(7). Non-bonding distances (Å): Rh1–N3, 3.43; Rh1–O3, 3.82; Rh1–C15, 3.20.

Not surprisingly, besides the single ^{15}N chemical shift, the three oxazolines of $To^{P}Ir(CO)_2$ appeared to be equivalent in the ^{1}H NMR spectrum as in the case of **2.2** and **2.3**.

Oxazoline N-methylation and substitution reactions of $To^{M}Rh(CO)_2$

The chemistry of $TpRh(CO)_2$ compounds have been reported to react with phosphines to provide mono-CO-substituted $TpRh(CO)(PR_3)$ complexes.[11,17] Therefore, we anticipated that **2.2** could react with one equivalent of PR_3 under the same reaction pathway. Treating **2.2** with either electron-donating PMe_3 or bulkier PPh_3 gives multiple products (immediately after addition at room temperature) and unreacted **2.2** (up to 80 °C for 5 h) respectively. Thus, we speculated that **2.2** could only tolerate electron-withdrawing and less bulky phosphites. Treating **2.2** with one equivalent of $P(OMe)_3$ at room temperature gives the complex $To^{M}Rh(CO)[(P(OMe)_3]$ (**2.4**) within 10 min (eq 2.3).

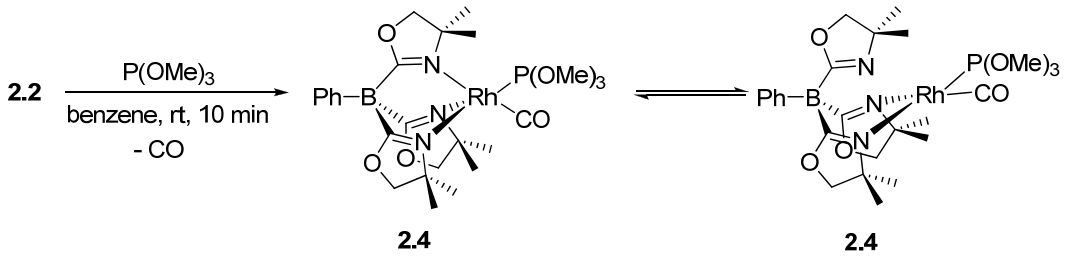

(2.3)

Once again, **2.4** is fluxional that all the three oxazolines are equivalent. The only $^{31}P\{^{1}H\}$ NMR signal was observed at –90.0 ppm ($^{1}J_{RhP}$ = 247.7 Hz) as a doublet coupled by the rhodium center. In the $^{13}C\{^{1}H\}$NMR spectrum, CO appeared at 189.6 ppm as a doublet of doublet ($^{1}J_{RhC}$ = 69.8 Hz, $^{2}J_{PC}$ = 28.5Hz). Both bidentate and tridentate

tris(oxazolinyl)phenylborate binding modes are present in **2.4** on the basis of its observed infrared spectrum (ν_{CO}: 1995 and 1965 cm^{-1}; ν_{CN}: 1610 and 1576 cm^{-1}).

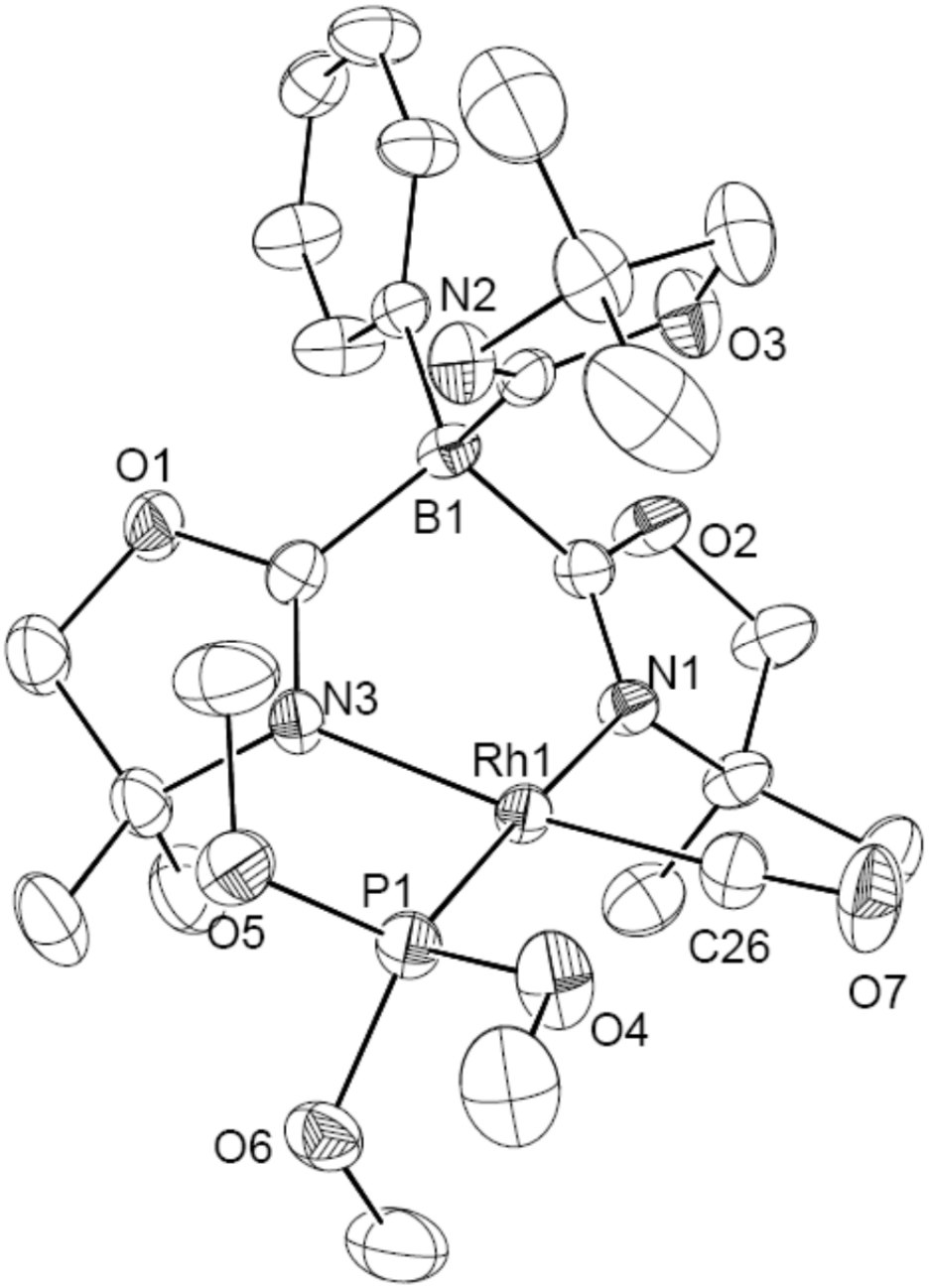

Figure 2.2. ORTEP diagram of **2.4** drawn at 50% probability. Hydrogens are omitted for clarity.

For the complex **2.4**, the distance between the pendant oxazoline nitrogen, N2, and the rhodium center (N2–Rh1, 3.69 Å) is somewhat longer than the one of **2.2** (3.43Å), presumably due to the steric effect. The carbonyl bond length of **2.4** (1.143(4) Å) is greater than that of **2.2** (1.136(2) Å), which is attributed to the less electron-withdrawing nature of $P(OMe)_3$ (compared to CO) so that the more electron-rich rhodium center of **2.4** back-donates more electron densities to the carbonyl and increase the bond length. Like the solid structure of **2.2**, **2.4** contains the six-membered ring formed by the two coordinated oxazolines and the rhodium center, adopting a boat conformation.

The dicarbonyl complex **2.2** reacts with MeOTf to give the compound [{*N*-Me-κ^2-To^M}$Rh(CO)_2$]OTf (**2.5**). The reaction proceeds *via* N-methylation route rather than the oxidative addition route on the rhodium center (eq 2.4). The N-methylated **2.5** exhibited a C_s symmetric pattern of the ancillary ligand To^M in the ^1H NMR spectrum. The dimethyl groups (as well as the methylene groups) of the two rhodium-bounded oxazolines are inequivalent whereas the unbounded oxazoline dimethy groups and methylene groups are equivalent (dissected by a mirror plane). The cross-peak between the methylated nitrogen (–211.0 ppm) and the methyl group (2.90 ppm) was observed in the ^1H–^{15}N HMBC experiment while the coordinated oxazoline nitrogens appeared at –179.7 ppm.

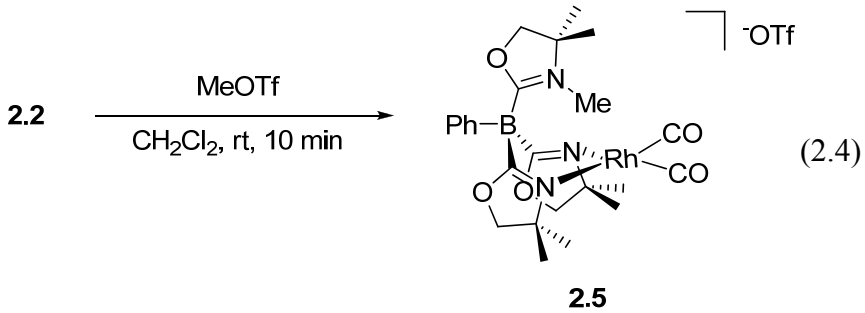

2.5 (2.4)

Two CO absorption bands showed at 2083 and 2012 cm^{-1}, which are close to the CO stretching frequency of the compound **2.2**. This provides further evidence that for this reaction, the reactive center is not located on the rhodium center (which gives Rh(III) oxidative product) but on the oxazoline nitrogen. The X-ray structure of **2.5** undoubtedly confirmed the connectivity proposed in the reaction (Fig 2.3).

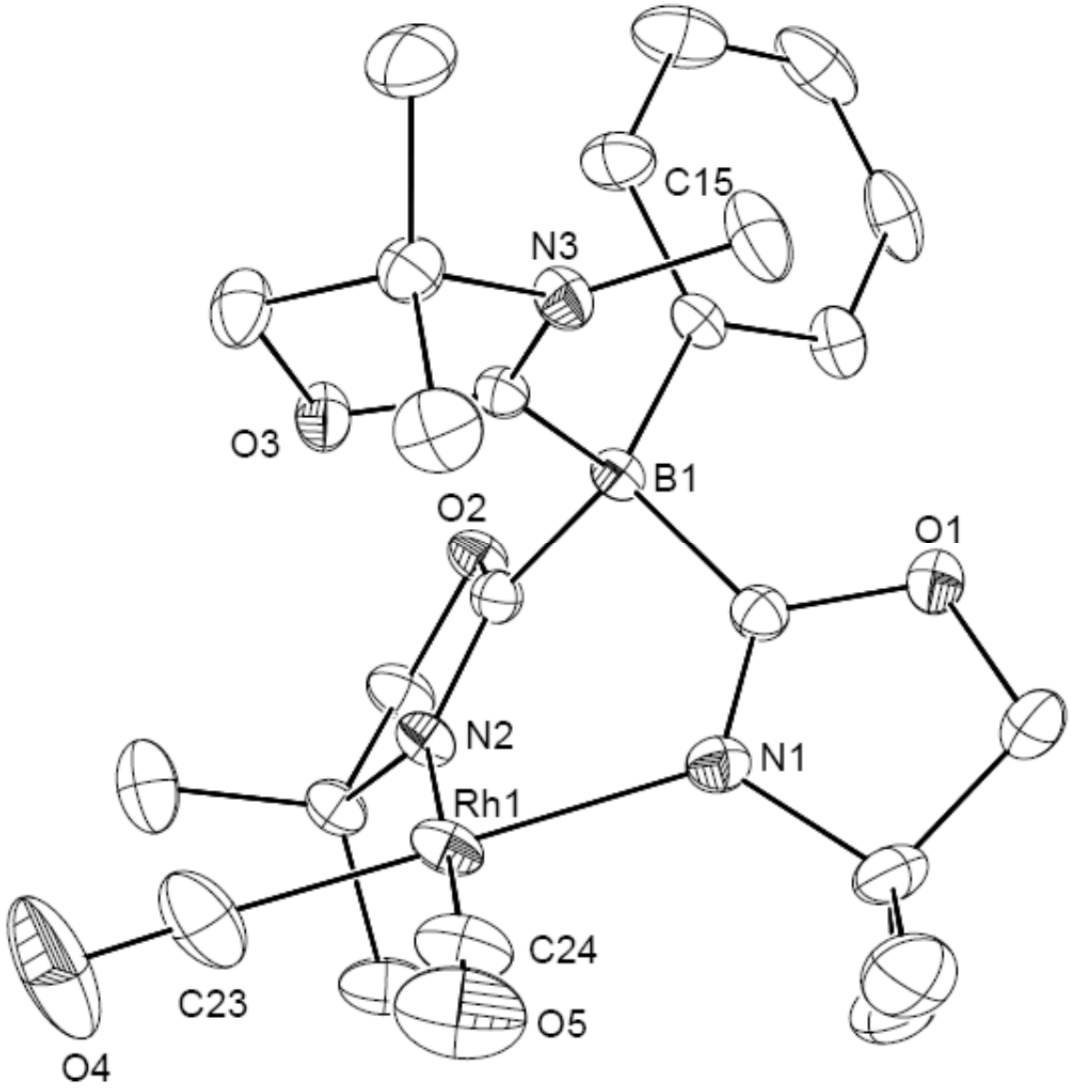

Figure 2.3. ORTEP diagram of **2.5** drawn at 50% probability. Hydrogens and the triflate are omitted for clarity.

For comparison, the precedent of N-protonation or N-methylation of $To^{P}Ir(COD)$[12b], $To^{P}Ir(CO)_2$[12b], $To^{M}Ir(COD)$[12c] and $To^{M}Ir(CO)_2$[12c] has established the foundation of the possible reaction pathways. Nevertheless, it has been studied that the reaction of $Tp^{*}Rh(CO)L$ (L = CO or phosphines) and MeI affords $[Tp^{*}RhI(COMe)L]$.[11] Given that the electron-donating ability of **2.2** is slightly greater than Tp^{*} analogues, the contrary consequence of proceeding *via* N-methylation route instead of the oxidative addition route has to be further investigated and rationalized. Thus, more details of the reactivities of **2.2** toward various electrophiles were explored and discussed in the context below.

Oxidative addition reactions of $To^{M}Rh(CO)_2$ and $To^{P}Rh(CO)_2$

Treatment of **2.2** with a large excess of allyl bromide gives the oxidative addition product, (κ^3-To^{M})Rh(η^1-C_3H_5)Br(CO) (**2.6**) after 5 h (eq 2.5). The crude product was purified by recrystallization from a concentrated acetonitrile solution at –30 ºC. The $^{13}C\{^1H\}$ NMR spectrum confirmed the connectivity of the metal-bonded η^1-C_3H_5 group where the allylic carbon bonded to the rhodium was observed at 20.5 ppm ($^1J_{RhC}$ = 16 Hz). A related structure, $Tp^{*}Rh(\eta^1$-$C_3H_5)Br(NCMe)$, has been reported to show a similar ^{13}C chemical shift and coupling constant (δ_{RhC} = 18.0; $^1J_{RhC}$ = 18 Hz).[18] Besides, the carbonyl group displayed a single resonance at 186.5 ppm ($^1J_{RhC}$ = 60 Hz) in the $^{13}C\{^1H\}$ NMR spectrum in addition to the only one CO band appearing at 2058 cm^{-1} in the IR spectrum, excluding the possibility of being an acyl group (Rh–(C=O)–(C_3H_5)). The assignment of the η^1-C_3H_5 group was supported by the COSY experiment that the internal vinylic proton (6.99 ppm) has correlations with both the allylic protons (4.57 and 3.64 ppm) and the terminal vinylic protons (5.58 and 5.24 ppm). The overall molecular symmetry of **2.6** (C_1) is in contrast to the

one of **2.5** (C_s), proven by the inequivalence of all the dimethyl and methylene groups on the oxazolines in the ^{1}H NMR spectrum.

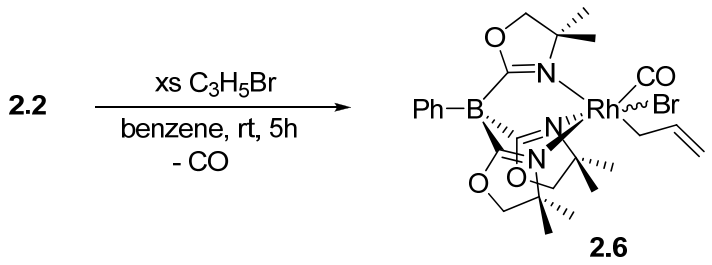

(2.5)

The two diastereotopic allylic protons of the η^1-C_3H_5 group were proved to be in close proximity to the two sets of dimethyl groups on the oxazolines by ^{1}H NOESY spectroscopy. These four methyl groups were thus assigned as *cis* with respect to the η^1-C_3H_5 group whereas the dimethyl group on the third ring was assigned as *trans*, showing no cross-peak in the NOESY spectrum (Fig 2.4).

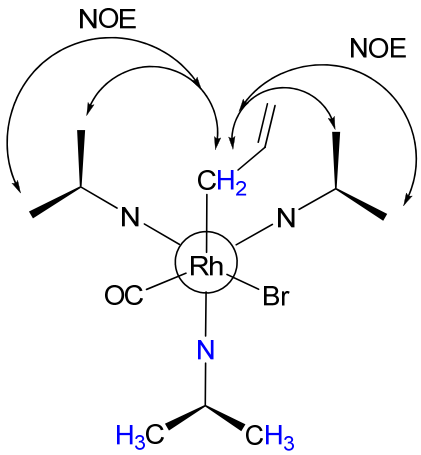

Figure 2.4. A Newman projection of one of two enantiomers of the racemic mixture of C_1-symmetric (κ^3-To^M)Rh(η^1-C_3H_5)Br(CO) (**2.6**) viewed along the Rh–B bond. Through-space close contacts between oxazoline methyl groups and the σ-allyl ligand, detected using a NOESY experiment, are illustrated with arrows. Through-bond coupling between an

oxazoline nitrogen and σ-allyl ligand is observed with a $^{1}H–^{15}N$ HMBC experiment and highlighted in blue.

The $^{1}H–^{15}N$ HMBC experiment also coincided with the assignments that were based on NOESY spectroscopy. The four *cis* methyl groups showed correlations with two of the oxazoline nitrogens (–163.5 and –187.8 ppm) and the rest two *trans* methyl groups correlated to the third nitrogen at –203.5 ppm.

To expand the oxidative chemistry, we chose $CHCl_3$ to react with compound **2.2**. The reaction of **2.2** and $CHCl_3$ undergoes at 60 ºC to generate C–Cl oxidative adduct (κ^3-To^{M})Rh($CHCl_2$)Cl(CO) (**2.7)** (eq 2.6). In comparison, a similar reaction type has been published that Tp^{Me2Cl}Rh$(CO)_2$ thermally reacts with $CHCl_3$ to afford Tp^{Me2Cl}Rh($CHCl_2$)Cl(CO) while no reaction occurs between Tp*Rh$(CO)_2$ and chloroform.[15b] In contrast, Tp*Rh$(CNCH_2CMe_3)_2$ reacts with $CHCl_3$ to give Tp*Rh($CHCl_2$)Cl($CNCH_2CMe_3$) as the photolytic product and Tp*RhCl_2 under thermal condition.[19] The overall molecular symmetry of **2.7** appears to be C_1, identical to compound **2.6**.

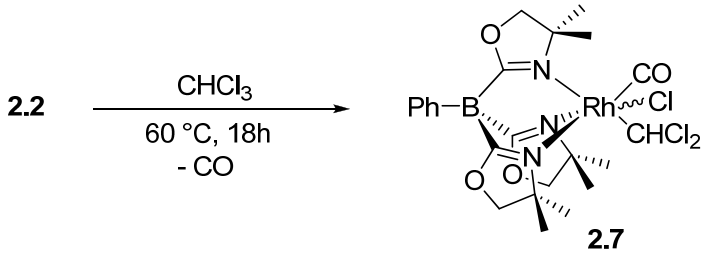

(2.6)

In the ^{1}H NMR spectrum, the proton signal of the dichloromethyl ligand was assigned as a doublet at 7.81 ppm ($^{2}J_{RhH}$ = 3.2 Hz). This dichloromethyl ligand showed at 63.7 ppm as a doublet ($^{1}J_{RhC}$ = 26 Hz) in the $^{13}C\{^{1}H\}$ NMR spectrum and correlated to its proton in a $^{1}H–^{13}C$ HMQC experiment. The stereo proximity could be determined by the NOESY

experiment that four methyls are assigned as *cis* due to the observation of cross-peaks between C*H*Cl_2 and the dimethyl hydrogens. These four methyls also correlated to the two oxazoline nitrogen resonances in the $^{1}H–^{15}N$ HMBC spectrum. In this spectrum, the most upfield nitrogen signal (–198.0 ppm) was assigned to the dimethyl *trans* to the $CHCl_2$ ligand, which was parallel to the compound **2.6** whose most upfield nitrogen resonance was associated with dimethyl trans to the η^1-C_3H_5 group.

So far, we have demonstrated the difference of regioselectivity between ally bromide, chloroform and MeOTf with **2.2**. For these three electrophiles, the former two are able to provide racemic products (**2.6** and **2.7**). Thus, we chose one of these (allyl bromide and chloroform) to study the stereoselectivity by utilizing an enantiopure ancillary ligand To^P to examine the formation of two diastereomers. Enantiopure compound **2.3** reacts with chloroform to give (κ^3-To^P)Rh($CHCl_2$)Cl(CO) (**2.8)** at room temperature with 100:3 ratio of diastereomers (eq 2.7). The diastereomer ratio of the crude product was determined by ^{1}H NMR spectroscopy. More specifically, the ratio was determined by the integration of C*H*Me_2 signals because the CH*Me*$_2$, oxazoline C*H*$_2$ and the C_6H_5 resonances are significantly overlapping. The major product could be obtained after column chromatography. The proton resonance of $CHCl_2$ ligand was detected at 7.11 ppm ($^{2}J_{RhH}$ = 3.2 Hz) in the ^{1}H NMR spectrum and the carbon resonance was found at 65.7 ppm ($^{1}J_{RhC}$ = 28.0 ppm) in the $^{13}C\{^{1}H\}$ NMR spectrum. The doublet of carbonyl signal of **2.8** (179.7 ppm) was comparatively more upfield than that of **2.7** (188.4 ppm).

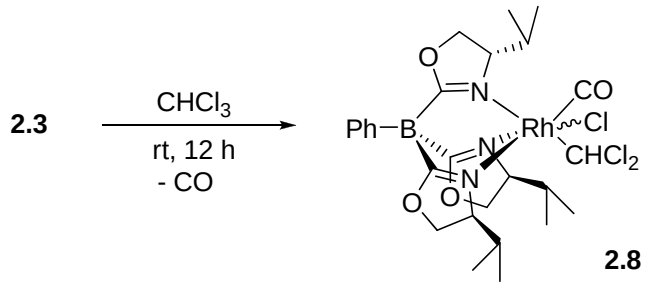

(2.7)

The isopropyl methine hydrogens at δ 2.37 and 2.17 contained cross-peaks associated with C*H*Cl_2 ligand and the two corresponding oxazolines were assigned as *cis* in a NOESY experiment. Moreover, the signals of the two nitrogens on these two *cis* oxazolines were detected at –204.3 and –217.7 ppm in the $^{1}H–^{15}N$ HMBC spectrum. Intriguingly, both **2.7** and **2.8** showed through-bond correlation between the C*H*Cl_2 ligand and *cis*/*trans* oxazoline nitrogens, however, the correlation between the η^1-C_3H_5 group and oxazoline nitrogens for **2.6** could not be observed.

The high diastereoselectivity for eq 2.7 implies that the oxidative addition chemistry for **2.2** would not proceed *via* radical mechanism. Indeed, the rate and the selectivity do not change when the reactions are performed in dark although the attempts to determine the rate law have been hindered by insufficiently separated resonances in the ^{1}H NMR spectrum. Yet, the similar reaction between $Tp^{Me2Cl}Rh(CO)_2$ and $CHCl_3$ has been proposed to undergo thermally *via* S_N2-type mechanism.[15b] Besides, the carbonyl group of **2.2** could be substituted by the phosphite (eq 2.3), which suggests that CO dissociation could occur prior to rhodium oxidation addition. While the absolute configuration of **2.8** remains unknown, the synergistic effect of the three chiral oxazolines provide an excellent control for the stereochemistry of the rhodium center during the formation of the SP and/or TBP intermediates (transition states).

Conclusion

Though the diverse regioselectivity of $Tp^*M(CO)_2$ (M = Rh or Ir) toward $HBF_4 \cdot Et_2O$ has been documented that $Tp^*Ir(CO)_2$ reacts with the acid to give the metal hydride,[10] our previously reported To^M and To^P iridium compounds have not given any oxidative chemistry on the metal center but underwent N-methylation and N-protonation exclusively.[12b, c] Instead, here we report that a combination of a fundamental study of both regioselectivity and stereoselectivity could be accomplished within a single system. Both Tl[To^M] and **2.1** are proved to be superior ligand transfer agents for synthesizing rhodium complexes and this would prompt us to further explore the reactivities of both compounds, which will be included in the next chapter. The regioselectivity of **2.2** is ascribed to the nature of electrophiles, relative bonding capability of OTf^- versus Br^- and Cl^- and electron donating ability of To^M and To^P versus Tp family. The ultra-high diastereoselectivity of **2.7** lays a foundation for future applications to asymmetric catalysis.

Experimental

General Procedures. All reactions were performed under an inert atmosphere using standard Schlenk techniques or in a glovebox unless otherwise indicated. Dry, oxygen-free solvents were used throughout. Benzene, toluene, pentane, diethyl ether, and tetrahydrofuran were degassed by sparging with nitrogen, filtered through activated alumina columns, and stored under N_2. Benzene-d_6 and toluene-d_8 were vacuum transferred from Na/K alloy and stored under N_2 in the glovebox. All organic reagents were purchased from Aldrich. Chloroform was distilled from calcium hydride, and allyl bromide was distilled prior to use. Li[To^M],[12a] Li[To^P],[12b] [Rh(μ-Cl)$(CO)_2]_2$,[20] were prepared by published procedures. ^1H, ^{11}B, and $^{13}C\{^1H\}$

NMR spectra were collected on Bruker DRX-400 and Avance II-700 spectrometers. ^{1}H and $^{13}C\{^{1}H\}$ resonances were assigned using standard 2D methods, including COSY, ^{1}H–^{13}C HMQC and ^{1}H–^{13}C HMBC experiments. ^{15}N chemical shifts were determined by ^{1}H–^{15}N HMBC experiments on a Bruker Avance II 700 spectrometer with a Bruker Z-gradient inverse TXI $^{1}H/^{13}C/^{15}N$ 5mm cryoprobe. ^{15}N chemical shifts were originally referenced to liquid NH_3 and recalculated to the CH_3NO_2 chemical shift scale by adding –381.9 ppm. ^{11}B NMR spectra were referenced to an external sample of $BF_3{\cdot}Et_2O$. Elemental analysis was performed using a Perkin-Elmer 2400 Series II CHN/S by the Iowa State Chemical Instrumentation Facility. X-ray diffraction data was collected on a Bruker APEX2 CCD Diffractometer.

Tl[To^{P}] (2.1). A suspension of Li[To^{P}] (1.38 g, 3.20 mmol) and Tl[OAc] (1.26 g, 4.78 mmol) was stirred in CH_2Cl_2 (100 mL) at room temperature overnight. The reaction mixture was then filtered to remove excess Tl[OAc] and Li[OAc], and the filtrate was evaporated under reduced pressure. The residue was crystallized from a concentrated diethyl ether solution at -80 °C to afford **2.1** as a white powder (1.26 g, 2.00 mmol, 62.6%). ^{1}H NMR (benzene-d_6, 400 MHz): δ 8.28 (d, 2 H, $^{3}J_{HH}$ = 7.2 Hz, *ortho*-C_6H_5), 7.57 (t, 2 H, $^{3}J_{HH}$ = 7.6 Hz, *meta*-C_6H_5), 7.35 (t, 1 H, $^{3}J_{HH}$ = 7.2 Hz, *para*-C_6H_5), 3.69 (m, 3 H, CNC(CHMe$_2$)*H*CH$_2$O), 3.51 (m, 6 H, CNC(CHMe$_2$)HC*H*$_2$O), 1.49 (m, 3 H, CNC(C*H*Me$_2$)HCH$_2$O), 0.76 (d, 9 H, CNC(CH*Me*$_2$)HCH$_2$O), 0.67 (d, 9 H, CNC(CH*Me*$_2$)HCH$_2$O). $^{13}C\{^{1}H\}$ NMR (benzene-d_6, 150 MHz): δ 136.46 (*ortho*-C_6H_5), 127.03 (*meta*-C_6H_5), 125.52 (*para*-C_6H_5), 71.51 (CNC(CHMe$_2$)H*C*H$_2$O), 70.07 (CN*C*(CHMe$_2$)HCH$_2$O), 33.25 (CNC(*C*HMe$_2$)HCH$_2$O), 19.42 (CNC(CH*Me*$_2$)HCH$_2$O), 18.65 (CNC(CH*Me*$_2$)HCH$_2$O). ^{11}B NMR (benzene-d_6, 128

MHz): δ −19.2. IR (KBr, cm^{-1}): ν 3046 (m), 2955 (s), 1590 (s, ν_{CN}), 1465 (m), 1430 (w), 1387 (w), 1367 (w), 1263 (w), 1166 (m), 1111 (m), 1036 (w), 969 (m), 735 (w), 730 (w), 702 (m). Anal. Calcd. for $C_{24}H_{35}BN_3O_3Tl$: C, 45.85; H, 5.61; N, 6.68. Found: C, 46.08; H, 5.53; N, 6.61. Mp 70–73 °C, dec.

$To^MRh(CO)_2$ (2.2). Benzene (50 mL) was added to a solid mixture of $Tl[To^M]$ (0.63 g, 1.07 mmol) and $[Rh(\mu\text{-}Cl)(CO)_2]_2$ (0.21 g, 0.54 mmol). The resulting mixture was allowed to stir at room temperature for 24 h and then filtered. The solvent was evaporated under vacuum. The residue was dissolved in diethyl ether, stirred for 2 h, and was then filtered. The filtrate was evaporated to dryness to give **2.2** as a pale green solid in excellent yield (0.53 g, 0.98 mmol, 92%). X-ray quality crystals were obtained from slow evaporation of a diethyl ether solution at −30 °C. ^{1}H NMR (benzene-d_6, 400 MHz): δ 8.08 (d, 2 H, $^3J_{HH}$ = 7.2 Hz, *ortho*-C_6H_5), 7.51 (t, 2 H, $^3J_{HH}$ = 7.6 Hz, *meta*-C_6H_5), 7.34 (t, 1 H, $^3J_{HH}$ = 7.2 Hz, *para*-C_6H_5), 3.50 (s, 6 H, $CNCMe_2CH_2O$), 1.07 (s, 18 H, $CNCMe_2CH_2O$). $^{13}C\{^1H\}$ NMR (benzene-d_6, 150 MHz): δ 188.42 (d, CO, $^1J_{RhC}$ = 66.6 Hz), 135.80 (*ortho*-C_6H_5), 127.40 (*meta*-C_6H_5), 126.12 (*para*-C_6H_5), 79.78 ($CNCMe_2CH_2O$), 67.60 ($CNCMe_2CH_2O$), 28.70 ($CNCMe_2CH_2O$). ^{11}B NMR (benzene-d_6, 128 MHz): δ −17.3. $^{15}N\{^1H\}$ NMR (benzene-d_6, 71 MHz): δ −163.1. IR (KBr, cm^{-1}): ν 2966 (s), 2933 (m), 2070 (s, ν_{CO}), 2048 (m, ν_{CO}), 2010 (s, ν_{CO}), 1997 (s, ν_{CO}), 1968 (m, ν_{CO}), 1616 (m, ν_{CN}), 1571 (s, ν_{CN}), 1361 (m), 1288 (m), 1204 (m), 965 (m). IR (CH_2Cl_2, cm^{-1}): ν 2963 (m), 2927 (w), 2069 (s, ν_{CO}), 2055 (w sh, ν_{CO}) 2010 (w), 1994 (s, ν_{CO}), 1967 (w), 1616 (w), 1566 (m, ν_{CN}), 1461 (w), 1360 (w), 1289 (w), 1202 (m), 963 (m), 736 (m), 706 (m). Anal. Calcd. for $C_{23}H_{29}BRhN_3O_5$: C, 51.04; H, 5.40; N, 7.76. Found: C, 51.51; H, 5.41; N, 7.76. Mp 204–206 °C, dec.

To^{P}Rh(CO)$_2$ (2.3). A 20 mL vial was charged with **2.1** (0.21 g, 0.34 mmol), [Rh(μ-Cl)(CO)$_2$]$_2$ (0.07 g, 0.17 mmol), and benzene (10 mL). The reaction mixture was allowed to stir at room temperature for 6 h and was then filtered. All volatiles were removed to afford **2.3** as a dark green solid (0.19 g, 0.33 mmol, 95%). ^{1}H NMR (benzene-d_6, 400 MHz): δ 8.15 (d, 2 H, $^3J_{HH}$ = 7.2 Hz, *ortho*-C$_6$H$_5$), 7.44 (t, 2 H, $^3J_{HH}$ = 7.4 Hz, *meta*-C$_6$H$_5$), 7.25 (t, 1 H, $^3J_{HH}$ = 7.4 Hz, *para*-C$_6$H$_5$), 3.64 (m, 9 H, overlapping CNC(CHMe$_2$)*H*C*H*$_2$O), 2.02 (m, 3 H, CNC(C*H*Me$_2$)HCH$_2$O), 0.72 (d, 9 H, CNC(CH*Me*$_2$)HCH$_2$O), 0.66 (d, 9 H, CNC(CH*Me*$_2$)HCH$_2$O). ^{13}C{^{1}H} NMR (benzene-d_6, 150 MHz): δ 186.11 (d, CO, $^1J_{RhC}$ = 65.0 Hz), 134.86 (*ortho*-C$_6$H$_5$), 127.68 (*meta*-C$_6$H$_5$), 126.28 (*para*-C$_6$H$_5$), 74.51 (CNC(CHMe$_2$)H*C*H$_2$O), 67.69 (CN*C*(CHMe$_2$)HCH$_2$O), 32.00 (CNC(*C*HMe$_2$)HCH$_2$O), 19.28 (CNC(CH*Me*$_2$)HCH$_2$O), 15.85 (CNC(CH*Me*$_2$)HCH$_2$O). ^{11}B NMR (benzene-d_6, 128 MHz): δ −17.3 ^{15}N{^{1}H} NMR (benzene-d_6, 71 MHz): δ −182.8. IR (KBr, cm^{-1}): ν 2959 (m), 2898 (w), 2873 (w), 2072 (s, ν_{XO}), 2002 (σ, ν_{CO}), 1572 (m, ν_{CN}), 1480 (w), 1464 (w), 1366 (w), 1210 (m), 1180 (w), 1134 (w), 1118 (w), 983 (m), 961 (m), 737 (w). IR (CH$_2$Cl$_2$, cm^{-1}): ν 2961 (w), 2077 (s, ν_{CO}), 2007 (s, ν_{CO}), 1575 (m, ν_{CN}), 1481 (w), 1366 (w), 1277 (w), 1209 (w), 1118 (w). Anal. Calcd. for C$_{26}$H$_{35}$BRhN$_3$O$_5$: C, 53.54; H, 6.05; N, 7.20. Found: C, 53.91; H, 5.54; N, 6.99. Mp 80–82 °C, dec.

To^{M}Rh(CO)[P(OMe)$_3$] (2.4). P(OMe)$_3$ (22 μL, 0.19 mmol) and **2.2** (100 mg, 0.185 mmol) were dissolved in benzene (10 mL) and allowed to stir for 10 min. All volatiles were removed under vacuum to give To^{M}Rh(CO)[P(OMe)$_3$] as a pale yellow solid in quantitative yield. X-ray quality crystals were obtained by slow diffusion of pentane into a concentrated toluene solution at –80 °C. ^{1}H NMR (dichloromethane-d_2, 400 MHz): δ 7.27 (d, 2 H, $^3J_{HH}$ =

6.8 Hz, *ortho*-C_6H_5), 7.13 (t, 2 H, $^3J_{HH}$ = 6.8 Hz, *meta*-C_6H_5), 7.03 (t, 1 H, $^3J_{HH}$ = 6.4 Hz, *para*-C_6H_5), 3.88 (s, 6 H, $CNCMe_2CH_2O$), 3.54 (d, 9 H, $^3J_{PH}$ = 12.4 Hz, $P(OMe)_3$), 1.27 (s, 18 H, $CNCMe_2CH_2O$). $^{13}C\{^1H\}$ NMR (benzene-d_6, 175 MHz): δ 189.63 (dd, CO, $^1J_{RhC}$ = 69.8 Hz, $^2J_{PC}$ = 27.5 Hz), 135.68 (*ortho*-C_6H_5), 127.20 (*meta*-C_6H_5), 125.46 (*para*-C_6H_5), 78.98 ($CNCMe_2CH_2O$), 68.16 ($CNCMe_2CH_2O$), 51.82 ($P(OMe)_3$), 28.84 ($CNCMe_2CH_2O$). ^{11}B NMR (benzene-d_6, 128 MHz): δ –16.4. $^{31}P\{^1H\}$ NMR (benzene-d_6, 162 MHz): δ –90.0 (d, $^1J_{RhP}$ = 247.7 Hz). IR (KBr, cm^{-1}): ν 2966 (s), 1995 (s, ν_{CO}), 1965 (m, ν_{CO}), 1610 (m, ν_{CN}), 1576 (s, ν_{CN}), 1462 (m), 1368 (m), 1279 (m), 1120 (s), 1017(s), 970 (m). Anal. Calcd. for $C_{25}H_{38}BRhN_3O_7P$: C, 47.12; H, 6.01; N, 6.59. Found: C, 47.17; H, 5.93; N, 6.52. Mp 159–163 °C, dec.

[{*N*-Me-κ^2-To^M}Rh(CO)$_2$]OTf (2.5). A benzene solution of **2.2** (0.052 g, 0.096 mmol) and MeOTf (0.063 g, 0.35 mmol) was stirred for 30 min and then evaporated to dryness. The residue was crystallized from a benzene/pentane solution at room temperature to give green X-ray quality crystals (0.038 g, 0.053 mmol, 55%). Trituration of the crystals with pentane provides a white powder without loss in yield. ^1H NMR (dichloromethane-d_2, 400 MHz): δ 7.30 (m, 3 H, *para*- and *meta*-C_6H_5), 7.14 (d, 2 H, $^3J_{HH}$ = 6.4 Hz, *ortho*-C_6H_5), 4.48 (s, 2 H, $CN(Me)CMe_2CH_2O$), 4.29 (d, 2 H, $^3J_{HH}$ = 9.0 Hz, $CN(Rh)CMe_2CH_2O$), 4.25 (d, 2 H, $^3J_{HH}$ = 9.0 Hz, $CN(Rh)CMe_2CH_2O$), 2.90 (s, 3 H, NCH_3), 1.51 (s, 6 H, $CN(Me)CMe_2CH_2O$), 1.44 (s, 6 H, $CN(Rh)CMe_2CH_2O$), 1.41 (s, 6 H, $CN(Rh)CMe_2CH_2O$). $^{13}C\{^1H\}$ NMR (dichloromethane-d_2, 175 MHz): δ 183.85 (d, CO, $^1J_{RhC}$ = 68.3 Hz), 133.35 (*ortho*-C_6H_5), 128.77 (*meta*-C_6H_5), 127.76 (*para*-C_6H_5), 121.54 (q, $^1J_{FC}$ = 319 Hz, OSO_2CF_3), 82.19 ($CN(Me)CMe_2CH_2O$), 81.25 ($CN(Rh)CMe_2CH_2O$), 69.21 ($CN(Rh)CMe_2CH_2O$), 67.30

(CN(Me)*C*Me$_2$CH$_2$O), 30.16 (N*C*H$_3$), 28.65 (CN(Rh)C*Me*$_2$CH$_2$O), 28.25 (CN(Rh)C*Me*$_2$CH$_2$O), 24.45 (CN(Me)C*Me*$_2$CH$_2$O). ^{11}B NMR (dichloromethane-d_2, 128 MHz): δ −17.3. ^{15}N{^{1}H} NMR (dichloromethane-d_2, 71 MHz): δ −179.7 (NRh), −211.0 (NMe). IR (KBr, cm^{-1}): ν 3074 (m), 2971 (s), 2083 (s, ν_{CO}), 2012 (s, ν_{CO}), 1580 (s, ν_{CN}), 1551 (m, ν_{CN}), 1462 (s), 1434 (m), 1390 (m), 1372 (m), 1362 (m), 1325 (m), 1262 (s), 1224 (s), 1205 (s), 1157 (s), 1031 (s), 998 (m), 964 (s), 748 (m), 736 (m), 710 (m). Anal. Calcd. for $C_{24}H_{32}N_3O_8SF_3RhB$: C, 41.58; H, 4.65; N, 6.06. Found: C, 42.00; H, 4.56; N, 5.70. Mp 132−134 °C, dec.

(κ^3-To^M)Rh(η^1-C$_3$H$_5$)Br(CO) (2.6). Excess allyl bromide (1.9 mL) and **2.2** (0.114 g, 0.211 mmol) were allowed to react in benzene for 5 h at room temperature. The solution was filtered, the volatiles were evaporated, and the solid residue was crystallized from a concentrated acetonitrile solution at −30 °C overnight to give a yellow solid (0.063 g, 0.098 mmol, 47%). ^{1}H NMR (benzene-d_6, 400 MHz, *cis*- and *trans*- designations for oxazoline rings are given with respect to η^1-C$_3$H$_5$ moiety): δ 8.25 (d, 2 H, $^3J_{HH}$ = 7.2 Hz, *ortho*-C$_6$H$_5$), 7.53 (t, 2 H, $^3J_{HH}$ = 7.2 Hz, *meta*-C$_6$H$_5$), 7.35 (t, 1 H, $^3J_{HH}$ = 7.2 Hz, *para*-C$_6$H$_5$), 6.99 (m, 1 H, RhCH$_2$C*H*CH$_2$), 5.58 (d, 1 H, $^3J_{HH}$ = 16.8 Hz, RhCH$_2$CHC*H*$_2$), 5.24 (d, 1 H, $^3J_{HH}$ = 9.6 Hz, RhCH$_2$CHC*H*$_2$), 4.57 (br, 1 H, RhC*H*$_2$CHCH$_2$), 3.66 (d, 1 H, $^2J_{HH}$ = 8.4 Hz, *cis*-CNCMe$_2$C*H*$_2$O), 3.64 (br, 1 H, RhC*H*$_2$CHCH$_2$), 3.40 (d, 1 H, $^2J_{HH}$ = 8.0 Hz, *cis*-CNCMe$_2$C*H*$_2$O), 3.35 (d, 1 H, $^2J_{HH}$ = 8.4 Hz, *cis*-CNCMe$_2$C*H*$_2$O), 3.24 (d, 1 H, $^2J_{HH}$ = 8.0 Hz, *cis*-CNCMe$_2$C*H*$_2$O), 3.21 (s, 2 H, *trans*-CNCMe$_2$C*H*$_2$O), 1.50 (s, 3 H, *cis*-CNC*Me*$_2$CH$_2$O), 1.44 (s, 3 H, *cis*-CNC*Me*$_2$CH$_2$O), 1.33 (s, 3 H, *cis*-CNC*Me*$_2$CH$_2$O), 1.31 (s, 3 H, *cis*-CNC*Me*$_2$CH$_2$O), 1.04 (s, 3 H, *trans*-CNC*Me*$_2$CH$_2$O), 0.81 (s, 3 H, *trans*-

CNC*Me*$_2$CH$_2$O). ^{13}C{^{1}H} NMR (benzene-d_6, 175 MHz, *cis*- and *trans*- designations for oxazoline groups are given with respect to η^1-C_3H_5 moiety): δ 186.45 (d, CO, $^1J_{RhC}$ = 59.5 Hz), 148.03 (RhCH$_2$*C*HCH$_2$), 136.34 (*ortho*-C_6H_5), 127.32 (*meta*-C_6H_5), 126.44 (*para*-C_6H_5), 112.97 (RhCH$_2$CH*C*H$_2$), 81.94 (*cis*-CNCMe$_2$*C*H$_2$O), 81.22 (*cis*-CNCMe$_2$*C*H$_2$O), 80.62 (*trans*-CNCMe$_2$*C*H$_2$O), 73.06 (*cis*-CN*C*Me$_2$CH$_2$O), 70.65 (*cis*-CN*C*Me$_2$CH$_2$O), 69.30 (*trans*-CN*C*Me$_2$CH$_2$O), 29.06 (*cis*-CNC*Me*$_2$CH$_2$O), 28.88 (*cis*-CNC*Me*$_2$CH$_2$O), 27.19 (*cis*-CNC*Me*$_2$CH$_2$O), 27.10 (*trans*-CNC*Me*$_2$CH$_2$O), 26.62 (*trans*-CNC*Me*$_2$CH$_2$O), 25.92 (*cis*-CNC*Me*$_2$CH$_2$O), 20.53 (d, Rh*C*H$_2$CHCH$_2$, $^1J_{RhC}$ = 15.8 Hz). ^{11}B NMR (benzene-d_6, 128 MHz): δ –18.0. ^{15}N{^{1}H} NMR (benzene-d_6, 71 MHz): δ –163.5 (*cis*), –187.8 (*cis*), –203.5 (*trans*). IR (KBr, cm^{-1}): ν 2967 (m), 2930 (m), 2058 (s, ν_{CO}), 1582 (s, ν_{CN}), 1462 (m), 1387 (w), 1367 (m), 1290 (m), 1203 (m), 1003 (m), 968 (m). Anal. Calcd. for $C_{25}H_{34}N_3O_4RhBBr$: C, 47.35; H, 5.40; N, 6.63. Found: C, 47.09; H, 5.39; N, 6.58. Mp 174–178 °C, dec.

(κ^3-To^M)Rh(CHCl$_2$)Cl(CO) (2.7). A solution of **2.2** (0.107 g, 0.20 mmol) in $CHCl_3$ (30 mL) was degassed by three freeze-pump-thaw cycles and then heated at 60 °C for 18 h. The reaction mixture was allowed to cool to ambient temperature, and then it was filtered. The solvent was removed from the filtrate under reduced pressure, and the residue was extracted with toluene (10 mL) and evaporated to dryness. The resulting solid was washed with CH_3CN (ca. 1 mL) at –30 °C to give an off-white solid (0.054 g, 0.080 mmol, 43%). ^{1}H NMR (benzene-d_6, 400 MHz, *cis*- and *trans*- designations for oxazoline rings are given with respect to $CHCl_2$ moiety): δ 8.18 (d, 2 H, $^3J_{HH}$ = 7.2 Hz, *ortho*-C_6H_5), 7.81 (d, 2 H, $^2J_{RhH}$ = 3.2 Hz, C*H*Cl$_2$), 7.50 (t, 2 H, $^3J_{HH}$ = 7.6 Hz, *meta*-C_6H_5), 7.34 (t, 1 H, $^3J_{HH}$ = 7.2 Hz, *para*-C_6H_5), 3.60 (d, 1 H, $^2J_{HH}$ = 8.4 Hz, *cis*-CNCMe$_2$C*H*$_2$O), 3.33 (m, 5 H, CNCMe$_2$C*H*$_2$O), 1.60,

(s, 3 H, *trans*-CNC*Me*$_2$CH$_2$O), 1.51 (s, 3 H, *cis*-CNC*Me*$_2$CH$_2$O), 1.29 (s, 3 H, *cis*-CNC*Me*$_2$CH$_2$O), 1.28 (s, 3 H, *cis*-CNC*Me*$_2$CH$_2$O), 1.11 (s, 3 H, *cis*-CNC*Me*$_2$CH$_2$O), 0.63 (s, 3 H, *trans*-CNC*Me*$_2$CH$_2$O). ^{13}C{^{1}H} NMR (benzene-d_6, 175 MHz): δ 188.42 (d, CO, $^1J_{RhC}$ = 59.5 Hz), 135.19 (*ortho*-C$_6$H$_5$), 127.38 (*meta*-C$_6$H$_5$), 126.70 (*para*-C$_6$H$_5$), 82.04 (*cis*-CNCMe$_2$*C*H$_2$O), 80.77 (*cis*-CNCMe$_2$*C*H$_2$O), 79.76 (*trans*-CNCMe$_2$*C*H$_2$O), 73.08 (*cis*-CN*C*Me$_2$CH$_2$O), 71.41 (*cis*-CN*C*Me$_2$CH$_2$O), 68.88 (*trans*-CN*C*Me$_2$CH$_2$O), 63.74 (d, *C*HCl$_2$, $^1J_{RhC}$ = 26.3 Hz), 28.87 (*cis*-CNC*Me*$_2$CH$_2$O), 28.71 (*cis*-CNC*Me*$_2$CH$_2$O), 27.48 (*trans*-CNC*Me*$_2$CH$_2$O), 26.96 (cis-CNC*Me*$_2$CH$_2$O), 23.68 (*trans*-CNC*Me*$_2$CH$_2$O), 21.08 (*cis*-CNC*Me*$_2$CH$_2$O). ^{11}B NMR (benzene-d_6, 128 MHz): δ −17.8. ^{15}N{^{1}H} NMR (benzene-d_6, 71 MHz): δ −177.6 (cis), −187.8 (*cis*), −198.0 (*trans*). IR (KBr, cm^{-1}): ν 3076 (m), 3042 (m), 2985 (s), 2969 (s), 2890 (s), 2088 (s, ν_{CO}), 2042 (w), 2037 (w), 1575 (s, ν_{CN}), 1548 (m), 1496 (m), 1464 (s), 1433 (m), 1388 (s), 1358 (s), 1293 (s), 1273 (s), 1251 (s), 1199 (s), 1155 (s), 1114(s), 1036(m), 1024 (m), 957 (s), 933 (s), 891 (m), 800 (m), 785 (m). Anal. Calcd. for $C_{23}H_{30}BN_3O_4Cl_3BRh$: C, 43.67; H, 4.78; N, 6.64. Found: C, 43.20; H, 4.52; N, 6.46. Mp 156−159 °C, dec.

(κ^3-To^P)Rh(CHCl$_2$)Cl(CO) (2.8). A solution of To^{P}Rh(CO)$_2$ (0.102 g, 0.175 mmol) in CHCl$_3$ (20 mL) was degassed by three freeze-pump-thaw cycles and then allowed to stir overnight at room temperature. All volatiles were evaporated and the residue was purified by silica gel column chromatography, eluting with hexane/ethyl acetate (85:15) to yield a yellow solid (0.060 g, 0.089 mmol, 51%). ^{1}H NMR (CDCl$_3$, 400 MHz, *cis*- and *trans*- designations for oxazoline rings are given with respect to CHCl$_2$ moiety): δ 7.65 (d, 2 H, $^3J_{HH}$ = 7.6 Hz, *ortho*-C$_6$H$_5$), 7.31 (t, 2 H, $^3J_{HH}$ = 7.2 Hz, *meta*-C$_6$H$_5$), 7.25 (t, 1 H, $^3J_{HH}$ = 7.2 Hz, *para*-C$_6$H$_5$),

7.11 (d, 2 H, $^{2}J_{RhH}$ = 3.2 Hz, C*H*Cl$_2$), 4.95 (m, 1 H, *cis*-CNC(CHMe$_2$)*H*CH$_2$O), 4.84 (m, 1 H, *cis*-CNC(CHMe$_2$)*H*CH$_2$O), 4.38 (m, 4 H, overlapping *cis*- and *trans*-CNC(CHMe$_2$)HC*H*$_2$O), 4.28 (t, 1 H, $^{2}J_{HH}$ = 9.6 Hz, *trans*-CNC(CHMe$_2$)HC*H*$_2$O), 4.09 (t, 1 H, $^{2}J_{HH}$ = 9.6 Hz, *cis*-CNC(CHMe$_2$)HC*H*$_2$O), 4.07 (m, 1 H, *trans*-CNC(CHMe$_2$)*H*CH$_2$O), 2.84 (m, 1 H, *trans*-CNC(C*H*Me$_2$)HCH$_2$O), 2.37 (m, 1 H, *cis*-CNC(C*H*Me$_2$)HCH$_2$O), 2.17 (m, 1 H, *cis*-CNC(C*H*Me$_2$)HCH$_2$O), 1.02 (d, 3 H, $^{3}J_{HH}$ = 6.8 Hz, *cis*-CNC(CH*Me*$_2$)HCH$_2$O), 0.92 (d, 3 H, $^{3}J_{HH}$ = 6.8 Hz, *cis*-CNC(CH*Me*$_2$)HCH$_2$O), 0.86 (d, 3 H, $^{3}J_{HH}$ = 7.2 Hz, *trans*-CNC(CH*Me*$_2$)HCH$_2$O), 0.75 (d, 3 H, $^{3}J_{HH}$ = 6.4 Hz, *cis*-CNC(CH*Me*$_2$)HCH$_2$O), 0.65 (d, 3 H, $^{3}J_{HH}$ = 6.8 Hz, *cis*-CNC(CH*Me*$_2$)HCH$_2$O), 0.56 (d, 3 H, $^{3}J_{HH}$ = 6.8 Hz, *trans*-CNC(CH*Me*$_2$)HCH$_2$O). ^{13}C{^{1}H} NMR (CDCl$_3$, 175 MHz): δ 179.71 (d, CO, $^{1}J_{RhC}$ = 59.5 Hz), 134.84 (*ortho*-C$_6$H$_5$), 127.22 (*meta*-C$_6$H$_5$), 126.63 (*para*-C$_6$H$_5$), 71.73 (*trans*-CN*C*(CHMe$_2$)HCH$_2$O), 70.71 (*cis*-CNC(CHMe$_2$)H*C*H$_2$O), 70.25 (*trans*-CNC(CHMe$_2$)H*C*H$_2$O), 69.69 (*cis*-CNC(CHMe$_2$)H*C*H$_2$O), 68.42 (*cis*-CN*C*(CHMe$_2$)HCH$_2$O), 65.67 (d, *C*HCl$_2$, $^{1}J_{RhC}$ = 28.0 Hz), 65.14 (*cis*-CN*C*(CHMe$_2$)HCH$_2$O), 29.17 (*cis*-CNC(*C*HMe$_2$)HCH$_2$O), 29.01 (*cis*-CNC(*C*HMe$_2$)HCH$_2$O), 28.64 (*trans*-CNC(*C*HMe$_2$)HCH$_2$O), 20.03 (*cis*-CNC(CH*Me*$_2$)HCH$_2$O), 19.17 (*cis*-CNC(CH*Me*$_2$)HCH$_2$O), 18.81 (*trans*-CNC(CH*Me*$_2$)HCH$_2$O), 14.71 (*cis*-CNC(CH*Me*$_2$)HCH$_2$O), 14.00 (*cis*-CNC(CH*Me*$_2$)HCH$_2$O), 13.82 (*trans*-CNC(CH*Me*$_2$)HCH$_2$O). ^{11}B NMR (CDCl$_3$, 128 MHz): δ –18.1. ^{15}N{^{1}H} NMR (CDCl$_3$, 71 MHz): δ –194.2 (*trans*-C*N*C(CHMe$_2$)HCH$_2$O), –204.3 (*cis*-C*N*C(CHMe$_2$)HCH$_2$O), –217.7 (*cis*-C*N*C(CHMe$_2$)HCH$_2$O). IR (KBr, cm^{-1}): ν 3001 (w), 2962 (m), 2929 (m), 2872 (m), 2092 (s, $\nu_{C=O}$), 1590 (s, $\nu_{C=N}$), 1479 (w), 1463 (w), 1372 (w), 1364 (w), 1223 (m). Anal. Calcd. for C$_{26}$H$_{36}$BN$_3$O$_4$RhCl$_3$: C, 46.29; H, 5.38; N, 6.23; Found: C, 46.11; H, 5.03; N, 5.99. Mp 116–118 °C, dec.

References

(1) Collman, J. P.; Hegedus, L. S.; Norton, J. R.; Finke, R. G. Eds. *Principles and Applications of Organotransition Metal Chemistry*; University Science Books: Mill Valley, CA, 1987.

(2) Crabtree, R. Ed. *The Organometallic Chemistry of the Transition Metals,* 3rd ed.; Wiley-Interscience John Wiley & Sons, INC., 2001; pp152-161.

(3) (a) Forster, D. *Adv. Organomet. Chem.* 1**979**, *17*, 255-267. (b) Howard, M. J.; Jones, M. D.; Roberts, M. S.; Taylor, S. A. *Catal. Today* **1993**, *18*, 325-354. (c) Haynes, A.; Mann, B. E.; Morris, G. E.; Maitlis, P. M. *J. Am. Chem. Soc.* **1993**, *115*, 4093-4100. (d) Sunley, G. J.; Watson, D. J. *Catal. Today* **2000**, *58*, 293-307.

(4) Janka, M.; Atesin, A. C.; Fox, D. J.; Flaschenriem, C.; Brennessel, W. W.; Eisenberg, R. *Inorg. Chem.* **2006**, *45*, 6559-6561.

(5) (a) Doppiu, A.; Englert, U.; Salzer, A. *Chem. Commun.* **2004**, 2166-2167. (b) Doppiu, A.; Englert, U.; Peters, V.; Salzer, A. *Inorg. Chim. Acta* **2004**, *357*, 1773-1780.

(6) Kataoka, Y.; Nakagawa, Y.; Shibahara, A.;Yamagata, T.; Mashima, K.; Tani, K. *Organometallics* **2004**, *23*, 2095–2099.

(7) Keyes, M. C.; Young, V. G., Jr.; Tolman, W. B. *Organometallics* **1996**, *15*, 4133– 4140.

(8) Mobley, T. A.; Bergman, R. G. J. Am. Chem. Soc. **1998**, *120*, 3253–3254.

(9) Henderson, R. A. *Angew. Chem., Int. Ed.* **1996**, *35*, 946-967.

(10) Ball, R. G.; Ghosh, C. K.; Hoyano, J. K.; McMaster, A. D.;Graham, W. A. G. *J. Chem. Soc., Chem. Commun.* **1989**, 341–342.

(11) (a) Chauby, V.; Daran, J.-C.; Berre, C. S.-L; Malbosc, F.; Kalck, P.; Gonzalez, O. D.; Haslam, C. E.; Haynes, A. *Inorg. Chem.* **2002**, *41*, 3280-3290.

(12) (a) Dunne, J. F.; Su, J. C.; Ellern, A.; Sadow, A. D. *Organometallics* **2008**, *27*, 2399-2401. (b) Baird, B.; Pawlikowski, A. V.; Su, J.; Wiench, J. W.; Pruski, M.; Sadow, A. D. *Inorg. Chem.* **2008**, *47*, 10208-10210. (c) Pawlikowski, A. V.; Gray, T. S.; Schoendorff, G.; Baird, B.; Ellern, A.; Windus, T. L.; Sadow, A. D. *Inorg. Chim. Acta* **2009**, *362*, 4517-4525.

(13) Ho, H.-A.; Dunne, J. F.; Ellern, A.; Sadow, A. D. *Organometallics* **2010**, *29*, 4105-4114.

(14) (a) Bucher, U. E.; Currao, A.; Nesper, R.; Rüegger, H.; Venanzi, L. M.; Younger, E., *Inorg. Chem.* **1995**, *34*, 66-74. (b) Bucher, U. E.; Fässler, T. F.; Hunziker, M.; Nesper, R.; Rüegger, H.; Venanzi, L. M., *Gazz. Chim. Ital.* **1995**, *125*, 181-188. (c) Del Ministro, E.; Renn, O.; Rüegger, H.; Venanzi, L. M.; Burckhardt, U.; Gramlich, V., *Inorg. Chim. Acta* **1995**, *240*, 631-639. (d) Albinati, A.; Bovens, M.; Rüegger, H.; Venanzi, L. M., *Inorg. Chem.* **1997**, *36*, 5991-5999.

(15) (a) Malbosc, F.; Chauby, V.; Berre, C. S.-L.; Etienne, M.; Daran, J.-C.; Kalck, P., *Eur. J. Inorg. Chem.* **2001**, 2689-2697. (b) Teuma, E.; Malbosc, F.; Etienne, M.; Daran, J.-C.; Kalck, P. *J. Organomet. Chem.* **2004**, *689*, 1763-1765.

(16) Slugovc, C.; Padilla-Martínez, I.; Sirol, S.; Carmona, E. *Coord. Chem. Rev.* **2001**, *213*, 129-157.

(17) (a) Connelly, N. G.; Emslie, D. J. H.; Metz, B.; Orpen, A. G.; Quayle, M. J., *Chem. Commun.* **1996**, 2289-2290. (b) Connelly, N. G.; Emslie, D. J. H.; Geiger, W. E.; Hayward, O. D.; Linehan, E. B.; Orpen, A. G.; Quayle, M. J.; Rieger, P. H., *J. Chem. Soc., Dalton Trans.* **2001**, 670-683.

(18) Ikeda, S.; Maruyama, Y.; Ozawa, F., *Organometallics* **1998**, *17*, 3770-3774.

(19) Vetter, A. J.; Rieth, R. D.; Brennessel, W. W.; Jones, W. D., *J. Am. Chem. Soc.* **2009**, *131*, 10742-10752.

(20) McCleverty, J. A. and Wilkinson, G. *Inorg. Synth.* **1966**, *8,* 211.

Chapter 3. Allylic C–H bond activation and functionalization mediated by tris(oxazolinyl)phenylborato rhodium(I) compounds

Modified from a paper published in *Dalton Transactions*[†]

Hung-An Ho,[‡] Tristan S. Gray,[¶] Benjamin Baird, Arkady Ellern, Aaron D. Sadow[*]

Abstract

Allylic C–H bond oxidative addition reactions, mediated by tris(oxazolinyl)phenylborato rhodium(I), provide the first step in a hydrocarbon functionalization sequence. The bond activation products $To^{M}RhH(\eta^3\text{-}C_8H_{13})$ (**3.1**), $To^{M}RhH(\eta^3\text{-}C_3H_5)$ (**3.2**) and $To^{M}RhH(\eta^3\text{-}C_3H_4Ph)$ (**3.3**) are synthesized by reaction of $Tl[To^{M}]$ and the corresponding metal olefin chloride dimers. Characterization of these rhodium allyl hydride complexes includes $^{1}H–^{15}N$ heteronuclear correlation NMR experiments that reveal through-metal magnetization transfer between metal-hydride and the *trans*-coordinated oxazoline nitrogen. Furthermore, the oxazoline ^{15}N NMR chemical shifts are affected by the *trans* ligand, with the resonances for the group *trans* to hydride typically downfield of those *trans* to η^3-allyl and tosylamide. These rhodium oxazolinylborate compounds have been studied to develop approaches allylic functionalization. However, this possibility is generally limited by the tendency of the allyl hydride compounds to undergo olefin reductive elimination. Reductive elimination products

---

[†] *Dalton Trans.* **2011**, *40*, 6500-6514

[‡] Primary researcher and author

[¶] Contributed synthesis of iridium analogues

[*] Author for correspondence

are formed upon addition of ligands such as CO and CN*t*-Bu. Also, $To^{M}RhH(\eta^3\text{-}C_8H_{13})$ and acetic acid react to give $To^{M}RhH(\kappa^2\text{-}OAc)$ (**3.4**) and cyclooctene. In contrast, treatment of $To^{M}RhH(\eta^3\text{-}C_3H_5)$ with TsN_3 (Ts = *p*-toluenesulfonyl) gives the complex $To^{M}Rh(NHTs)(\eta^3\text{-}C_3H_5)$ (**3.7**). Interestingly, the reaction of $To^{M}RhH(\eta^3\text{-}C_8H_{13})$ and TsN_3 yields $To^{M}RhH(NHTs)OH_2$ (**3.8**) and 1,3-cyclooctadiene *via* β-hydride elimination and Rh–H bond amination. Ligand-induced reductive elimination of **3.7** provides $HN(CH_2CH{=}CH_2)Ts$; these steps combine to give a propene C–H activation/functionalization sequence.

Introduction

The process of so called C–H activation/functionalization has served as a long-term "holy grail" for inert C–H bond transformation in organometallic chemistry.[1] The advance in this field would provide more efficient routes to construct desired molecules in both industrial and pharmaceutical communities.[2] However, so far, numerous cases have shown that the hydrocarbon C–H oxidative addition process could not further proceed due to easily accessible reverse pathway, namely C–H reductive elimination, although stoichiometric functionalizations have been commonly seen for the past few decades. Fortunately, a lot more cases with C–H transformations have been achieved by using catalytic amount of metal catalysts. With regard to this issue, we are interested in investigating stepwise C–H activation/functionalization sequence in a manner of isolating the intermediate products in each stage, which may possess potential of developing an unprecedented catalytic route as well as a more comprehensive understanding of the reaction mechanism.

More recently, the allylic C–H functionalizations to form C–C,[3] C–N[4,5] and C–O[6] bonds *via* electrophilic palladium(II)-catalyzed transformation under oxidizing conditions have drawn much attention. These are classified as the electrophilic type functionalization which is quite dissimilar to the traditional two-electron oxidative addition of C–H bonds[7] that have been typically observed for group 9 rhodium and iridium complexes.[8] While rhodium(I)-catalyzed allylic substitution reactions have been well-studied,[9] a non-cycloaddition type[10] allylic C–H functionalization reaction catalyzed by Rh(I) has never been reported.[11] These invoked our curiosity that whether the group 9 rhodium located adjacent to palladium on periodic table could generally accomplish such a transformation.

For stoichiometric allylic C–H activation paradigm, $IrCl(N_2)(PPh_3)_2$ has represented a classic example of activating allylbenzene to give Ir(III) allyl hydride species.[12] *Fac*-coordinating ancillary ligands were later shown to facilitate allylic C–H bond activations. For instance, Oro has reported an example of vinylic sp^2 C–H activation by treating Na[Tp] with $[Ir(\mu\text{-}Cl)(COE)_2]_2$ (COE = cyclooctadiene) to afford hydrido complex, $TpIr(H)(\sigma\text{-}C_8H_{13})(\eta^2\text{-}C_8H_{14})$.[13] In contrast, it has been demonstrated that the allylic C-H activation product could be obtained by mixing K[Tp] and $[Ir(\mu\text{-}Cl)(COE)_2]_2$ to give η^3-coordinated compound, $TpIr(H)(\eta^3\text{-}C_8H_{13})$.[14] Later on, Tilley has shown the feasibility of the same type of activation by treating $[Li(TMEDA)][PhB(CH_2PPh_2)_3]$ ligand with this iridium dimer to give η^3-coordinated complex as well.[15] Meanwhile, regarding to the rhodium version activation, the photolysis of $Tp^*Rh(CNneo)(PhN{=}C{=}Nneo)$ in liquid propylene to generate $\eta^1\text{-}C_3H_5$ allylic activation product $Tp^*Rh(CNneo)(CH_2CH{=}CH_2)H$.[16] Recently, A photo-induced allylic

activation by irradiating $Cp^*Rh(CH_2=CHMe)_2$ (Cp^* = pentamethylcyclopentadienyl) yields $Cp^*RhH(\eta^3\text{-}C_3H_5)$.[17]

On this premise, we sought to utilize the platform mentioned above to furnish the stepwise activation/functionalization process to have deeper insights into overall mechanism and develop related functionalization strategies. Herein, we report allylic C–H activation of cyclooctene, propene and allylbenzene mediated by the *fac*-coordinated rhodium metal center as well as the first example of azide insertion into a Rh–H bond. Subsequent reductive elimination provides a functionalized propene derivative. Stereo conformation and configuration (*endo*/*exo*, *syn*/*anti*) has been assigned by using $^1H–^{15}N$ HMBC, NOESY and COSY experiments to establish the relationship between metal hydride and oxazoline nitrogen coordination environment.

Results

Synthesis and characterization of allylic C-H activation complexes

In Chapter 2, we have discussed the counter ion effect for ligand transfer. The reaction of $M[To^M]$ (M = Li, K) and $[Rh(\mu\text{-}Cl)(COE)_2]_2$ in a solvent (benzene, thf, methylene chloride and acetonitrile) give complex mixtures that were unable to isolated and characterize at either elevated temperature (60 °C) or room temperature. Once again, $Tl[To^M]$ is proved to be an excellent transfer agent that it reacts with $[Rh(\mu\text{-}Cl)(COE)_2]_2$ to provide $To^MRhH(\eta^3\text{-}C_8H_{13})$ (**3.1**). Slightly excess of the rhodium dimer (1.4 equivalent) was used to drive the reaction to completion within 5 h and the reaction could be scaled up to 1.8 millimoles. Analytical pure product was isolated after pentane extraction (eq 3.1).

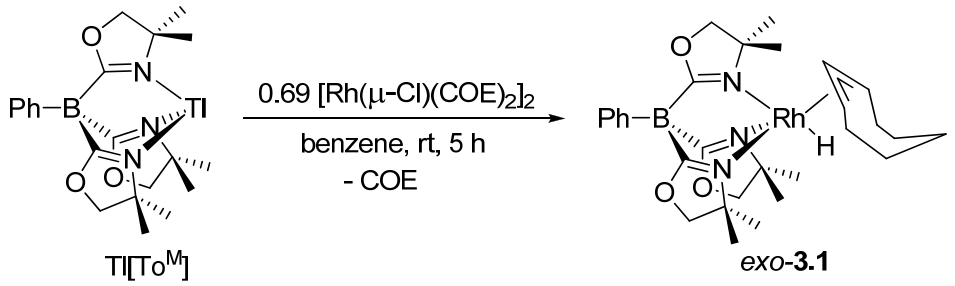

(3.1)

In the ^{1}H NMR spectrum, the characteristic metal hydride signal showed at –24.3 ppm ($^{1}J_{RhH}$ = 11.6 Hz). Like compound **2.5**, the overall symmetry of **3.1** exhibited a C_s symmetric pattern of the ancillary ligand To^{M} in the ^{1}H NMR experiment. For the π-allyl ligand, the central C*H* and the C*H* on the two sides appeared at 5.16 ppm (1 H) as a triplet and 3.95 ppm (2 H) as a doublet of doublet respectively. The NOESY experiment indicated that the cross-peaks were found between oxazoline dimethyl *trans* to metal hydride and both π-allyl central C*H* and the two *syn*-π-C*H* on each side. In addition, the rhodium hydride showed no cross-peaks with all the π-allyl-C*H*. Thus, we assigned the conformation of **3.1** as an *exo* structure. In the ^{13}C{^{1}H} NMR spectrum, the resonance at 93.9 ppm ($^{1}J_{RhC}$ = 6.0 Hz) and 52.2 ppm ($^{1}J_{RhC}$ = 11.4 Hz) were assigned as π-allyl central C*H* and the two *syn*-π-C*H* respectively, which also correlated to the protons in a ^{1}H–^{13}C HMQC experiment.

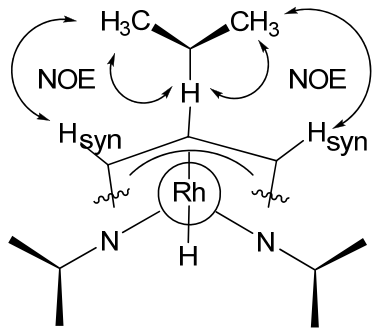

Figure 3.1. A Newman projection of $To^{M}RhH(\eta^3\text{-}C_8H_{13})$ (**3.1**) viewed along the Rh–B bond. Through-space close contacts between oxazoline methyl groups π-allyl ligand, detected using a NOESY experiment, are illustrated with arrows.

Two distinct nitrogen resonances at –164.2 and –173.4 ppm were detected in the $^{1}H–^{15}N$ HMBC experiment. The former chemical shift represented the oxazoline nitrogen *trans* to Rh–H bond while the latter one represented the two equivalent oxazoline nitrogens bisected by symmetry mirror plane. Moreover, the through bond cross-peak between the rhodium hydride and the *trans* oxazoline nitrogen was observed. The hydride resonance was further supported by the IR spectroscopy (ν_{RhH} = 2158 cm^{-1}).

To expand the substrate scope of the allylic C–H activation, the parent π-allyl analogue is obtained by bubbling propene into a solution of $[Rh(\mu\text{-}Cl)(COE)_2]_2$ in benzene at room temperature to generate $[Rh(\mu\text{-}Cl)(C_3H_6)_2]_2$ *in situ* in the first step followed by adding $Tl[To^{M}]$ in the second step to give $To^{M}RhH(\eta^3\text{-}C_3H_5)$ (**3.2**). During the course of the reaction, the *exo* conformer formed exclusively within 1 h with complete conversion (monitored by ^{1}H NMR spectroscopy in benzene-d_6). The final ratio turns out to be 4:1 (*exo*:*endo*) after 2 h at room temperature. Prolonged sitting (up to 2 d) or heating at elevated temperature (80 °C, 2 h) would not change the ratio (eq 3.2). This is somewhat contrast to the observation of $Tp^{*}RhMe(\eta^3\text{-}C_3H_5)$ that the *endo* isomer is the only conformer obtained after heating at 60 °C when starting with 7:1 (*endo*:*exo*) mixture.[18]

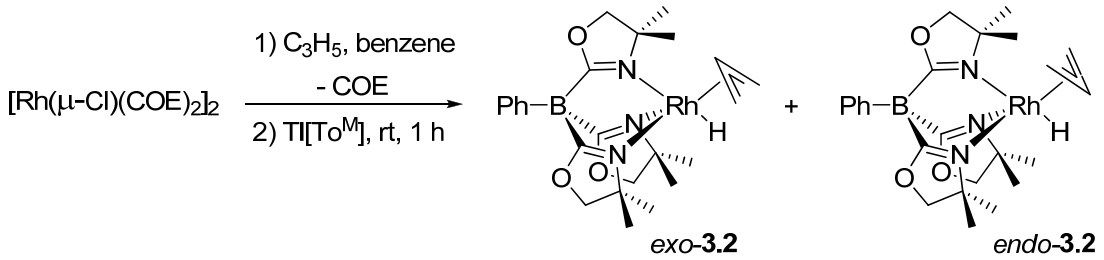

(3.2)

The NOESY experiment confirmed the conformer assignment that a cross-peak was detected between the central π-allyl C*H* and the rhodium hydride of *endo*-**3.2**. The hydride signal of *endo*-**3.2** appeared at –22.7 ppm as a broad singlet while the hydride of *exo*-**3.2** showed at –23.3 ppm as a doublet ($^1J_{RhH}$ = 10.0 Hz) in the ^{1}H NMR spectrum. Also, in the same spectrum, the coupling constant between the central and terminal *syn*-π-allyl C*H* was identical (7.2 Hz) whereas the one between central and terminal anti-π-allyl C*H* was slightly different (11.2 Hz for *endo* and 11.6 Hz for *exo*). Both *endo* and *exo* conformers display a C_s symmetry splitting pattern like the case of *exo*-**3.1**. The two rhodium hydrides of both conformers and the corresponding *trans* oxazoline nitrogen displayed a cross-signal in the ^{1}H–^{15}N HMBC experiment. The existence of metal hydrides was confirmed by stretching frequency of Rh–H showing at 2090 and 2080 cm^{-1} in the IR spectrum.

X-ray crystal structure was obtained at –30 °C and revealed that both conformers co-crystallize (Fig 3.2). The Rh–N bonds *trans* to hydride Rh1–N3 (*endo*: 2.298(3) □ and Rh2–N5 (*exo*: 2.223(3) Å) are longer than the two Rh–N bonds *trans* to the allyl ligand (*endo*: Rh1–N1, 2.107(3); Rh1–N2, 2.109(3); *exo*: Rh2–N4, 2.128(3); Rh2–N6, 2.141(3) Å). The Rh–N distances *trans* to the allyl ligand in the *exo* conformer are slightly longer than the

Rh–N distances in the *endo* conformer. Lastly, both conformers of **3.2** could be obtained by treating **3.1** with propene in benzene-d_6 at room temperature with elimination of cyclooctene.

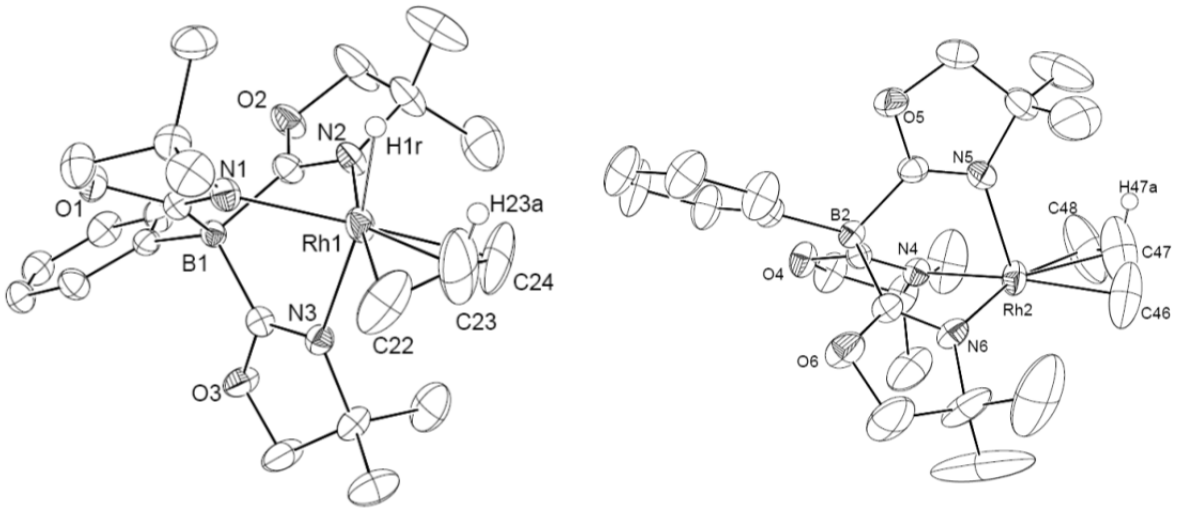

Figure 3.2. ORTEP diagram of *endo*-**3.2** (left) and *exo*-**3.2** (right) drawn at 50% probability. All hydrogens (except the central π-allyl C*H* and the hydride) are omitted for clarity. The two isomers co-crystallize, but their relative orientation has been altered above to more clearly illustrate the rhodium centers' coordination geometry, and this figure does not represent their relative positions in the unit cell. Selected bond distances (Å) for *endo*-**3.2**: Rh1–H1r, 1.67(6); Rh1–N1, 2.107(3); Rh1–N2, 2.109(3); Rh1–N3, 2.298(3); Rh1–C22, 2.160(5); Rh1–C23, 2.099(6), Rh1–C24, 2.139(5). Selected bond distances (Å) for *exo*-**3.2**: Rh2–N4, 2.128(3); Rh2–N5, 2.223(3), Rh2–N6, 2.141(3); Rh2–C46, 2.147(7); Rh2–C47, 2.035(8); Rh2–C48, 2.096(7) .

Similar to the preparation of **3.2**, the synthesis of $To^{M}RhH(\eta^3\text{-}C_3H_4Ph)$ (**3.3**) is carried out by treating $[Rh(\mu\text{-}Cl)(COE)_2]_2$ dimer with excess of allylbenzene to *in situ* generate $[Rh(\mu\text{-}Cl)(C_3H_5Ph)_2]_2$ followed by $Tl[To^{M}]$ addition (eq 3.3).

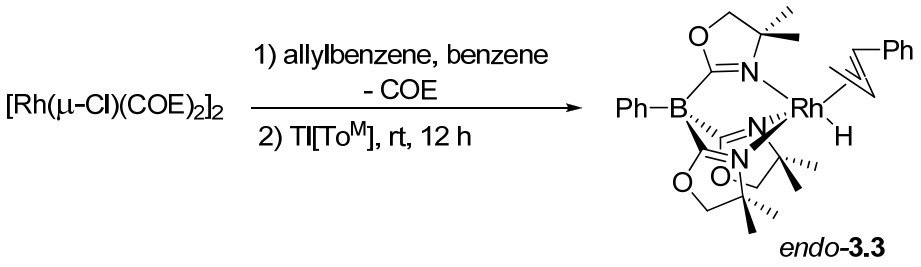

(3.3)

3.3 adopts an *endo* conformation as well as a *syn* configuration (the phenyl group is *syn* to central π-allyl C*H*). The diagnostic rhodium hydride appeared at –22.5 ppm in the ^{1}H NMR spectrum and a cross-peak between the hydride and the central π-allyl C*H* was identified. The assignment of the four Hs of the π-allyl group was determined by COSY experiment that the central C*H* (5.62 ppm) correlated with both the internal benzylic proton (3.98 ppm) and two terminal protons (*syn*, 3.22 ppm; *anti*, 2.84 ppm). The coupling constant (^{3}J) of the latter ones is 9.6 (*syn*) and 11.2 Hz (*anti*) respectively. In the ^{13}C NMR spectrum, the central π-allyl carbon appeared at 90.06 ppm ($^{1}J_{RhC}$ = 3.5 Hz) where the terminal π-allyl carbon and the benzylic π-allyl carbon showed at 36.54 ($^{1}J_{RhC}$ = 12.25 Hz) and 54.52 ppm ($^{1}J_{RhC}$ = 10.5 Hz), which further supports the structure proposed. Due to the C_1 symmetry of the whole molecule, the three oxazoline nitrogens are inequivalent, exhibiting three different signals (–168.2, –172.1 and –179.9 ppm) in the ^{1}H–^{15}N HMBC spectrum. As the case with **3.1** and **3.2**, the oxazoline nitrogen *trans* to the hydride gave a cross-peak between that itself and the hydride.

The solid state structure was obtained from a concentrated toluene solution at –30 °C. The C–C distances in the group appear to be almost equivalent (C22–C23, 1.416(5) and C22–C30, 1.406(5) Å). The steric repulsion between the π-allyl phenyl and the ancillary To^{M}

results in longer distance of Rh1–C23 (2.195(4) Å) compared to the Rh1–C30 (1.406(5) Å) (Fig 3.3).

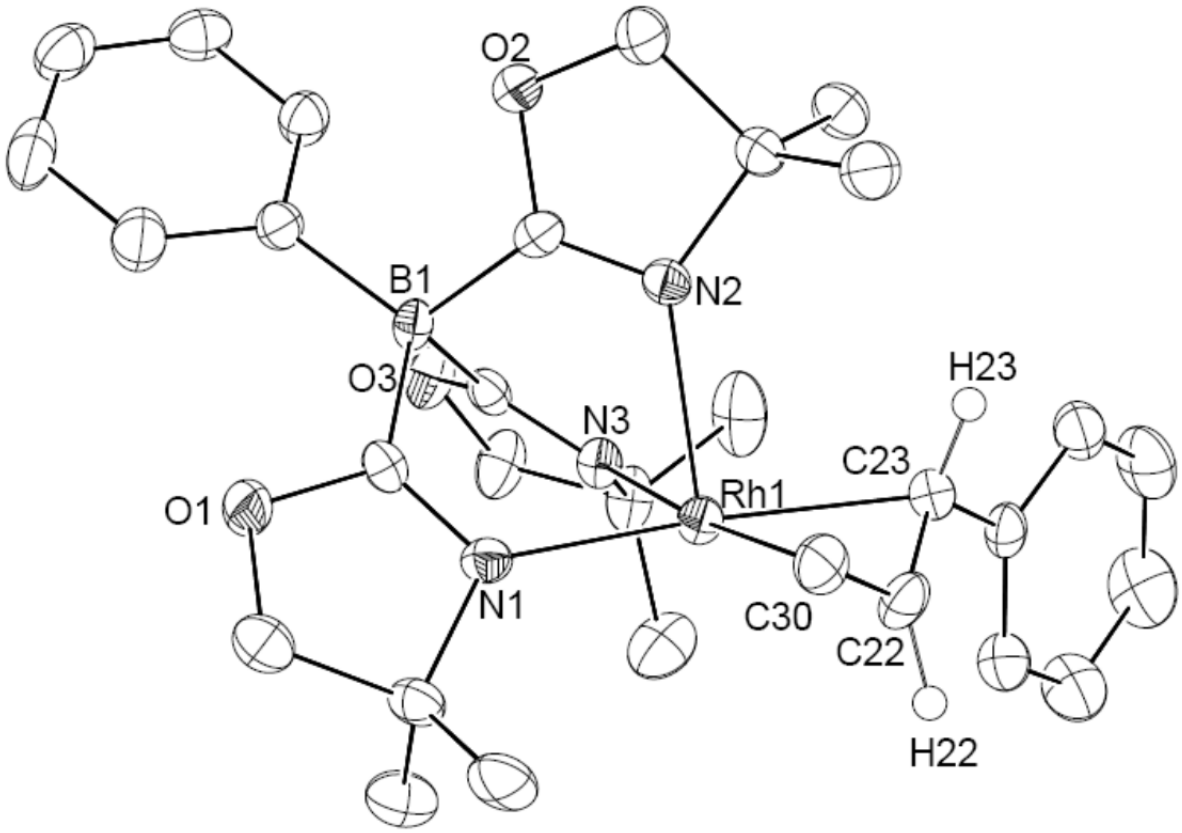

Figure 3.3. ORTEP diagram of **3.3** drawn at 50% probability. Hydrogens are omitted for clarity except H22 and H23. Selected bond distances (Å): Rh1–N1, 2.101(3); Rh1–N2, 2.280(3); Rh1–N3, 2.132(3); Rh1–C22, 2.113(4); Rh1–C23, 2.195(4), Rh1–C30, 2.148(4). Selected angles (°): N1–Rh1–N2, 87.5(1); N1–Rh1–N3, 84.1(1); N2–Rh1–N3, 84.9(1); C23–C22–C30, 120.6(4).

We have discussed three examples of allylic C–H activation, which fulfill the first step of stepwise C–H activation/functionalization. We will continue to illustrate the reactivities of the succeeding functionalization attempts in the following context.

Reactions of To^{M}RhH(η^3-allyl) toward C–E (E = C, N, O)bond formation

We tested a broad scope of oxygen, nitrogen and carbon-based nucleophiles (Nuc) to study the reactivities of To^{M}RhH(η^3-allyl) toward these nucleophiles. These nucleophile reagents include alcohols, amines, alkoxide and enolates. We did not observe the C(allyl)–Nuc bond formation however the reductive elimination pathway dominates. For example, the reaction between **3.1** and neopentyl alcohol or *tert*-butyl amine gives the formation of cyclooctene along with rhodium black precipitate in benzene-d_6 solution at 60 to 80 ºC. Nevertheless, a weaker nucleophile such as a Brønsted acid could provide identifiable product although cyclooctene generated by reductive elimination (or protonation) mechanism is still the major outcome. For instance, treating **3.1** with acetic acid in benzene at room temperature gives To^{M}RhH(κ^2-OAc) (**3.4**). The crude product is purified by pentane extraction and then toluene recrystallization to give analytical pure product in moderate yield (eq 3.4).

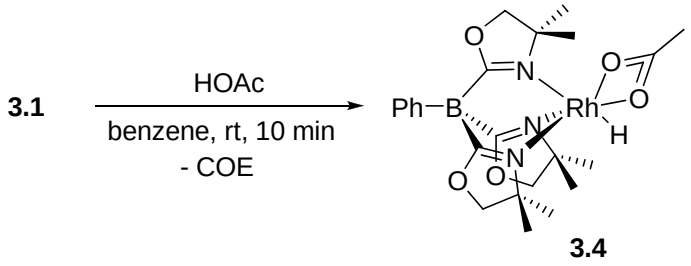

3.4 (3.4)

Reaction with acetic acid-d_1 provides a mixture of **3.4** and To^{M}RhD(κ^2-OAc) (**3.4**-d_1) in a 3:1 ratio. This implies that the reductive elimination of cyclooctene (followed by O–H oxidative addition) is the minor pathway whereas the major one is the direct protonation of η^3-C_8H_{13} (followed by substitution). **3.4** could also be generated when treating **3.3** with Ac_2O

overnight in benzene at 80 °C. The featured hydride appeared at −13.2 ppm ($^1J_{RhH}$ = 11.6 Hz) in the ^{1}H NMR spectrum while the carbonyl carbon of the OAc was detected at 190.3 ppm in the $^{13}C\{^1H\}$ NMR spectrum. Two nitrogen signals were observed in the ^1H–^{15}N HMBC spectrum owing to the C_s symmetry of the whole molecule. The oxazoline nitrogen *trans* to the hydride was assigned at −154.3 ppm. The X-ray structure was obtained in concentrated toluene at −30 °C (Fig 3.4).

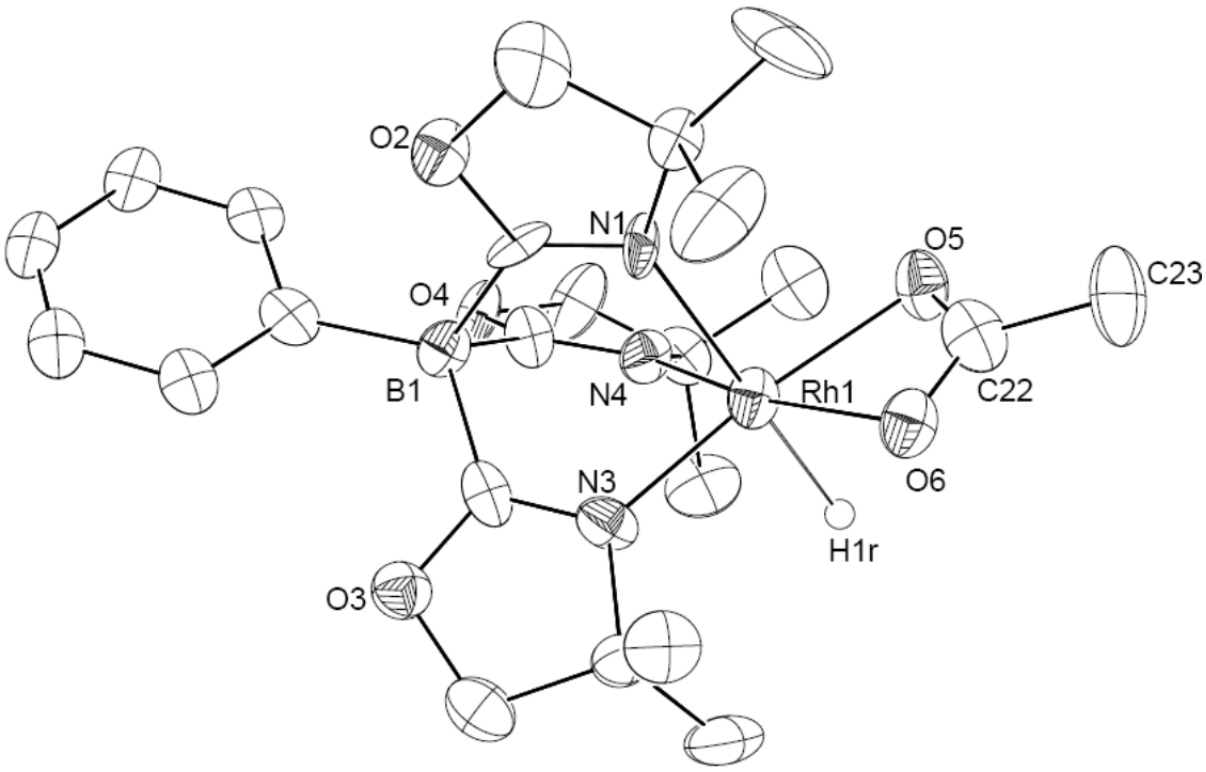

Figure 3.4. ORTEP diagram of **3.4** drawn at 50% probability. Hydrogens (except hydride) are omitted for clarity. Selected bond distances (Å): Rh1–H1r, 1.7(1); Rh1–N1, 2.20(1); Rh1–N2, 1.97(1); Rh1–N3, 2.01(1); Rh1–O4, 2.069(9); Rh1–O5, 2.092(9). Selected bond angles (°): N1–Rh1–H1r, 177(4); N1–Rh1–N2, 87.7(4); N1–Rh1–N3, 85.8(4); N2–Rh1–N3, 85.2(5); N2–Rh1–O4, 167.7(4); N3–Rh1–O5, 168.6(4); O4–R1–O5, 61.8(4).

Next, we anticipated that a viable alternative route is to transform the complexes to cationic species, which would be more vulnerable toward nucleophilic attack (either the metal center or π-allyl group). Thus, the reaction of **3.2** and Lewis-acidic electrophile $B(C_6F_5)_3$ in benzene-d_6 at 60 °C or methylene chloride-d_2 at 40 °C overnight affords a mixture of unidentified products. No free olefin was detected in these reaction mixtures. However, it reacts with a weaker electrophile to form the Rh–Ele bond (Ele = electrophile). For instance, treating **3.3** with NBS gives $To^{M}RhBr(\eta^3\text{-}C_3H_4Ph)$ (**3.5**) overnight at room temperature (eq 3.5).

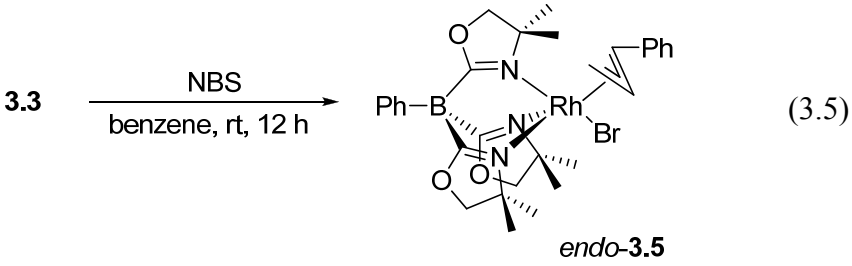

(3.5)

Like **3.3**, the proton assignment of π-allyl group of could be accomplished by the COSY experiment while the coupling constants and the NOESY experiment unambiguously indicated the configuration and the conformation of **3.5**, which remains identical to **3.3** as *endo*-*syn*. Based on the COSY experiment, the central π-allyl C*H* (6.54 ppm) correlated with the benzylic C*H* (5.43 ppm) as well as the terminal *syn* (4.45 ppm) and *anti* (4.14 ppm) π-allyl protons. Due to the C_1 symmetry of **3.5**, three nitrogen cross-peaks were detected in the $^{1}H–^{15}N$ HMBC spectrum whereas the most upfield resonance (−181.5 ppm) was assigned as the one *trans* to bromide.

To this point, our approach has been focusing on nucleophilic and electrophilic substitution reactions and now it is necessary to vary the synthetic route which might benefit and achieve the catalytic functionalization goal. Ligand insertion followed by reductive elimination, however, is a commonly utilized strategy to construct C–E bonds. We began the examination with simple unsaturated hydrocarbons such as ethylene and $Me_3SiC{\equiv}CH$. Unfortunately, for example, the reaction of ethylene and both **3.1** (benzene-d_6, room temperature, overnight) and **3.2** (benzene-d_6, 80 ºC, overnight) result in decomposition of the starting complexes. Moreover, neither **3.1** nor **3.2** give insertion products (the acetylene decomposed instead) when reacting with $Me_3SiC{\equiv}CH$. Yet, both **3.1** (benzene-d_6, room temperature, 2 h) and **3.2** (benzene-d_6, 60 ºC, 2 h) react with CO to give dicarbonyl complex $To^MRh(CO)_2$ (**2.2)** *via* reductive elimination of cyclooctene. Subsequently, we discovered that isoelectronic isocyanide would also react with **3.1** to give $To^MRh(CN\textit{t}\text{-Bu})_2$ (**3.6**) at room temperature (eq 3.6) with cyclooctene elimination although the insertion reaction pathway has not been observed in both cases (CO and CN*t*-Bu).

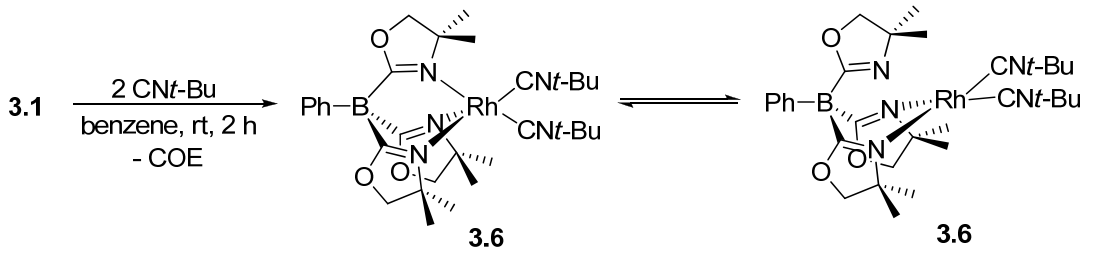

(3.6)

In a solution phase, **3.6** behaves like **2.2** that the constitutional equilibrium (κ^2 and κ^3) cause the equivalency of oxazoline dimethyl and methylene groups. Therefore, in the ^1H NMR spectrum, methylene signal was detected at 3.71 ppm (6 H) whereas the dimethyl one was assigned at 1.35 ppm (18 H) respectively. The ^1H–^{15}N HMBC experiment also supports

this observation that only one oxazoline cross-peak was detected at −159.6 ppm while the isocyanide nitrogen exhibited at −201.1 ppm. IR spectroscopic evidence further indicated the

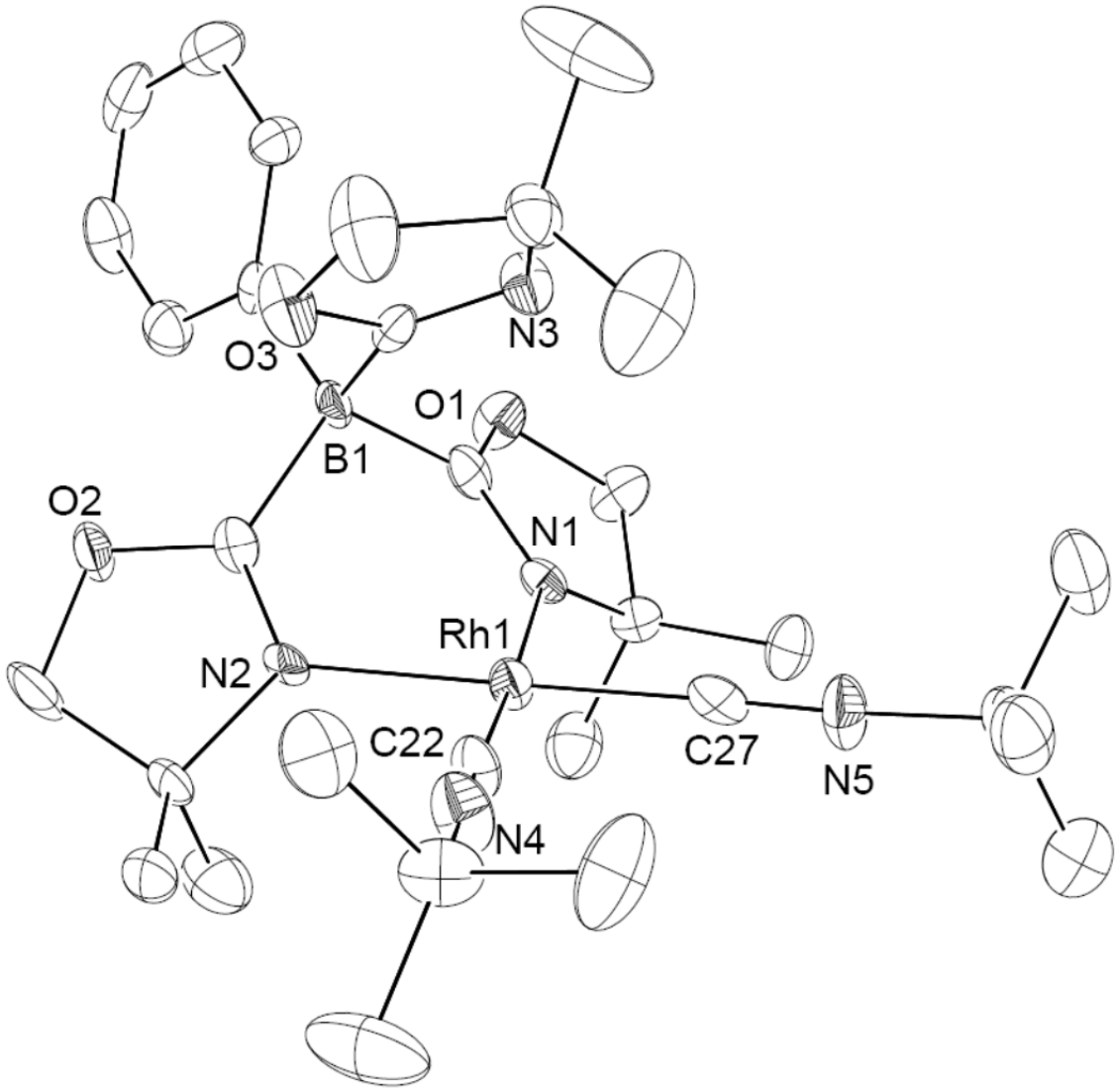

Figure 3.5. ORTEP diagram of **3.6**. Ellipsoids are shown at 50% probability. Hydrogens are omitted for clarity. Selected bond distances (Å): Rh1−N1, 2.094(4); Rh1−N2, 2.087(4); Rh1−C22, 1.881(6); Rh1−C27, 1.884(7). Selected bond angles (°): N1−Rh1−C22, 174.9(2); N2−Rh1−C27, 178.4(2); N1−Rh1−N2, 85.2(2); C22−Rh1−C27, 84.8(2).

presence of two isomers in solution that four isocyanide C≡N stretching frequencies were observed. The X-ray structure was obtained by slow evaporation of ether into methylene chloride solution at –30 ºC. Undoubtedly, the structural connectivity shows κ^2 coordination is the only isomer in the solid state (Fig 3.5).

Up to now, several non-polar and polar multiple bond species have been examined for insertion chemistry and none of them give satisfactory desire inserted products. Thus, we decided to consider other possible insertion routes. 1,3-dipolar dinitrogen compounds (nitrous oxide, diazos and azides) have been well known to undergo 1,3-dipolar cycloaddition. Meanwhile, these three compounds could also serve as good atom transfer carriers that deliver oxygen, carbon and nitrogen respectively with extrusion of molecular nitrogens. For example, N_2O[19] has been applied to inserting oxygen into a M–C or M–H bond and azides (RN_3)[20] have been reported to give corresponding nitrene insertion consequences as well.

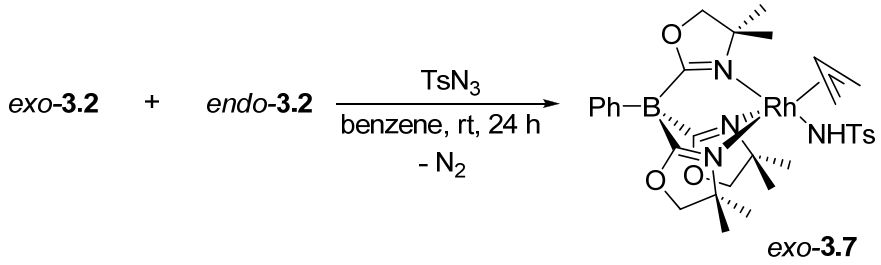

(3.7)

Treating **3.2** with N_2O in benzene-d_6 at 80 °C affords unidentified products over 2 h. The reaction between **3.2** and diazoacetate does not render any detectable insertion products but decomposition result. Nonetheless, TsN_3 reacts with two isomeric mixture **3.2** to give the nitrene insertion compound $To^MRh(NHTs)(\eta^3\text{-}C_3H_5)$ (**3.7**) at room temperature for 24 h (eq

3.7). *exo*-**3.7** adopts C_s symmetry for the whole molecule and is the only isomer that exists in this reaction.

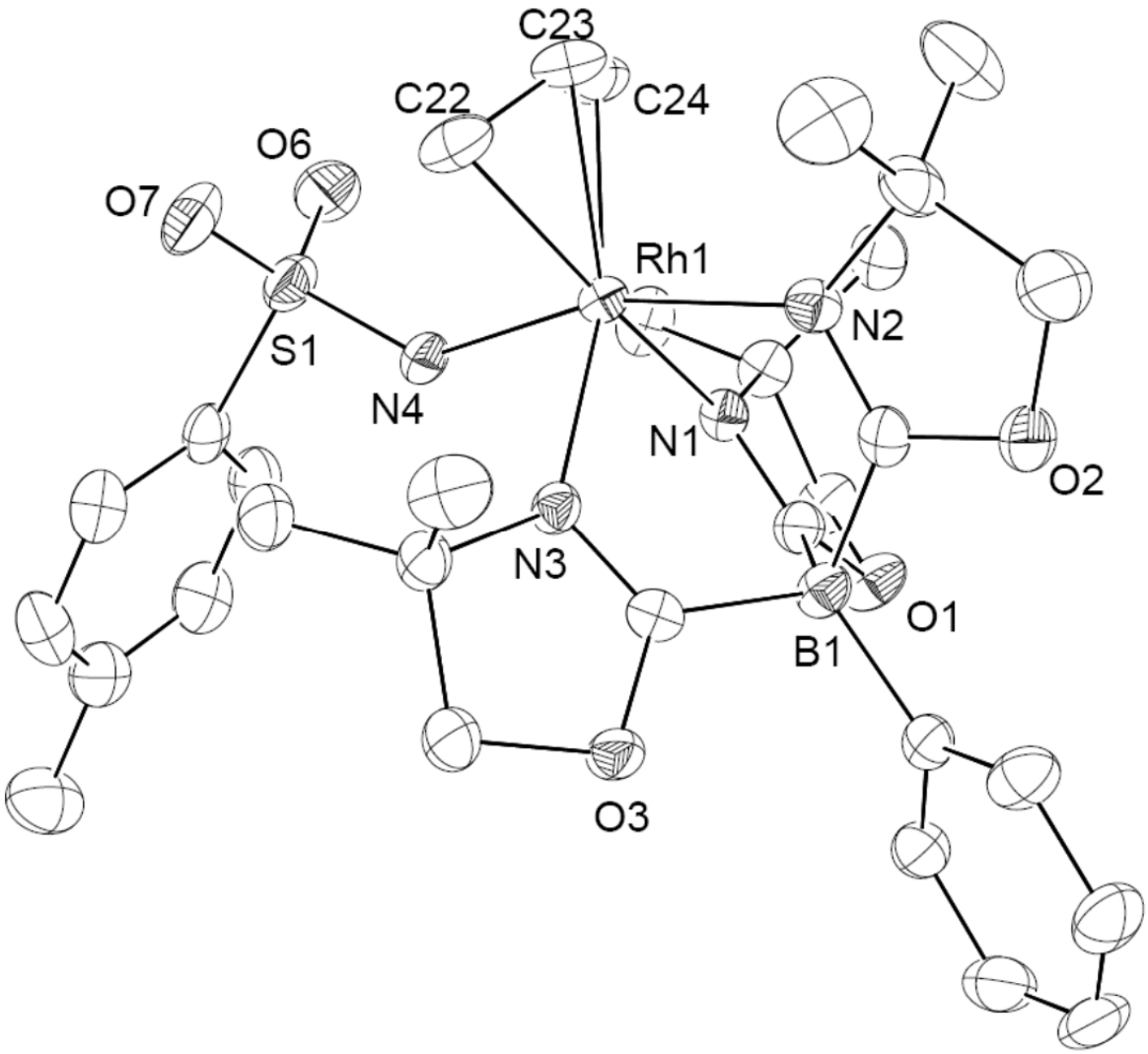

Figure 3.6. ORTEP diagram of **3.7**. Ellipsoids are drawn at 50% probability. Hydrogens are omitted for clarity. Selected bond distances (Å): Rh1–N1, 2.140(2); Rh1–N2, 2.119(3); Rh1–N3, 2.121(3); Rh1–N4, 2.085(3); Rh1–C22, 2.181(3); Rh1–C23, 2.145(3); Rh1–C24, 2.181(3). Selected bond angles (°): N1–Rh1–N4, 83.8(1); N2–Rh1–N4, 163.0(1); N3–Rh1–N4, 84.4(1); Rh1–N4–S1, 138.5(2).

The stereo conformation was confirmed by NOESY experiment and two ^{15}N cross-peaks (–177.6 and –255.4 ppm) were found in the ^{1}H–^{15}N HMBC experiment that the latter one is the oxazoline nitrogen *trans* to NHTs group. The π-allyl group displayed three signals at 5.60, 5.17 and 4.19 ppm, representing the central proton, two *anti* terminal protons ($^{3}J_{HH}$ = 12.4 Hz) and two *syn* terminal proton ($^{3}J_{HH}$ = 8.8 Hz) respectively in the ^{1}H NMR spectrum. X-ray structure (obtained from vapor diffusion of pentane into toluene solution at –30 ºC) further validates the conformation assignment (Fig 3.6), which disclose the exo-η^3-C_3H_5 disposition.

Later, we predicted that the reaction between **3.1** and TsN_3 would follow the same pathway to give the complex $To^{M}Rh(NHTs)(\eta^3\text{-}C_8H_{13})$. Surprisingly, when the reaction is carried out at room temperature, it proceeds to completion within 2 h to afford the complex $To^{M}RhH(NHTs)(OH_2)$ (**3.8**) instead. By monitoring the reaction of **3.1** and TsN_3 in benzene-d_6 by NMR spectroscopy, the formation of 1,3-COD was observed along with vigorous N_2 evolution (eq 3.8).

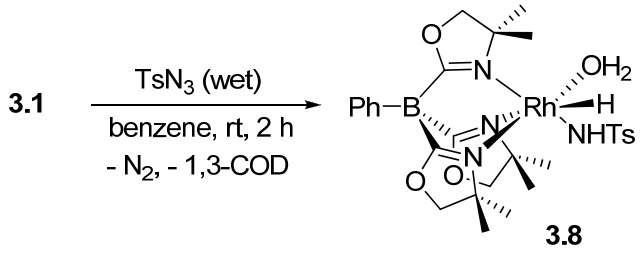

(3.8)

The distinctive hydride peak was located at –15.75 ppm ($^{1}J_{RhH}$ = 9.2 Hz) in the ^{1}H NMR spectrum and the related absorption was detected at 2067 cm^{-1} in the IR spectrum. The C_1 symmetry of the complex **3.8** was noted to display three different cross-peaks (–228.6, –205.8 and –154.1 ppm) of ^{15}N signal for oxazoline nitrogens in the ^{1}H–^{15}N HMBC

spectrum. The X-ray quality structure was obtained by vapor diffusion of pentane into benzene solution at room temperature (Fig 3.7)

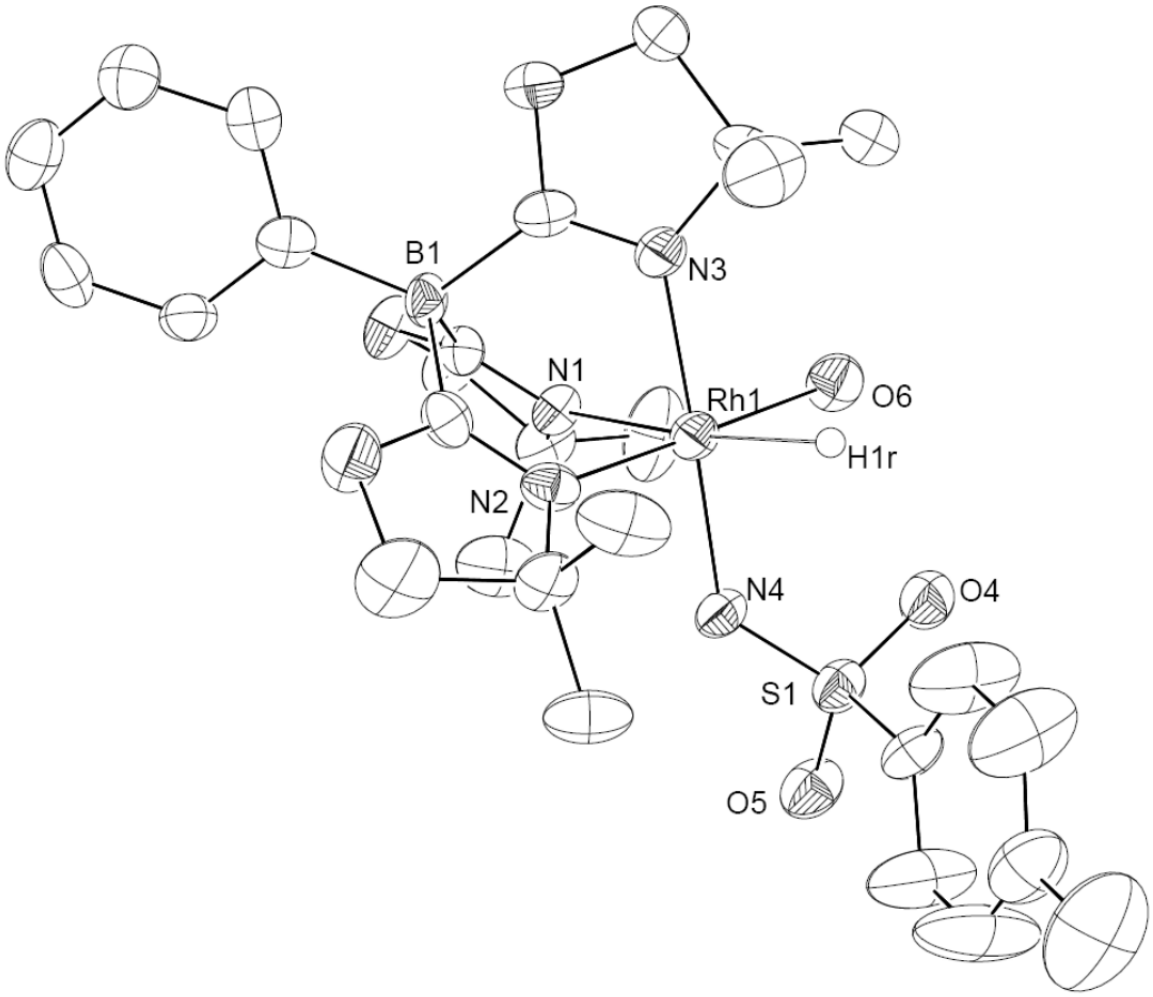

Figure 3.7. ORTEP diagram of **3.8** drawn at 50% probability. Hydrogens (except hydride) are omitted for clarity. Selected bond distances (Å): Rh1–H1r, 1.88(7); Rh1–N1, 2.234(6); Rh1–N2, 2.016(7); Rh1–N3, 2.064(7); Rh1–N4, 2.088(6); Rh1–O6, 2.101(6). Selected bond angles (Å): N1–Rh1–H1r, 173(2); N2–Rh1–O6, 179.2(3); N3–Rh1–N4, 176.9(3); Rh1–N4–S1, 131.5(4).

Unfortunately, the reaction of **3.3** and TsN_3 could not give any identifiable products (benzene-d_6, overnight, room temperature). Moreover, neither Adm-N_3 (Adm = adamantyl)

nor Me_3Si-N_3 gives insertion amido products (M–NHR, R = Adm or Me_3Si) for complexes **3.1-3.3**.

Excitingly in the end, the reaction of **3.7** and CO at 65 °C results in C–N bond reductive elimination and CO coordination to give $To^MRh(CO)_2$ (**2.2**, 81% yield) and allyl(tosyl)amine (eq. 3.9). The organic product, identified by GC-MS and ^1H NMR, is formed in 29% yield.

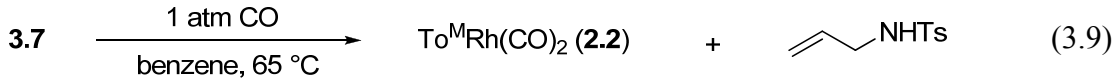

(3.9)

Discussion

Attempt to synthesize $To^PRhH(\eta^3\text{-}C_8H_{13})$ could not be achieved by introducing a similar synthetic route for **3.1** synthesis. In fact, the reaction between **2.1** and $[Rh(\mu\text{-}Cl)(COE)_2]_2$ renders an isolable $\{To^PRh\}$ species. Coordinated cyclooctene and metal hydrides were not observed, which indicates that the ancillary ligand, To^P, is not able to mediate allylic C–H activation. This is somewhat unexpected due to similar electronic and steric properties of To^M and To^P. On the other hand, the richness of the chemistry included in this chapter is once more attributed to the important starting material, $Tl[To^M]$. As was mentioned earlier in Chapter 2, $Tl[To^M]$ serves as the best ligand transfer agent comparing to the analogues, $Li[To^M]$ and $K[To^M]$. For comparison,[11, 12] counter ion effect has been brought up in the context above that different coordinated cations would lead to diverse reaction pathways. Therefore, it is reasonable that $Li[To^M]$ and $K[To^M]$ afford complex mixtures.

Several possible azide insertion reactions and mechanisms have been proposed. To rationalize the mechanism in our system, 1) $Co(Me)_3(PMe_3)_3$ has been reported to react with

TsN_3 to give the N(γ)-inserted (1,1-insertion) triazenide complex, Co(κ^2-(MeN(γ)-N_2Ts)$(Me)_2(PMe_3)_3$.[21] 2) The triazenide complex has also been synthesized as the intermediate of hafnium amido complex inserted by azide reagents. The isotope study suggested that it proceeds *via* 1,3-hydrogen migration (from N(γ) to N(α)) followed by N_2 extrusion.[22] 3) More recently, Leung and his co-workers has discovered the insertion of nitrene (from PhINTs) into Ir–C bond *via* proposed formation of Ir(V) imido intermediate.[23] Presumably, this intermediate is generated *via* N(α) coordination followed by N_2 extrusion. To summarize, Scheme 3.1 shows the two possible mechanisms for rhodium amido formation where (1) involves the formation of Rh(III) triazenide intermediate. The second and third step of this proposed mechanism is based on the first two points mentioned above. In contrast, pathway (2) proceeds *via* formation of Rh(V) imido intermediate. Again, dinitrogen extrusion and subsequent insertion steps are based on the third point noted above.

Besides, the isomerization of **3.2** was monitored during the course of the formation of the two isomers. The isomerization implies the un-coordination and re-coordination (η^3-η^1-η^3) process of the π-allyl group. In addition, $PhB(CH_2PPh_2)_3IrH(\eta^3$-$C_8H_{13})$ has been documented to undergo β-eleimination in the presence of $PMePh_2$ to give the compound $[Ir](H)_2PMePh_2$ accompanied by cyclooctene elimination,[13b] in which the ancillary phosphine arm

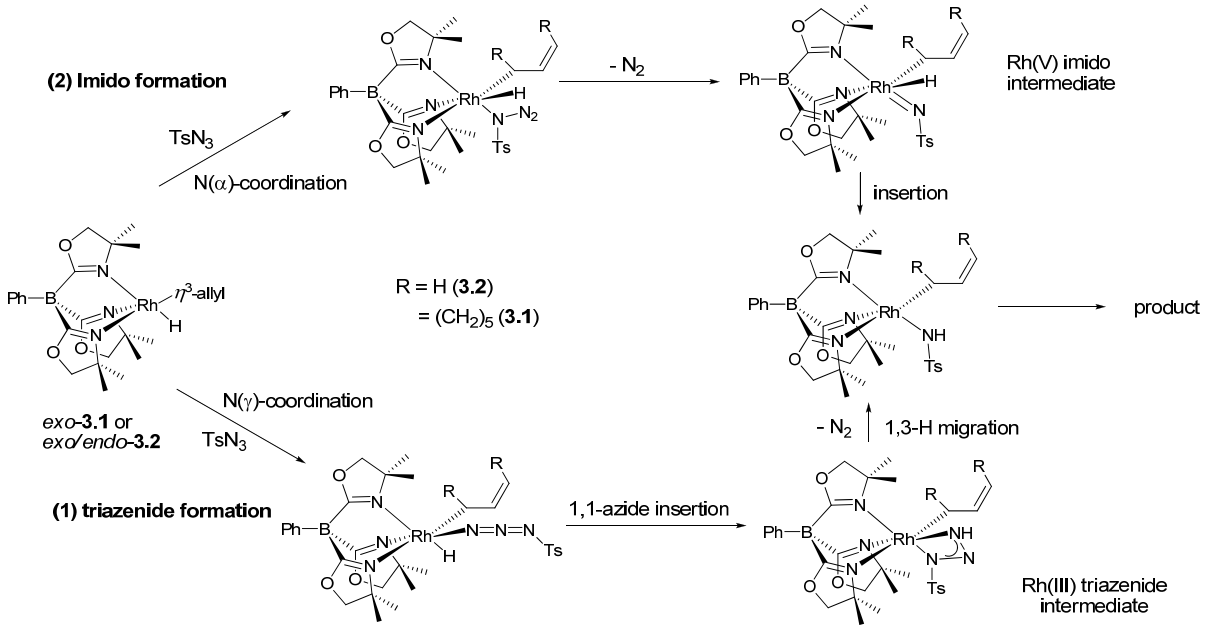

Scheme 3.1. Two possible mechanisms for the reaction of **3.2** and tosylazide that gives a tosylamide.

dissociation is less likely to occur. Thus, it is reasonable to propose the η^1-allyl intermediate rather than oxazoline dissociation that generate an open site for azide nitrogen coordination in the first step of both possible mechanisms (Scheme 3.1). To further argue the rationale of the two mechanisms, both CO and CN*t*-Bu could act as 1,1-insertion substrates. However, in our system, both ligands promote reductive elimination of cyclooctene instead of undergoing insertion into Rh–H bond. This is perhaps the azide insertion product is irreversibly trapped by 1,3-coordination in the beginning followed by 1,3-hydrogen migration and N_2 elimination. Moreover, Rh(V) imido species is a highly reactive intermediate if it ever exists. Therefore, mechanism (1) is a more plausible reaction pathway for rhodium amido formation.

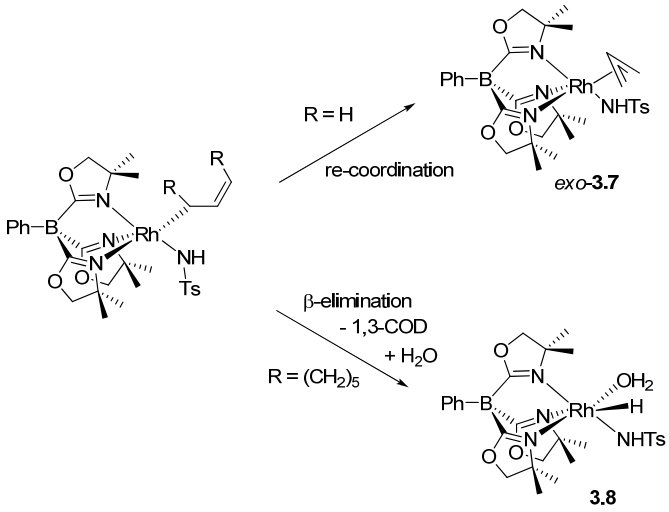

Scheme 3.2. Proposed mechanism for divergent pathways in reactions of **3.1** and **3.2** with tosylazide.

The fate of the insertion intermediate is demonstrated in Scheme 3.2 that **3.1** undergoes *β*-elimination to form 1,3-cyclooctadiene and the compound **3.8** whereas **3.2** undergoes re-coordination of η^1-C_3H_5 to give the complex **3.7**.

We have demonstrated in the previous chapter that ^{15}N NMR spectroscopy plays a crucial role and a powerful tool for structural and stereo assignment. The through-metal ^{1}H–^{15}N correlations confirmed the connectivity of the ancillary ligand, the metal center and the actor ligand. Table 3.1 shows the ^{15}N chemical shift values relative to the *trans* ligand and Rh–N distances for the compounds reported in this chapter. The ^{15}N NMR chemical shift of the oxazoline *trans* to hydrides in **3.1** and **3.2** are the farthest downfield while **3.3** is about 15 ppm upfield with respect to them. The oxazoline *trans* to the tosylamide has the farthest upfield ^{15}N NMR chemical shift, and those *trans* to weak-field bromide, water, and acetate ligands also have upfield chemical shifts.

Table 3.1. ^{15}N NMR chemical shift data and M–N distances for oxazoline nitrogen in {To^{M}Rh} compounds.

Compound	^{15}N *trans* to hydride	M–N distance trans to H (Å)	^{15}N *trans* to allyl	M–N distance *trans* to allyl	^{15}N *trans* to a heteroatomic ligand
To^{M}RhH(η^3-C_8H_{13}) (**3.1**)	–164.2	n.a.[a]	–173.4	n.a.[a]	n.a.[c]
endo-To^{M}RhH(η^3-C_3H_5) (*endo*-**3.2**)	–165.6	2.298(3)	–173.8	2.107(3) 2.109(3)	n.a.[c]
exo-To^{M}RhH(η^3-C_3H_5) (*exo*-**3.2**)	–164.8	2.223(3)	–173.1	2.141(3) 2.128(3)	n.a.[c]
To^{M}RhH(η^3-C_3H_4Ph) (**3.3**)	–179.9	2.280(3)	–168.2, –172.1	2.101(3) 2.132(3)	n.a.[c]
ToMRhH(κ^2-O_2CMe) (**3.4**)	–154.3	2.20(1)	n.a.[d]	n.a.[d]	–221.0 (OAc)
To^{M}RhBr(η^3-C_3H_4Ph) (**3.5**)	n.a.[b]	n.a.[a,b]	–191.1, –181.5	n.a.[a]	–217.6 (Br)
To^{M}Rh(NHTs)(η^3-C_3H_5) (**3.7**)	n.a.[b]	n.a.[b]	–177.6	2.140(2) 2.121(3)	–225.4 (NHTs)
To^{M}RhH(NHTs)OH_2 (**3.8**)	–154.1	2.234(6)	n.a.[d]	n.a.[d]	–228.6 (NHTs) –205.8 (OH_2)

[a] An X-ray crystal structure was not obtained. [b] The compound does not contain a metal hydride. [c] The compound does not contain a heteroatomic ligand. [d] The compound does not contain an allyl group.

Conclusion

Although Rh(II)-catalyzed insertion chemistry of carbene and nitrene into C–H bonds to give functionalized C–C and C–N bond formation products has been well developed and extensively applied,[24] we are currently investigating a new catalytic route for functionalizing

allylic C–H bonds, in which, to the best of our knowledge, disclosing the first example of nitrene insertion into Rh–H bonds. We have completed the non-catalytic stepwise allylic C–H activation/nitrene insertion/reductive elimination process (Scheme 3.3). Although the third step gives the non-regenerated Rh(I) dicarbonyl complex as well as the allyl(tosyl)amine product, we will be continuing to seek for a suitable method to invoke the reductive elimination and accomplish the catalytic cycle.

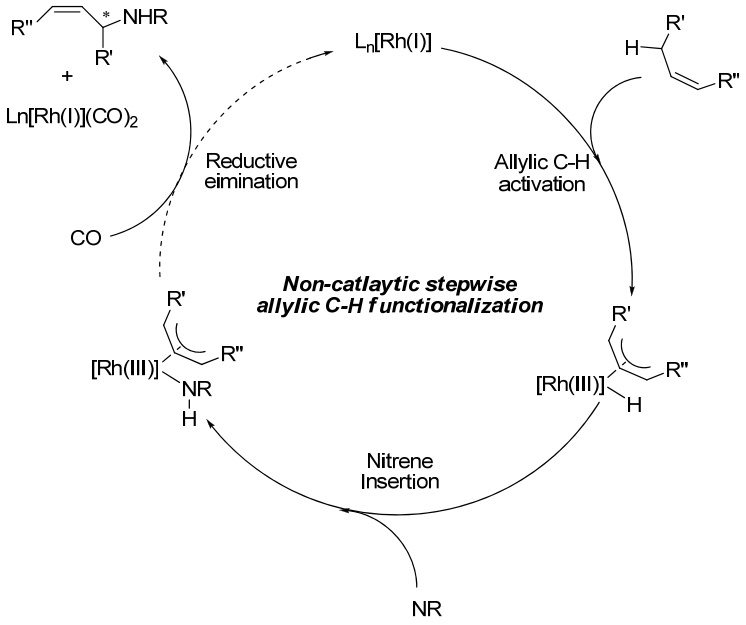

Scheme 3.3. Stepwise functionalization of an allylic C–H bond to generate the C–N bond formation product.

In addition, we have proved the *fac*-coordinated To^M is a proper ancillary ligand for the allylic C–H activation even though the electronically and sterically similar To^P ligand could not promote such a transformation. However, we have illustrated a potentially possible reaction method that is able to expand to asymmetric functionalization of allylic C-H bonds

as long as an appropriate chiral ancillary ligand could facilitate this type of chemistry. All the issues addressed above are all under investigation.

Experimental

General Procedures. All reactions were carried out under an inert atmosphere using standard Schlenk techniques or in a glovebox. All solvents were dried and degassed unless otherwise indicated. All reagents were purchased from Sigma-Aldrich and used without further purification. $Tl[To^M]$[25], $[Rh(\mu\text{-}Cl)(COE)_2]_2$[26], and TsN_3[27] were prepared according to reported procedures. All NMR spectra were obtained at room temperature using Bruker DRX-400 and Avance II-700 spectrometers. ^{15}N NMR chemical shifts were determined by ^1H-^{15}N HMBC experiments recorded on an Avance II-700 spectrometer; the chemical shift values are reported relative to CH_3NO_2. ^{11}B NMR spectra chemical shifts are reported relative to $BF_3{\cdot}Et_2O$. GC-MS data were obtained on an Agilent 7890 A GC system containing an HP-5MS capillary column and an Agilent 5975C mass selective detector. Elemental analyses were obtained at the Iowa State Chemical Instrumentation Facility using a Perkin-Elmer 2400 Series II CHN/S. Single crystal X-ray analysis was carried out on a Bruker APEX2 CCD Diffractometer.

$To^MRhH(\eta^3\text{-}C_8H_{13})$ (3.1). Benzene (50 mL) was added to a solid mixture of $Tl[To^M]$ (0.187 g, 0.319 mmol) and $[Rh(\mu\text{-}Cl)(COE)_2]_2$ (0.160 g, 0.223 mmol) giving a suspension. The resulting mixture was stirred at room temperature for 5 h and then filtered. The solvent was removed from the filtrate under reduced pressure. The resulting residue was extracted with pentane (3 × 25 mL), and the extractions were combined and evaporated to dryness to give analytically pure $To^MRhH(\eta^3\text{-}C_8H_{13})$ (**3.1**, 0.134 g, 0.225 mmol, 70.6%) as a brown solid in

good yield. ^{1}H NMR (benzene-d_6, 400 MHz): δ 8.45 (d, 2 H, $^{3}J_{HH}$ = 7.6 Hz, *ortho*-C_6H_5), 7.58 (t, 2 H, $^{3}J_{HH}$ = 7.6 Hz, *meta*-C_6H_5), 7.38 (t, 1 H, $^{3}J_{HH}$ = 7.2 Hz, *para*-C_6H_5), 5.16 (t, 1 H, C*H*$(CH)_2(CH_2)_5$, $^{3}J_{HH}$ = 8.0 Hz), 3.95 (dd, 2 H, $^{3}J_{HH}$ = 16.4 Hz, $^{3}J_{HH}$ = 8.0 Hz, CH(C*H*$)_2(CH_2)_5$), 3.74 (d, 2 H, $^{2}J_{HH}$ = 8.4 Hz, $CNCMe_2CH_2O$), 3.60 (d, 2 H, $^{2}J_{HH}$ = 8.4 Hz, $CNCMe_2CH_2O$), 3.33 (s, 2 H, $CNCMe_2CH_2O$), 2.51 (m, 2 H, $(CH)_3CH_2(CH_2)_3CH_2$), 2.21 (m, 1 H, $(CH)_3(CH_2)_2CH_2(CH_2)_2$), 1.74 (m, 2 H, $(CH)_3CH_2(CH_2)_3CH_2$), 1.50 (m, 1 H, $(CH)_3(CH_2)_2CH_2(CH_2)_2$), 1.45 (m, 4 H, $(CH)_3CH_2CH_2CH_2CH_2CH_2$), 1.17 (s, 6 H, $CNCMe_2CH_2O$), 1.12 (s, 6 H, $CNCMe_2CH_2O$), 0.82 (s, 6 H, $CNCMe_2CH_2O$), –24.27 (d, 1 H, $^{1}J_{RhH}$ = 11.6 Hz, Rh*H*). ^{13}C{^{1}H} NMR (benzene-d_6, 175 MHz): δ 136.81 (*ortho*-C_6H_5), 126.93 (*meta*-C_6H_5), 125.75 (*para*-C_6H_5), 93.93 (d, $^{1}J_{RhC}$ = 6.0 Hz, *C*H$(CH)_2(CH_2)_5$), 81.96 ($CNCMe_2CH_2O$), 80.93 ($CNCMe_2CH_2O$), 68.41 ($CNCMe_2CH_2O$), 67.92 ($CNCMe_2CH_2O$), 52.15 (d, $^{1}J_{RhC}$ = 11.4 Hz, CH$(CH)_2(CH_2)_5$), 38.41 ($(CH)_3CH_2(CH_2)_3CH_2$), 29.52 ($(CH)_3CH_2CH_2CH_2CH_2CH_2$), 29.49 ($(CH)_3CH_2CH_2CH_2CH_2CH_2$), 28.82 ($CNCMe_2CH_2O$), 28.57 ($CNCMe_2CH_2O$), 28.33 ($CNCMe_2CH_2O$). ^{11}B NMR (benzene-$d_6$, 128 MHz): δ –18.7. ^{15}N NMR (benzene-d_6, 71 MHz): δ –164.2 (*trans* to RhH), –173.4 (*cis* to RhH) IR (KBr, cm^{-1}): ν 3076 (w), 3040 (w), 2959 (m), 2927 (m), 2843 (m), 2158 (m, ν_{RhH}), 1598 (s, ν_{CN}), 1462 (m), 1383 (m), 1363 (m), 1275 (m), 1195 (m), 1156 (m), 996 (m), 972 (m), 933 (w). Anal. Calcd. for $C_{29}H_{43}BRhN_3O_3$: C, 58.50; H, 7.28; N, 7.06. Found: C, 58.85; H, 7.48; N, 7.10. Mp: 132–135 °C, dec.

To^{M}RhH(η^3-C_3H_5) (3.2). Propene was bubbled through a solution of $[Rh(\mu\text{-Cl})(COE)_2]_2$ (0.500 g, 0.697 mmol) in benzene (100 mL) for 10 min to form $[Rh(\mu\text{-Cl})(C_3H_6)_2]_2$. Tl[To^{M}] (0.56 g, 0.96 mmol) was added as a solid to the $[Rh(\mu\text{-Cl})(C_3H_6)_2]_2$ solution at room

temperature, and the resulting mixture was stirred for 1 h. The solution was then filtered, and the volatile materials in the filtrate were evaporated to dryness. The resulting residue was extracted with pentane (3 × 50 mL) and stored at −35 °C overnight. The solids were then collected as an analytically pure, light-brown, flaky powder (0.39 g, 76%). This powder was then recrystallized from toluene at −30 °C to obtain X-ray quality crystals of co-crystallized *exo*-**3.2** and *endo*-**3.2**. IR (KBr, cm^{-1}): ν 3075 (m), 3035 (m), 2967 (m), 2927 (m), 2899 (m), 2090 (s, ν_{RhH}), 2080 (s, ν_{RhH}), 1598 (s, ν_{CN}), 1567 (m, ν_{CN}), 1460 (m), 1382 (m), 1365 (m), 1351 (m), 1275 (m), 1197 (m), 1155 (m), 1021 (w), 992 (m), 975 (m), 902 (m), 703 (m). Anal. Calcd. for $C_{24}H_{35}BRhN_3O_3$: C, 54.67; H, 6.69; N, 7.97. Found: C, 54.71; H, 6.37; N, 7.71. Mp: 204–206 °C, dec. Although the two conformers are not independently isolated, the NMR spectroscopic data for each is provided separately facilitate interpretation. ***exo*-3**: ^{1}H NMR (benzene-d_6, 400 MHz): δ 8.46 (d, 2 H, $^3J_{HH}$ = 7.6 Hz, *ortho*-C_6H_5), 7.58 (t, 2 H, $^3J_{HH}$ = 7.6 Hz, *meta*-C_6H_5), 7.38 (t, 1 H, $^3J_{HH}$ = 7.6 Hz, *para*-C_6H_5), 4.91 (m, 1 H, C*H*$(CH_2)_2$), 3.66 (d, 2 H, $^2J_{HH}$ = 8.4 Hz, CNCMe$_2$C*H*$_2$O), 3.61 (d, 2 H, $^2J_{HH}$ = 8.4 Hz, CNCMe$_2$C*H*$_2$O), 3.34 (s, 2 H, CNCMe$_2$C*H*$_2$O), 2.91 (d, 2 H, $^3J_{HH}$ = 7.2 Hz, *syn*-CH(C*H*$_2$)$_2$), 2.28 (d, 2 H, $^3J_{HH}$ = 11.6 Hz, *anti*-CH(C*H*$_2$)$_2$), 1.05 (s, 6 H, CNC*Me*$_2$CH$_2$O), 1.02 (s, 6 H, CNC*Me*$_2$CH$_2$O), 0.79 (s, 6 H, CNC*Me*$_2$CH$_2$O), −23.20 (d, 1 H, $^1J_{RhH}$ = 10.0 Hz, Rh*H*). ^{13}C{^{1}H} NMR (benzene-d_6, 175 MHz): δ 136.71 (*ortho*-C_6H_5), 126.97 (*meta*-C_6H_5), 125.78 (*para*-C_6H_5), 93.41 (d, $^1J_{RhC}$ = 7.0 Hz, *C*H$(CH_2)_2$), 81.82 (CNCMe$_2$*C*H$_2$O), 80.53 (CNCMe$_2$*C*H$_2$O), 69.00 (CN*C*Me$_2$CH$_2$O), 67.74 (CN*C*Me$_2$CH$_2$O), 32.99 (d, $^1J_{RhC}$ = 10.5 Hz, CH(*C*H$_2$)$_2$), 28.72 (CNC*Me*$_2$CH$_2$O), 28.38 (CNC*Me*$_2$CH$_2$O), 28.11 (CNC*Me*$_2$CH$_2$O). ^{11}B NMR (benzene-d_6, 128 MHz): δ −18.4. ^{15}N NMR (benzene-d_6, 71 MHz): δ −165.6 (*trans* to RhH), −173.1 (*cis*

to RhH). ***endo*-3**: ^{1}H NMR (benzene-d_6, 400 MHz): δ 8.56 (d, 2 H, $^{3}J_{HH}$ = 6.8 Hz, *ortho*-C_6H_5), 7.63 (t, 2 H, $^{3}J_{HH}$ = 7.6 Hz, *meta*-C_6H_5), 7.41 (t, 1 H, $^{3}J_{HH}$ = 7.2 Hz, *para*-C_6H_5), 5.10 (m, 1 H, C*H*(CH_2), 3.64 (d, 2 H, $^{2}J_{HH}$ = 8.4 Hz, CNCMe$_2$C*H*$_2$O), 3.47 (d, 2 H, $^{2}J_{HH}$ = 8.4 Hz, CNCMe$_2$C*H*$_2$O), 3.29 (s, 2 H, CNCMe$_2$C*H*$_2$O), 3.01 (d, 2 H, $^{3}J_{HH}$ = 7.2 Hz, *syn*-CH(C*H*$_2$)$_2$), 2.51 (d, 2 H, $^{3}J_{HH}$ = 11.2 Hz, *anti*-CH(C*H*$_2$)$_2$), 0.94 (s, 6 H, CNC*Me*$_2$CH$_2$O), 0.79 (s, 6 H, CNC*Me*$_2$CH$_2$O), 0.76 (s, 6 H, CNC*Me*$_2$CH$_2$O), –22.74 (s, br, 1 H, Rh*H*). ^{13}C{^{1}H} NMR (benzene-d_6, 175 MHz): δ 136.77 (*ortho*-C_6H_5), 127.05 (*meta*-C_6H_5), 125.81 (*para*-C_6H_5), 88.28 (d, $^{1}J_{RhC}$ = 7.0 Hz, *C*H(CH_2)$_2$), 80.11 (CNCMe$_2$*C*H$_2$O), 79.97 (CNCMe$_2$*C*H$_2$O), 69.53 (CN*C*Me$_2$CH$_2$O), 67.36 (CN*C*Me$_2$CH$_2$O), 37.46 (d, $^{1}J_{RhC}$ = 10.5 Hz, CH(*C*H$_2$)$_2$), 28.38 (CNC*Me*$_2$CH$_2$O), 27.85 (CNC*Me*$_2$CH$_2$O), 27.63 (CNC*Me*$_2$CH$_2$O). ^{11}B NMR (benzene-d_6, 128 MHz): δ –17.7 ^{15}N NMR (benzene-d_6, 71 MHz): δ –164.8 (*trans* to RhH), –173.8 (*cis* to RhH).

To^{M}RhH(η^3-C$_3$H$_4$Ph) (3.3). Allylbenzene (0.59 mL) and [Rh(μ-Cl)(COE)$_2$]$_2$ (0.159 g, 0.22 mmol) were allowed to react in benzene (10 mL) for 30 min to generate [Rh(μ-Cl)(C_3H_5Ph)$_2$]$_2$. The resulting solution was then added solid Tl[To^{M}] (260 mg, 0.44 mmol) and stirred overnight. Solids were filtered off and the filtrate was evaporated to dryness. The residue was washed with pentane (2 × 2 mL) and the resulting solid was dissolved in toluene (10 mL). The toluene solution was concentrated to 0.5 mL and the solid was collected as a green powder (0.160 g, 0.265 mmol, 59.8%). ^{1}H NMR (benzene-d_6, 400 MHz): δ 8.51 (d, 2 H, $^{3}J_{HH}$ = 7.6 Hz, *ortho*-C_6H_5), 7.60 (t, 2 H, $^{3}J_{HH}$ = 7.6 Hz, *meta*-C_6H_5), 7.44 (d, 2 H, $^{3}J_{HH}$ = 7.6 Hz, *ortho*-$CH_2CHCHPh$), 7.39 (t, 1 H, $^{3}J_{HH}$ = 7.6 Hz, *para*-C_6H_5), 7.11 (t, 2 H, $^{3}J_{HH}$ = 7.2 Hz, *meta*-$CH_2CHCHPh$), 7.09 (t, 1 H, $^{3}J_{HH}$ = 7.2 Hz, *para*-$CH_2CHCHPh$), 5.62 (m, 1 H,

$CH_2CHCHPh$), 3.98 (d, 1 H, $^3J_{HH}$ = 10.4 Hz, $CH_2CHCHPh$), 3.64 (d, 1 H, $^2J_{HH}$ = 8.4 Hz, $CNCMe_2CH_2O$), 3.48 (dd, 2 H, $^2J_{HH}$ = 8.4 Hz, $CNCMe_2CH_2O$), 3.40 (dd, 2 H, $^2J_{HH}$ = 8.0 Hz, $CNCMe_2CH_2O$), 3.22 (d, 1 H, $^3J_{HH}$ = 9.6 Hz, *syn*-$CH_2CHCHPh$), 3.20 (d, 1 H, $^2J_{HH}$ = 8.4 Hz, $CNCMe_2CH_2O$), 2.84 (d, 1 H, $^3J_{HH}$ = 11.2 Hz, *anti*-$CH_2CHCHPh$), 1.02 (s, 3 H, $CNCMe_2CH_2O$), 0.91 (s, 3 H, $CNCMe_2CH_2O$), 0.83 (s, 3 H, $CNCMe_2CH_2O$), 0.76 (s, 3 H, $CNCMe_2CH_2O$), 0.72 (s, 3 H, $CNCMe_2CH_2O$), 0.39 (s, 3 H, $CNCMe_2CH_2O$), –22.48 (s, br, 1 H, Rh*H*). $^{13}C\{^1H\}$ NMR (benzene-d_6, 175 MHz): δ 145.57 (*ipso*-$CH_2CHCHPh$), 136.74 (*ortho*-C_6H_5), 129.43 (*meta*-$CH_2CHCHPh$), 129.21 (*ortho*-$CH_2CHCHPh$), 127.09 (*meta*-C_6H_5), 125.86 (*para*-C_6H_5), 125.54 (*para*-$CH_2CHCHPh$), 90.06 (d, $^1J_{RhC}$ = 3.5 Hz, $CH_2CHCHPh$), 81.39 ($CNCMe_2CH_2O$), 79.89 ($CNCMe_2CH_2O$), 79.38 ($CNCMe_2CH_2O$), 69.91 ($CNCMe_2CH_2O$), 68.06 ($CNCMe_2CH_2O$), 67.56 ($CNCMe_2CH_2O$), 54.52 (d, $^1J_{RhC}$ = 10.5 Hz, $CH_2CHCHPh$), 36.54 (d, $^1J_{RhC}$ = 12.25 Hz, $CH_2CHCHPh$), 28.52 ($CNCMe_2CH_2O$), 27.91 ($CNCMe_2CH_2O$), 27.59 ($CNCMe_2CH_2O$), 27.48 ($CNCMe_2CH_2O$), 27.03 ($CNCMe_2CH_2O$), 26.89 ($CNCMe_2CH_2O$). ^{11}B NMR (benzene-d_6, 128 MHz): δ –19.7. ^{15}N NMR (benzene-d_6, 71 MHz): δ –168.17 (*cis* to RhH), –172.10 (*cis* to RhH), –179.94 (*trans* to RhH). IR (KBr, cm^{-1}): ν 3041 (m), 2967 (m), 2927 (m), 2882 (m), 2081 (m, ν_{RhH}), 1590 (s, ν_{CN}), 1462 (w), 1366 (m), 1351 (m), 1276 (m), 1198 (m), 1177 (m), 1153 (m), 1022 (w), 999 (m), 970 (m). Anal. Calcd. for $C_{30}H_{39}BRhN_3O_3$: C, 59.72; H, 6.52; N, 6.96. Found: C, 60.18; H, 6.11; N, 6.88. Mp: 191–192 °C, dec.

To^{M}RhH(κ^2-OAc) (3.4). Acetic acid (0.021 g, 0.346 mmol) and **3.1** (0.103 g, 0.173 mmol) were allowed to react in benzene (10 mL) at room temperature for 10 min. The resulting mixture was then evaporated to dryness. The residue was extracted with pentane (15 mL),

dried under vacuum, and crystallized in toluene at −35 °C to give a brown solid (0.043 g, 0.076 mmol, 44.0%). ^{1}H NMR (benzene-d_6, 400 MHz): δ 8.40 (d, 2 H, $^{3}J_{HH}$ = 7.2 Hz, *ortho*-C_6H_5), 7.57 (t, 2 H, $^{3}J_{HH}$ = 7.6 Hz, *meta*-C_6H_5), 7.38 (t, 1 H, $^{3}J_{HH}$ = 7.2 Hz, *para*-C_6H_5), 3.78 (s, 2 H, CNCMe$_2$C*H*$_2$O), 3.52 (d, 2 H, $^{2}J_{HH}$ = 8.4 Hz, CNCMe$_2$C*H*$_2$O), 3.47 (d, 2 H, $^{2}J_{HH}$ = 8.4 Hz, CNCMe$_2$C*H*$_2$O), 1.59 (s, 3 H, O$_2$C*Me*), 1.25 (s, 6 H, CNC*Me*$_2$CH$_2$O), 1.17 (s, 6 H, CNC*Me*$_2$CH$_2$O), 1.11 (s, 6 H, CNC*Me*$_2$CH$_2$O), −13.23 (d, 1 H, $^{1}J_{RhH}$ = 11.6 Hz, Rh*H*). ^{13}C{^{1}H} NMR (benzene-d_6, 175 MHz): δ 190.29 (O$_2$*C*Me), 136.31 (*ortho*-C_6H_5), 127.36 (*meta*-C_6H_5), 126.38 (*para*-C_6H_5), 82.22 (CNCMe$_2$*C*H$_2$O), 80.33 (CNCMe$_2$*C*H$_2$O), 68.42 (CN*C*Me$_2$CH$_2$O), 67.03 (CN*C*Me$_2$CH$_2$O), 28.38 (CNC*Me*$_2$CH$_2$O), 27.66 (CNC*Me*$_2$CH$_2$O), 23.91 (O$_2$C*Me*). ^{11}B NMR (benzene-d_6, 128 MHz): δ −18.2. ^{15}N NMR (benzene-d_6, 71 MHz): δ −154.3 (*trans* to RhH), −221.0 (*cis* to RhH). IR (KBr, cm^{-1}): ν 2963 (m), 2927 (m), 2076(m, ν_{RhH}), 1597 (s, ν_{CN}), 1470 (s, ν_{COO}), 1387 (w), 1367 (m), 1284 (m), 1263 (m), 1202 (m), 1162 (m), 1026 (w), 999 (w), 968 (m). Anal. Calcd. for $C_{23}H_{33}BRhN_3O_5$: C, 50.66; H, 6.10; N, 7.71. Found: C, 51.05; H, 6.23; N, 7.50. Mp 115−118 °C, dec.

To^{M}RhBr(η^3-C$_3$H$_4$Ph) (3.5). A benzene solution of **3.3** (0.104g, 0.172 mmol) and NBS (0.031 g, 0.174 mmol) was stirred at room temperature overnight. The resulting solution was evaporated to dryness and washed with pentane (2 mL) and ether (4 × 1.5 mL). The residue was dried under vacuum to give a brown solid (0.049 g, 0.072 mmol, 42%). ^{1}H NMR (methylene chloride-d_2, 700 MHz): δ 7.91 (d, 2 H, $^{3}J_{HH}$ = 6.3 Hz, *ortho*-CH$_2$CHCHPh), 7.79 (d, 2 H, $^{3}J_{HH}$ = 7.0 Hz, *ortho*-C_6H_5), 7.39 (t, 1 H, $^{3}J_{HH}$ = 7.0 Hz, *para*-CH$_2$CHCHPh), 7.33 (t, 2 H, $^{3}J_{HH}$ = 7.7 Hz, *meta*-CH$_2$CHCHPh), 7.21 (t, 2 H, $^{3}J_{HH}$ = 7.0 Hz, *meta*-C_6H_5), 7.14 (t, 1 H, $^{3}J_{HH}$ = 7.0 Hz, *para*-C_6H_5), 6.54 (m, 1 H, CH$_2$C*H*CHPh), 5.43 (d, 1 H, $^{3}J_{HH}$ = 13.3 Hz,

$CH_2CHCHPh$), 4.45 (d, 1 H, $^3J_{HH}$ = 8.4 Hz, *syn*-$CH_2CHCHPh$), 4.14 (d, 1 H, $^3J_{HH}$ = 11.9 Hz, *anti*-$CH_2CHCHPh$), 4.11 (d, 1 H, $^2J_{HH}$ = 7.7 Hz, $CNCMe_2CH_2O$), 3.98 (d, 1 H, $^2J_{HH}$ = 8.4 Hz, $CNCMe_2CH_2O$), 3.96 (d, 1 H, $^2J_{HH}$ = 8.4 Hz, $CNCMe_2CH_2O$), 3.92 (d, 1 H, $^2J_{HH}$ = 7.7 Hz, $CNCMe_2CH_2O$), 3.77 (d, 1 H, $^2J_{HH}$ = 7.7 Hz, $CNCMe_2CH_2O$), 3.70 (d, 1 H, $^2J_{HH}$ = 8.4 Hz, $CNCMe_2CH_2O$), 1.52 (s, 3 H, $CNCMe_2CH_2O$), 1.40 (s, 3 H, $CNCMe_2CH_2O$), 1.31 (s, 3 H, $CNCMe_2CH_2O$), 1.18 (s, 3 H, $CNCMe_2CH_2O$), 0.98 (s, 3 H, $CNCMe_2CH_2O$), 0.75 (s, 3 H, $CNCMe_2CH_2O$). $^{13}C\{^1H\}$ NMR (methylene chloride-d_2, 175 MHz): δ 141.77 (*ipso*-$CH_2CHCHPh$), 135.85 (*ortho*-C_6H_5), 129.38 (*meta*-$CH_2CHCHPh$), 128.61 (*ortho*-$CH_2CHCHPh$), 127.04 (*para*-$CH_2CHCHPh$), 126.59 (*meta*-C_6H_5), 125.67 (*para*-C_6H_5), 112.29 ($CH_2CHCHPh$), 81.40 ($CNCMe_2CH_2O$), 80.74 ($CNCMe_2CH_2O$), 80.56 ($CNCMe_2CH_2O$), 72.26 ($CNCMe_2CH_2O$), 72.12 ($CNCMe_2CH_2O$), 70.22 ($CNCMe_2CH_2O$), 64.71 ($CH_2CHCHPh$), 37.34 (d, $^1J_{RhC}$ = 12.25 Hz, $CH_2CHCHPh$), 28.18 ($CNCMe_2CH_2O$), 27.86 ($CNCMe_2CH_2O$), 27.81 ($CNCMe_2CH_2O$), 27.45 ($CNCMe_2CH_2O$), 26.75 ($CNCMe_2CH_2O$), 26.21 ($CNCMe_2CH_2O$). ^{11}B NMR (methylene chloride-d_2, 128 MHz): δ –18.2. ^{15}N NMR (methylene chloride-d_2, 71 MHz): δ –181.5 (*cis* to RhBr), –191.1 (*cis* to RhBr), –217.6 (*trans* to RhBr). IR (KBr, cm^{-1}): ν 3039 (w), 2975 (w), 2883 (w), 1590 (s, ν_{CN}), 1466 (w), 1387 (w), 1368 (w), 1286 (m), 1245 (w), 1202 (m), 1028 (w), 1001 (w), 973 (m). Anal. Calcd. for $C_{30}H_{38}BRhN_3O_3Br$: C, 52.81; H, 5.61; N, 6.16; Found: C, 52.86; H, 5.48; N, 5.90. Mp: 215–218 °C, dec.

$To^MRh(CNt\text{-}Bu)_2$ (3.6). CN*t*-Bu (51 μL, 0.46 mmol) was added to a benzene solution of **3.1** (0.138 g, 0.232 mmol). The resulting solution was stirred for 2 h, and then the volatile materials were evaporated under reduced pressure. The residue was then washed with ether

to give a yellow solid (0.100 g, 0.153 mmol, 66.2%). ^{1}H NMR (benzene-d_6, 400 MHz): δ 8.42 (d, 2 H, $^{3}J_{HH}$ = 7.2 Hz, *ortho*-C_6H_5), 7.48 (t, 2 H, $^{3}J_{HH}$ = 7.6 Hz, *meta*-C_6H_5), 7.25 (t, 1 H, $^{3}J_{HH}$ = 7.2 Hz, *para*-C_6H_5), 3.71 (s, 6 H, $CNCMe_2CH_2O$), 1.35 (s, 18 H, $CNCMe_2CH_2O$), 0.97 (s, 18 H, $CNCMe_3$). $^{13}C\{^{1}H\}$ NMR (benzene-d_6, 175 MHz): δ 135.47 (*ortho*-C_6H_5), 128.50 (d, $^{1}J_{RhC}$ = 63.5 Hz, $RhCNCMe_3$), 127.35 (*meta*-C_6H_5), 125.37 (*para*-C_6H_5), 79.00 ($CNCMe_2CH_2O$), 68.33 ($CNCMe_2CH_2O$), 55.98 ($CNCMe_3$), 30.76 ($CNCMe_2CH_2O$), 28.70 ($CNCMe_3$). ^{11}B NMR (benzene-d_6, 128 MHz): δ –18.0. ^{15}N NMR (benzene-d_6, 71 MHz): δ –159.6 ($CNCMe_2CH_2O$), –201.1 ($CNCMe_3$). IR (CH_2Cl_2, cm^{-1}): ν 2962 (m), 2924 (m), 2892 (m), 2865 (w), 2208 (w, $\nu_{C\equiv N}$), 2147 (s, $\nu_{C\equiv N}$), 2103 (s, $\nu_{C\equiv N}$), 2068 (s, $\nu_{C\equiv N}$), 1614 (m, $\nu_{C=N}$), 1585 (s, $\nu_{C=N}$), 1460 (m), 1431 (w), 1368 (m), 1352 (m), 1274 (m), 1196 (m), 1173 (w), 1162 (w), 1119 (w), 1036 (w), 966 (m). Anal. Calcd. for $C_{31}H_{47}BN_5O_3Rh$: C, 57.15; H, 7.27; N, 10.75 Found: C, 57.00; H, 6.94; N, 10.32. Mp: 216–219 ºC , dec.

***exo*-To^{M}Rh(NHTs)(η^3-C_3H_5) (3.7). 3.2** (0.101 g, 0.192 mmol) was added to a solution of TsN_3 (38 mg, 0.19 mmol) in benzene (10 mL). The resulting solution was stirred for 24 h. The benzene solvent was evaporated in vacuo, and the residue was dissolved in a minimal amount of toluene and cooled to –30 °C for crystallization. Orange needles were collected by filtration at –30 °C, giving analytically pure To^{M}Rh(NHTs)(η^3-C_3H_5) (**3.7**) in good yield (0.109 g, 0.157 mmol, 81.7%). ^{1}H NMR (benzene-d_6, 400 MHz): δ 8.26 (d, 2 H, $^{3}J_{HH}$ = 7.2 Hz, *ortho*-C_6H_5), 7.86 (d, 2 H, $^{3}J_{HH}$ = 8.4 Hz, *ortho*-C_6H_4Me), 7.54 (t, 2 H, $^{3}J_{HH}$ = 7.6 Hz, *meta*-C_6H_5), 7.36 (t, 1 H, $^{3}J_{HH}$ = 7.2 Hz, *para*-C_6H_5), 6.87 (d, 2 H, $^{3}J_{HH}$ = 8.0 Hz, *meta*-C_6H_4Me), 5.60 (m, 1 H, $CH(CH_2)_2$), 5.17 (d, 2 H, $^{3}J_{HH}$ = 12.4 Hz, *anti*-$CH(CH_2)_2$), 4.19 (d, 2 H, $^{3}J_{HH}$ = 8.8 Hz, *syn*-$CH(CH_2)_2$), 3.58 (d, 2 H, $^{2}J_{HH}$ = 8.0, $CNCMe_2CH_2O$), 3.39 (d, 2 H,

$^{2}J_{HH}$ = 8.4 Hz, $CNCMe_2CH_2O$), 3.03 (s, 2 H, $CNCMe_2CH_2O$), 1.97 (s, 3 H, C_6H_4Me), 1.40 (s, 6 H, $CNCMe_2CH_2O$), 0.92 (s, 6 H, $CNCMe_2CH_2O$), 0.37 (s, 6 H, $CNCMe_2CH_2O$). $^{13}C\{^{1}H\}$ NMR (benzene-d_6, 175 MHz): δ 147.44 (*ipso*-C_6H_4Me), 140.17 (*para*-C_6H_4Me), 136.40 (*ortho*-C_6H_5), 129.34 (*meta*-C_6H_4Me), 127.18 (*meta*-C_6H_5), 126.71 (*ortho*-C_6H_4Me), 126.32 (*para*-C_6H_5), 103.09 (d, $^{1}J_{RhC}$ = 5.3 Hz, $CH(CH_2)_2$), 82.78 ($CNCMe_2CH_2O$), 80.63 ($CNCMe_2CH_2O$), 70.07 ($CNCMe_2CH_2O$), 69.08 ($CNCMe_2CH_2O$), 47.49 (d, $^{1}J_{RhC}$ = 10.5 Hz, $CH(CH_2)_2$), 28.31 ($CNCMe_2CH_2O$), 27.58 ($CNCMe_2CH_2O$), 27.51 ($CNCMe_2CH_2O$), 21.45 (C_6H_4Me). ^{11}B NMR (benzene-d_6, 128 MHz): δ −18.3. $^{15}N\{^{1}H\}$ NMR (benzene-d_6, 71 MHz): δ −177.59 (*cis* to RhNHTs), −255.43 (*trans* to RhNHTs). IR (KBr, cm^{-1}): ν 3341 (m, ν_{NH}), 3000 (m), 2970 (m), 2928 (m), 2885 (m), 1591 (s, ν_{CN}), 1462 (m), 1370 (m), 1287 (s, ν_{SO2}), 1262 (m), 1203 (s, ν_{SO2}), 1158 (m), 1134 (s, ν_{SO2}), 1088 (s), 998 (m), 965 (s, ν_{SO2}). Anal. Calcd. for $C_{31}H_{42}BN_4O_5RhS$: C, 53.46; H, 6.08; N, 8.04. Found: C, 53.90; H, 6.38; N, 7.85. Mp: 200–202 °C, dec.

$To^{M}RhH(NHTs)OH_2$ (3.8). 3.1 (0.166 g, 0.279 mmol) was added to a solution of TsN_3 (0.055 g, 0.279 mmol) in 10 mL of benzene (10 mL). The resulting mixture was stirred at room temperature for 3 h. All volatiles were evaporated, and the residue was washed with pentane (2 × 2 mL) to give a brown solid (0.126 g, 0.187 mmol, 67.0%). ^{1}H NMR (benzene-d_6, 400 MHz): δ 8.39 (d, 2 H, $^{3}J_{HH}$ = 6.8 Hz, *ortho*-C_6H_5), 8.19 (d, 2 H, $^{3}J_{HH}$ = 8.0 Hz, *ortho*-C_6H_4Me), 7.56 (t, 2 H, $^{3}J_{HH}$ = 7.2 Hz, *meta*-C_6H_5), 7.37 (t, 1 H, $^{3}J_{HH}$ = 7.6 Hz, *para*-C_6H_5), 6.88 (d, 2 H, $^{3}J_{HH}$ = 8.0 Hz, *meta*-C_6H_4Me), 3.79 (d, 1 H, $^{2}J_{HH}$ = 8.4 Hz, $CNCMe_2CH_2O$), 3.73 (d, 1 H, $^{2}J_{HH}$ = 8.4 Hz, $CNCMe_2CH_2O$), 3.58 (d, 1 H, $^{2}J_{HH}$ = 8.4 Hz, $CNCMe_2CH_2O$), 3.47 (d, 1 H, $^{2}J_{HH}$ = 8.4 Hz, $CNCMe_2CH_2O$), 3.38 (d, 1 H, $^{2}J_{HH}$ = 8.4 Hz, $CNCMe_2CH_2O$),

3.30 (d, 1 H, $^{2}J_{HH}$ = 8.8 Hz, CNCMe$_2$C*H*$_2$O), 2.32 (s, 1 H, N*H*Ts), 1.92 (s, 3 H, C$_6$H$_4$*Me*), 1.63 (s, 3 H, CNC*Me*$_2$CH$_2$O), 1.61 (s, 3 H, CNC*Me*$_2$CH$_2$O), 1.08 (s, 3 H, CNC*Me*$_2$CH$_2$O), 1.06 (s, 3 H, CNC*Me*$_2$CH$_2$O), 0.89 (s, 3 H, CNC*Me*$_2$CH$_2$O), 0.71 (s, 3 H, CNC*Me*$_2$CH$_2$O), –15.75 (d, 1 H, $^{1}J_{RhH}$ = 9.2 Hz, Rh*H*). ^{13}C{^{1}H} NMR (benzene-d_6, 175 MHz): δ 142.41 (*ipso*-C$_6$H$_4$Me), 142.31 (*para*-C$_6$H$_4$Me), 136.38 (*ortho*-C$_6$H$_5$), 129.78 (*meta*-C$_6$H$_4$Me), 127.30 (*meta*-C$_6$H$_5$), 126.37 (*ortho*-C$_6$H$_4$Me), 126.31 (*para*-C$_6$H$_5$), 82.25 (CNCMe$_2$*C*H$_2$O), 80.70 (CNCMe$_2$*C*H$_2$O), 79.70 (CNCMe$_2$*C*H$_2$O), 69.48 (CN*C*Me$_2$CH$_2$O), 67.14 (CN*C*Me$_2$CH$_2$O), 66.98 (CN*C*Me$_2$CH$_2$O), 28.93 (CNC*Me*$_2$CH$_2$O), 28.79 (CNC*Me*$_2$CH$_2$O), 27.77 (CNC*Me*$_2$CH$_2$O), 27.57 (CNC*Me*$_2$CH$_2$O), 27.53 (CNC*Me*$_2$CH$_2$O)**,** 27.29 (CNC*Me*$_2$CH$_2$O), 21.51 (C$_6$H$_4$*Me*). ^{11}B NMR (benzene-d_6, 128 MHz): δ –18.2. ^{15}N{^{1}H} NMR (benzene-d_6, 71 MHz): δ –154.1 (*trans* to RhH), –205.8 (*trans* to RhOH$_2$), –228.6 (*trans* to RhNHTs). IR (KBr, cm^{-1}): ν 3379 (br, ν_{OH}), 3300 (w, ν_{NH}), 3042 (w), 2964 (m), 2927 (m), 2889 (m), 2067 (m, ν_{RhH}), 1594 (s, ν_{CN}), 1495 (w), 1462 (m), 1433 (w), 1388 (w), 1367 (m), 1357 (m), 1289 (s, ν_{SO2}), 1267 (s, ν_{SO2}), 1205 (s, ν_{SO2}), 1160 (m), 1126 (w), 1090 (m), 1028 (w), 991 (m), 969 (s, ν_{SO}), 881 (w). Anal. Calcd. for C$_{28}$H$_{40}$BN$_4$O$_6$RhS: C, 49.86; H, 5.98; N, 8.31 Found: C, 49.91; H, 6.01; N, 8.30. Mp: 184–186 °C, dec.

References

(1) (a) Yu, J.-Q.; Shi, Z. *Top. Curr. Chem.* **2010**, *292*, 1-378. (b) Goldberg, K. I.; Goldman, A. S. Eds. *Activation and Functionalization of C–H Bonds*; ACS, Washington, D.C., 2004.

(2) Bergman, R. G. *Science* **2007**, *446*, 391-394.

(3) (a) Young, A. J.; White, M. C. *J. Am. Chem. Soc.* **2008**, *130*, 14090-14091, and references therein. (b) Young, A. J.; White, M. C. J. *Angew. Chem., Int. Ed.* **2011**, *50*, 6824-6827.

(4) Examples of intramolecular oxidative allylic amination: (a)Wu, L. ; Qiu, S.; Liu, G. *Org. Lett.* **2009**, *11*, 2707-2710. (b) Scarborough, C. C.; Bergant, A.; Sazama, G. T.; Guzei, I. A.; Spencer, L. C.; Stahl, S. S. *Tetrahedron.* **2009**, *65*, 5084-5092. (c) Yu, H.; Fu, Y.; Guo, Q.; Lin, Z. *Organometallics* **2009**, *28*, 4507-4512. (d) Fraunhoffer, K. J.; White, M. C. *J. Am. Chem. Soc.* **2007**, *129*, 7274-7276, and references cited therein.

(5) Examples of intermolecular oxidative allylic amination: (a) Reed, S. A.; White, M. C. *J. Am. Chem. Soc.* **2008**, *130*, 3316-3318. (b) Reed, S. A.; Mazzotti, A. R.; White, M. C. *J. Am. Chem. Soc.* **2009**, *131*, 11701-11706. (c) Liu, G.; Yin, G.; Wu, L. *Angew. Chem., Int. Ed.* **2008**, *47*, 4733-4736. (d) Shimizu, Y.; Obora, Y.; Ishii, Y. *Org. Lett.* **2010**, *12*, 1372-1374.

(6) (a) Hansson, S.; Heumann, A.; Rein, T.; Akermark, B. *J. Org. Chem.* **1990**, *55*, 975-984. (b) Åkermark, B.; Larsson, E. M.; Oslob, J. D. *J. Org. Chem.* **1994**, *59*, 5729-5733. (c) Grennberg, H.; BäcLckvall, J.-E. *Chem.–Eur. J.* **1998**, *4*, 1083-1089. (d) Grennberg, H.; Simon, V.; BäcLckvall, J.-E. *J. Chem. Soc., Chem. Commun.* **1994**, 265-266. (e) Chen, M. S.; White, M. C. *J. Am. Chem. Soc.* **2004**, *126*, 1346-1347. (f) Delcamp, J. H.; White, M. C. *J. Am. Chem. Soc.* **2006**, *128*, 15076-15077. (g) Pilarski, L. T.; Slander, N.; Böse, D.; Szabó, K. J. *Org. Lett.* **2009**, *11*, 5518-5521.

(7) Labinger, J. A.; Bercaw, J. E. *Nature* **2002**, *417*, 507-514.

(8) (a) Bergman, R. G. Science **1984**, *223*, 902-908. (b) Jones, W. D.; Feher, F. J. *Acc. Chem. Res.* **1989**, *22*, 91-100. (c) Arndtsen, B. A.; Bergman, R. G.; Mobley, T. A.; Peterson, T. H. *Acc. Chem. Res.* **1995**, *28*, 154-162.

(9) Evans, P. A. Ed. *Modern Rhodium-Catalyzed Organic Reactions*; Wiley-VCH Verlag GmbH & Co. KGaA, Weinheim, FRG., 2005; pp 191-212.

(10) Examples of cycloaddition type: (a) Li, Q.; Yu, Z.-X. *J. Am. Chem. Soc.* **2010**, *132*, 4542-4543. (b) Li, Q.; Yu, Z.-X. *Angew. Chem. Int. Ed.* **2010**, *50*, 2144-2147.

(11) (a) Colby, D. A.; Bergman, R. G.; Ellman, J. A. *Chem. Rev.* **2010**, *110*, 624-655. (b) Song, G.; Wang, F.; Li, X. *Chem. Soc. Rev.* **2012**, Advance Article, DOI: 10.1039/c2cs15281a.

(12) Tulip, T. H.; Ibers, J. A. *J. Am. Chem. Soc.* **1979**, *101*, 4201-4211.

(13) Fernández, M. J.; Rhodriguez, M. J.; Oro, L. A.; Lahoz, F. J. *J. Chem. Soc., Dalton Trans.* **1989**, 2073-2076.

(14) Tanke, R. S.; Crabtree, R. H. *Inorg. Chem.* **1989**, *28*, 3444-3447.

(15) (a) Peters, J. C.; Feldman, J. D. *J. Am. Chem. Soc.* **1999**, *121*, 9871-9872. (b) Feldman, J. C.; Peters, J. C.; Tilley, T. D. *Organometallics* **2002**, *21*, 4050-4064.

(16) Wick, D. D.; Jones, W. D. *Organometallics* **1999**, *18*, 495-505.

(17) Sexton, C. J.; López-Serrano, J.; Lledós, A.; Duckett, S. B. *Chem. Commun.* **2008**, 4834-4836.

(18) Ikeda, S.; Maruyama, Y.; Ozawa, F. *Organometallics* **1998**, *17*, 3770-3774.

(19) Yu, H.; Jia, G.; Lin, Z. *Organometallics* **2008**, *27*, 3825-3833 and references therein.

(20) Cenini, S.; Gallo, E.; Caselli, A.; Ragaini, F.; Fantauzzi, S.; Piangiolino, C. *Coord. Chem. Rev.*, **2006**, *250*, 1234-1253.

(21) Chiu, K. W.; Wilkinson, G.; Thornton-Pett, M.; Hursthouse, M. B. *Polyhdedron* **1984**, *3*. 79-85.

(22) Hillhouse, G. L.; Bercaw, J. E. *Organometallics* **1982**, *1*, 1025-1029.

(23) Sau, Y.-K.; Yi, X.-Y.; Chan, K.-W.; Lai, C.-S.; Williams, I. D.; Leung, W.-H. *J. Organomet. Chem.* **2010**, *695*, 1399-1404.

(24) (a) Davies, H. M. L.; Manning, J. R. *Nature*, **2008**, *451*, 417-424. (b) Collet, F.; Dodd, R. H.; Dauban, P. *Chem. Commun.* **2009**, 5061-5074. (c) Giri, R.; Shi, B.-F.; Engle, K. M.; Maugel, N.; Yu, J.-Q *Chem. Soc. Rev.* **2009**, *38*, 3242-3272.

(25) Ho, H.-A.; Dunne, J. F.; Ellern, A.; Sadow, A. D. *Organometallics* **2010**, *29*, 4105-4114.

(26) von der Ent, A.; Onderdelinden, A. L. *Inorg. Synth.* **1990**, *28*, 90.

(27) Ghosh, A. K.; Bischoff, A.; Cappiello, J. *Eur. J. Org. Chem.* **2003**, 821-832.

Chapter 4. Acceptorless photolytic alcohol decarbonylation and amine coupling catalyzed by tris(oxazolinyl)boratorhodium compounds

Modified from a paper to be submitted to *Angewandte Chemie International Edition*

Hung-An Ho,[‡] Arkady Ellern, Aaron D. Sadow[*]

Abstract

The compound $To^{M}RhH(\eta^3\text{-}C_8H_{13})$ (**3.1)** reacts with an excess amount of methanol, ethanol and benzylalcohol to afford the complex $To^{M}Rh(H)_2CO$ (**4.1**). We carried out catalytic primary alcohol decarbonylation by using **4.1** as the catalyst under photolytic condition, which generates hydrocarbons, CO and H_2 as the products. A series of rhodium and iridium complexes were examined for screening the catalyst efficiency of an alcohol decarbonylation, and it turned out that the compound $To^{M}Rh(CO)_2$ (**2.2)** is even more reactive than **4.1** for decarbonylation of primary alcohols. To further expand the generality, alkyl and aryl alcohols have been investigated by using 10 mol% of **2.2** to produce hydrocarbons in excellent yields under UV irradiation. Several alkyl and aryl amines were also studied under the same catalytic conditions. The net reaction of the amine transformation is the imine formation resulting from amine coupling and it serves as the first example of photocatalytic amine coupling under oxidant-free condition. To study the reaction mechanism, $To^{M}RhH(Ph)CO$ (**4.2**) and $To^{M}RhH(C_4H_3O)CO$ (**4.3**) are synthesized by treating **3.1** with benzaldehyde and furfural respectively. Also, **3.1** and 1 atm of H_2 react in

---

[‡] Primary researcher and author

[*] Author for correspondence

acetonitrile to give the complex $To^{M}Rh(H)_2(NCMe)$ (**4.4**). These compounds react with alcohol and benzaldehyde under thermal and/or photolytic conditions. Our mechanistic studies suggest photo-chemical ligand dissociation is not turnover-limiting, and studies of putative intermediates suggest several pathways may be involved in these conversions.

Introduction

Strategic substrate dehydrogenation has become a popular method for both bond formation and functional group transformation, where alcohols and amines have served as central roles for substrates selection.[1]

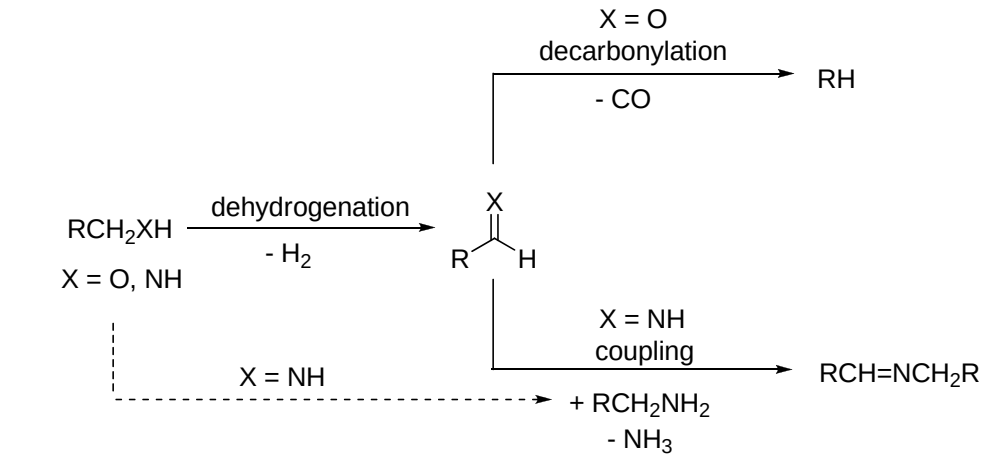

Net,

$$RCH_2OH \longrightarrow RH + CO + H_2 \qquad \Delta H = 22\text{-}30 \text{ Kcal/mol}$$

$$RCH_2NH_2 \longrightarrow \frac{1}{2} RCH{=}NCH_2R + \frac{1}{2} NH_3 + \frac{1}{2} H_2 \qquad \Delta H = 7 \text{ Kcal/mol}$$

Scheme 4.1. Catalytic hydrocarbon formation and imine synthesis *via* dehydrogenation and decarbonylation/coupling process.

The dehydrogenated products of primary alcohols and amines could be further converted to hydrocarbons and imines *via* aldehyde decarbonylation and amine coupling respectively, in

which the net reactions are both endothermic (22–30 Kcal/mol for alcohol decarbonylation and 7 Kcal/mol for amine coupling) (Scheme 4.1).[2] The alcohol decarbonylation process contains potential to be applied to removing highly oxygenated biomass-derived materials to become value-added fuels[3,4] while imines are important synthetic intermediates in organic synthesis, such that direct transformation of amines to imines has drawn much attention.[5]

Numerous examples have been demonstrated for stoichiometric alcohol decarbonylation. The original synthesis of Vaska's iridium complex involved ethylene glycol decarbonylation.[6] The reaction between $Cp^*IrCl_2(PMe_3)$ and primary alcohols gives the carbonyl-incorporated complex $[Cp^*IrR(CO)(PMe_3)]Cl$ (R = Me, Et, Ph) as the product.[7] Some iridium pincer compounds have also been documented to decarbonylate alcohols under thermal or photolytic conditions.[8] $Tp^*Rh(1,3\text{-COD})$ reacts with methanol photolytically to afford the dihydride carbonyl complex $Tp^*Rh(H)_2CO$.[9] Also, Tp-coordinated ruthenium complex $TpRuCl(PPh_3)(CH_3CN)$ undergoes decarbonylation with various primary alcohols in the presence of $NaBH_4$.[10] Under basic conditions, Wilkinson and his co-workers have disclosed decarbonylation of methoxide by the complex $RuHCl(PPh_3)_3$ to generate $Ru(H)_2(CO)(PPh_3)_3$.[11] Some other ruthenium complexes have been investigated to mediate the alcohol decarbonylations.[12] Meanwhile, limited catalytic cycles have been furnished and typically require a CO trap (for Pauson-Khand type reactions)[13] or a base to couple with CO to expel thermodynamically favorable CO_2 to increase the decarbonylation efficiency.[14]

On the other hand, photocatalytic amine coupling under aerobic conditions for imine synthesis have been a hot topic very recently. This type of reaction often needs molecular oxygen as an oxidant either at high pressure or atmospheric pressure. Zhao and co-workers

reported selective formation of imines by aerobic photocatalytic oxidation of amines on TiO_2.[15] Another example of using inorganic metal oxide for amine oxidation includes using Nb_2O_5 photocatalyst under 1 atm of O_2 with visible light.[16] In addition, mesoporous graphite carbon nitride (mpg-C_3N_4) species for oxidation of amines into imines under 0.5 MPa O_2 in excellent yields.[17] Herein, we report an acceptorless (a CO trap and/or a base is not needed) alcohol decarbonylation as well as the first example of photocatalytic amine coupling under oxidant-free condition.

Results and Discussion

Stoichiometric alcohol and aldehyde decarbonylation reactions

In Chapter 3, we reported the synthesis of **3.1** *via* salt metathesis of Tl[To^M] and [Rh(μ-Cl)(COE)$_2$]$_2$. Reductive elimination of **3.1** in reactions with various nucleophiles or 2 electron donors give the related complexes as well as cyclooctene as the major reaction pathway. That is, **3.1** could be viewed as a masked equivalent of the reactive {To^{M}Rh(I)} species precursor, and we attempt to utilize this pathway to react with primary alcohols (methanol, ethanol and benzyl alcohol). We initially added excess methanol to the solution of **3.1** in benzene-d_6. At room temperature, only starting materials are observed in mixtures of **3.1** and MeOH. However, **3.1** reacts with excess of methanol upon heating to 60 ºC in benzene-d_6 to give To^{M}Rh(H)$_2$CO (**4.1**) within 3 h in moderate yield (eq 4.1).

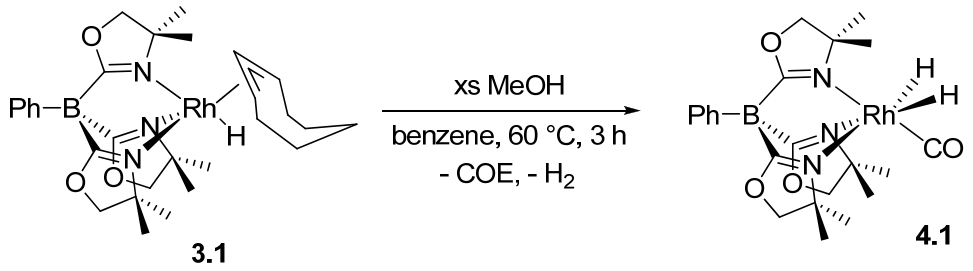

(4.1)

Intriguingly, treating **3.1** with either ethanol or benzyl alcohol under the same condition gives **4.1** as the only major product accompanied with methane or benzene formation respectively. These reactions were monitored by ^{1}H NMR spectroscopy in benzene-d_6.

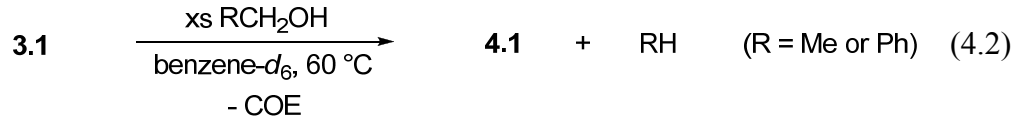

(4.2)

The reaction between **3.1** and ethanol-d_6 in benzene affords To^{M}Rh(D)$_2$CO, revealing that the metal hydride is originated from alcohols. **4.1** is C_s symmetric as evidenced by the splitting pattern in the ^{1}H NMR spectrum in which three singlets were observed at 1.03, 0.99 and 0.98 ppm for the methyl groups in the oxazolines. However, the chemical shifts of all the methylene protons are too close to be distinguished. More importantly, the distinctive dihydride resonance displayed a doublet at −13.33 ppm ($^{1}J_{RhH}$ = 18.4 Hz). In the ^{13}C{^{1}H} NMR spectrum, the carbonyl signal was detected at 192.05 ppm ($^{1}J_{RhC}$ = 68.3 Hz). The through-bond cross-peak between the rhodium hydride and the *trans* oxazoline nitrogen was detected in ^{1}H–^{15}N HMBC experiment (−166.6 ppm) like the cases in the previous chapter whereas the oxazoline nitrogen *trans* to CO was observed at −176.8 ppm. Lastly, the absorption band at 2019 cm^{-1} in the IR spectrum indicated the presence of CO.

A reasonable and possible intermediate of the alcohol decarbonylation is the formation of an aldehyde. Therefore, it is realistic to investigate the interaction between **3.1** and an aldehyde. Treating **3.1** with benzaldehyde in benzene-d_6 gives the complex To^{M}RhH(Ph)CO-d_6 (**4.2**-d_6) at room temperature over 6 h (eq 4.3).

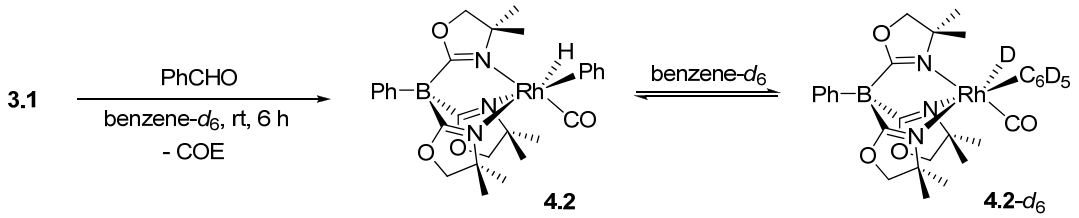

(4.3)

On the other hand, photolysis of the dicarbonyl complex **2.2** (To^{M}Rh(CO)$_2$) in benzene-d_6 with UV light provides the same product, **4.2**-d_6 (eq 4.4). For comparison, benzene C–H bond activation mediated by Tp*Rh(CO)$_2$ was reported two decades ago. The benzene C–H activation product, Tp*RhH(Ph)CO, is known to react with benzene-d_6 to give Tp*RhH(Ph)CO-d_6.[18]

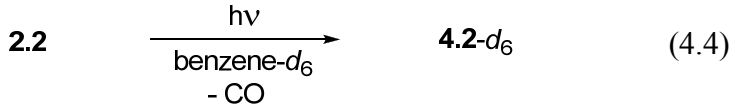

(4.4)

Owing to the C_1 symmetry of the complex **4.2**-d_6, six distinct oxazoline dimethyl and methylene peaks displayed in the ^{1}H NMR spectrum. The ^{13}C signal of the phenyl *ipso* carbon bonded to the rhodium center was detected at 143.07 ppm ($^{1}J_{RhC}$ = 25.7 Hz). The chemical shift at 192.71 ppm ($^{1}J_{RhC}$ = 65.8 Hz) in the ^{13}C{^{1}H} NMR spectrum as well as an absorption at 2030 cm^{-1} in the IR spectrum confirmed the presence of CO.

To further expand the generality of an aldehyde-decarbonylated complex such as **4.2**, the reaction between furfural and **3.1** was carried out to give the compound $To^{M}RhH(C_4H_3O)CO$ (**4.3**) at room temperature over 20 min (eq 4.5).

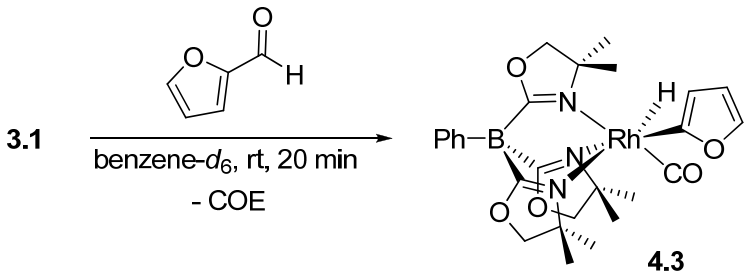

(4.5)

The complex **4.3** does not undergo hydrocarbon exchange with the solvent to give **4.2**-d_6. In addition, like the complex **4.2**, **4.3** was not isolated because it decomposes upon evaporation of the solvent. The diagnostic hydride appeared at –12.08 ppm ($^1J_{RhH}$ = 18.8 Hz) in the ^1H NMR spectrum. Also, three sets of doublet of doublet peaks for rhodium-bonded furyl group were observed at 7.59, 6.41 and 6.32 ppm representing 5-, 4- and 3-furyl protons respectively. This assignment was based on both chemical shifts and coupling constants. Moreover, the ^{13}C chemical shift of the furyl carbon bonded to the rhodium center was detected at 150.71 ppm ($^1J_{RhC}$ = 32.0 Hz) as well as the one at 3- position (119.72 ppm, $^2J_{RhC}$ = 4.4 Hz). Besides, the peak at 190.65 ppm in the $^{13}C\{^1H\}$ NMR spectrum was assigned as CO resonance ($^1J_{RhC}$ = 61.8 Hz). Regarding to the IR spectrum, the indicative absorption at 2280 and 2045 cm^{-1} were assigned to hydride and CO respectively.

Even though **4.3** could not be isolated, its reactions with $P(OMe)_3$ generates the CO-monosubstituted compound **2.4** along with the reductively eliminated furan (eq 4.6).

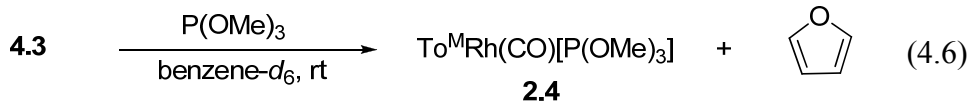

(4.6)

This reaction strongly supports the proposed structure and the connectivity of **4.3**.

In addition to an aldehyde, $\{To^{M}Rh(H)_2\}$ is also a highly possible intermediate during the decarbonylation process. We therefore sought a $\{To^{M}Rh(H)_2\}$ compound with a labile ligand, treating **3.1** under 1 atm H_2 in acetonitrile affords $To^{M}Rh(H)_2NCCH_3$ (**4.4**) at room temperature in 3 h (eq 4.7).

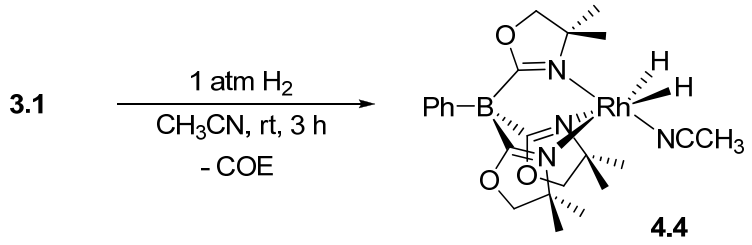

(4.7)

The proton signal of the acetonitrile in **4.4** appeared at 0.61 ppm and the distinctive hydride peak displayed at –16.20 ppm ($^{1}J_{RhH}$ = 18.4 Hz) as a doublet in the ^{1}H NMR spectrum. The ^{1}H–^{15}N HMBC experiment showed that the through metal cross-peak was observed between the metal hydride and the *trans* oxazoline nitrogen at –159.8 ppm whereas the oxazoline nitrogen *trans* to the acetonitrile was observed at –192.5 ppm as well as the nitrile nitrogen ($NCCH_3$) at –198.7 ppm. The hydride absorption bands in the IR spectrum were detected at 2054 and 2034 cm^{-1}. The X-ray quality crystal was obtained by slow vapor diffusion of ether into CH_2Cl_2 solution of **4.4** at –30 °C.

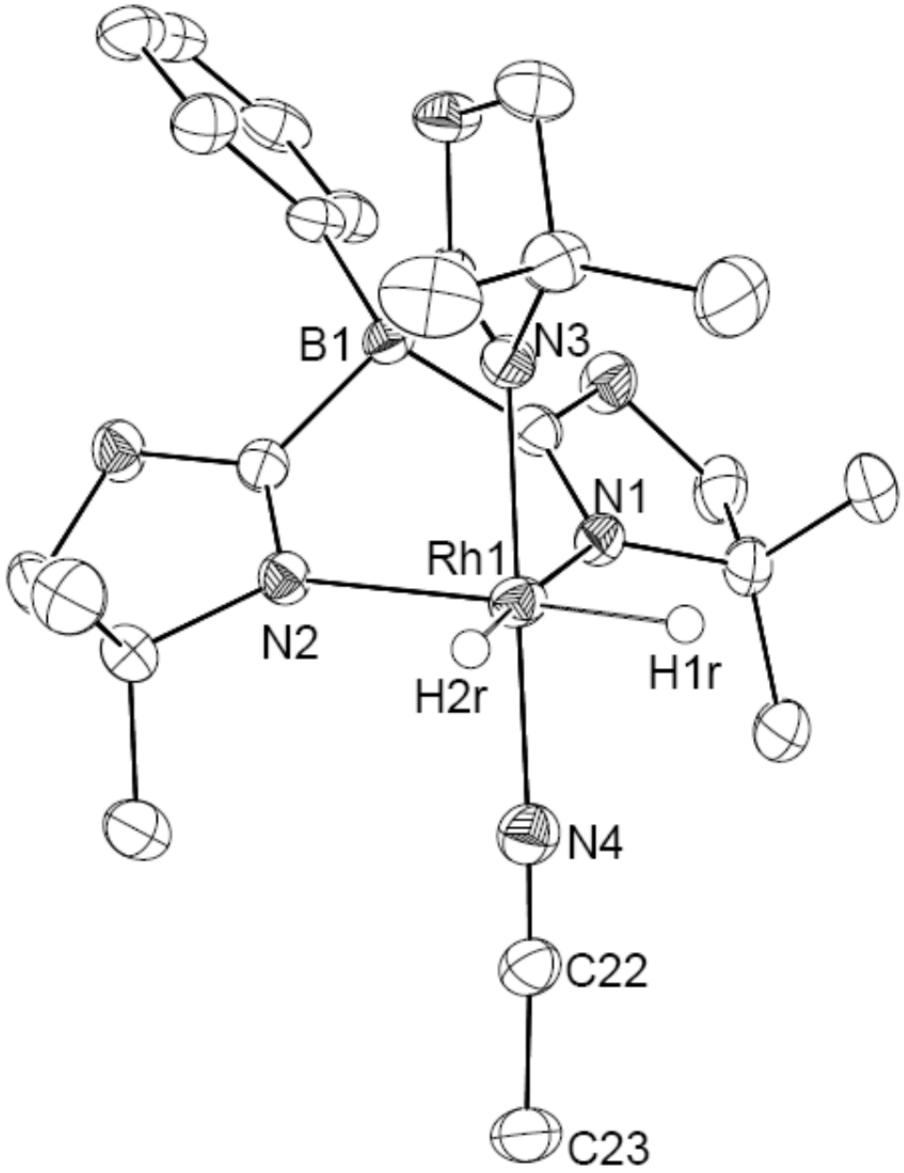

Figure 4.1. ORTEP diagram of **4.4**. Ellipsoids are drawn at 50% probability. All hydrogens except the hydrides are omitted for clarity. Selected bond distances (Å): Rh1–N1, 2.193(3); Rh1–N2, 2.173(3); Rh1–N3, 2.041(3); Rh1–N4, 1.987(3), Rh1–H1r, 1.53(4), Rh1–H2r, 1.56(4). Selected bond angles (°): N2–Rh1–N1, 86.90(10); N4–C22–C23, 178.1(4); H1r–Rh1–H2r, 80.(2); N1–Rh1–H1r, 95.5(14); N2–Rh1–H2r, 97.9(16).

In Chapter 3, **3.1** reacts with acetic acid *via* protonation of η^3-C_8H_{13} to give **3.4** (eq 3.4), and this was observed by a labeling experiment with AcOD. However, treating **3.1** with methanol-d_4 does not generate cyclooctene-d_1. This indicates that the reductive elimination is the only reaction mechanism for alcohol decarbonylations. Additionally, **3.1** is unchanged when heated at 60 °C in benzene for 6 h in the absence of aldehydes and alcohols and the reductive elimination rate decreases in the following order: CO ~ CN*t*-Bu > aldehyde > alcohol. These observations clearly suggest the substrate-induced reductive elimination of **3.1** is the first step for alcohol and aldehyde decarbonylations.

Catlaytic alcohol decarbonylations and amine couplings

Several attempts were made to develop the catalysis for this conversion. Initially, we used 10 mol% of **4.1** as the catalyst and cyclohexanemethanol ($CyCH_2OH$)[19] as the substrate in toluene-d_8. This mixture was heated at 120 °C for 24 h, but the resulting mixture contained only the alcohol starting material and black precipitate afterward. Next, we considered about using sacrificial reagent to assist in removing the major side products, H_2 and CO. For example, norbornene has been reported as an excellent hydrogen acceptor especially in alkane dehydrogenations.[20] Thus, one or more equivalents of norbornene was added to the mixture of $CyCH_2OH$ and **4.1** in toluene-d_8, heated at 120 °C. However, decomposition of rhodium species occurs after 12 h without conversion of $CyCH_2OH$. For another example, trimethylamine *N*-oxide (Me_3NO) has been known as a reagent for metal carbonyl decarbonylation to give trimethylamine and CO_2.[21] Unfortunately, Me_3NO is an ineffective additive when employing in the reaction at room temperature.

We then attempted on other strategies to achieve catalytic conversion. Light has been well studied for photo-induced CO dissociation from a metal complex. A classic example involves the photolysis of $W(CO)_6$ in the presence of 2 electron donor (L) to obtain $W(CO)_5L$, as well as many other types of reactions.[22] Initially, we investigated the photolysis of benzene solution of $CyCH_2OH$ with 10 mol% of **4.1** at room temperature under flood lamp (60 W) irradiation. The result showed that all the materials remained and no change was detected. A small amount of $CyCH_2OH$ could be converted to cyclohexane (CyH) after irradiating with rayonet reactor (250 nm) within 24 h (2.1%). Excitingly, photolysis of the reaction mixture with 450 W medium pressure mercury UV lamp gives 68% yield of CyH. The yield exceeds 95% after continuous 72 h irradiation (eq 4.8, Table 4.1, entry 1). GC-MS of aliquots of the catalytic reaction mixtures of $CyCH_2OH$ indicates the presence of the aldehyde, CyCHO. The gas phase withdrawn from a head space in this reaction was analyzed by GC-MS, revealing that D_2 and CO were formed during the decarbonylation process.[23]

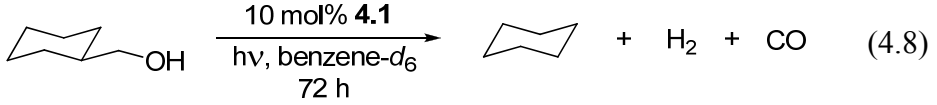

(4.8)

Switching the solvent to either acetonitrile-d_3 or methylene chloride-d_2 under the same conditions does not give any converted product (Table 4.1, entries 2 and 3). The sacrificial "acceptor" reagents did not increase the conversion efficiency. Instead, the reaction is inhibited by adding norbornene, which gives only 15% yield (Table 4.1, entry 4). Meanwhile, addition of Me_3NO results in catalyst decomposition (Table 4.1, entry 5). Several rhodium chloride dimers commonly used in catalysis were investigated in this reaction. However, none of these readily available rhodium complexes catalyze the conversion of $CyCH_2OH$

Table 4.1. Conditions and catalysts tested for the catalytic decarbonylation of $CyCH_2OH$.[a]

Entry	Solvent	Catalyst/ Additive	Time (h)	Yield (%)[b]
1	C_6D_6	**4.1**	72	> 95
2	CD_2Cl_2	**4.1**	24	0
3	CD_3CN	**4.1**	24	0
4	C_6D_6	**4.1**/ norbornene[c]	24	15
5	C_6D_6	**4.1**/ Me_3NO[c]	24	0
6	C_6D_6	$[Rh(CO)_2Cl]_2$	24	0
7	C_6D_6	$[Rh(COE)_2Cl]_2$	24	0
8	C_6D_6	$[Rh(COD)_2Cl]_2$	24	0
9	C_6D_6	$[Rh(CO)_2Cl_2]_2$/ dppm	24	0
10	C_6D_6	$[Rh(CO)_2Cl_2]_2$/ dppp	24	0.8
			72	1.6
11[d]	C_6D_6	$[Rh(dppp)_2Cl]$	24	0
12[d]	C_6D_6	$[Rh(CO)Cl(dppp)]_2$	24	0
13[d]	C_6D_6	$[Rh(dppe)_2Cl]$	24	0
14[d]	C_6D_6	[Rh(dppe)ClCO]	24	0
15	C_6D_6	$Cp^*Rh(CO)_2$	24	0
16	C_6D_6	$Cp^*Ir(CO)_2$	24	0
17	C_6D_6	$Tp^*Rh(CO)_2$	72	36
18	C_6D_6	$To^MRh(CO)_2$ (**2.2**)	24	> 95
19	C_6D_6	$To^PRh(CO)_2$ (**2.3**)	72	56
20	C_6D_6	$To^MIr(CO)_2$	24	0
21	C_6D_6	$(acac)Rh(CO)_2$	24	0
22	C_6D_6	$Bp^*Rh(CO)_2$	24	0
23	C_6D_6	[{*N*-Me-κ^2-To^M}$Rh(CO)_2$]OTf (**2.5**)	24	0

[a] Reaction conditions: 0.09 mmol of $CyCH_2OH$, 0.009 mmol of catalyst, 0.7 mL of solvent, 450 W medium pressure Hg lamp. [b] NMR yield. [c] 1 equiv of the additive. [d] Thermal conditions, in the dark at 110 ºC.

(Table 4.1, entries 6–8).

Furthermore, the combination of $[Rh(CO)_2Cl]_2$ and dppm shows no conversion at all whereas the carbonyl dimer with dppp gives 0.8 and 1.6 % conversion after 24 h and 72 h respectively (Table 4.1, entries 9 and 10). Rhodium(I) phosphine-based aldehyde decarbonylation catalysts are not active for alcohol dehydrogenation/decarbonylation under thermal or photochemical conditions.[24] For example, $[Rh(dppp)_2]Cl$ does not provide detectable quantities of cyclohexane under photolytic conditions, and a mixture of $[RhCl(CO)_2]_2$ and dppp gives only 1.6% conversion after 72 h of photolysis (Table 4.1, entries 11–14).

$Cp^*M(CO)_2$ (M = Rh, Ir) and $Tp^*Rh(CO)_2$ are known to react with C–H bonds under photochemical conditions.[18,25] However, neither $Cp^*M(CO)_2$ compound provides cyclohexane from $CyCH_2OH$ under the photolytic conditions (Table 4.1, entries 15 and 16). Interestingly, $Tp^*Rh(CO)_2$ catalyzes the partial conversion of $CyCH_2OH$ to CyH, CO, and H_2 under photolytic conditions (Table 4.1, entry 17). κ^2-Tp^*RhCO was proposed as a photochemically generated intermediate in C–H bond activation studies;[26] an isoelectronic [To^MRhCO] intermediate should be accessible from the photolysis of the dicarbonyl **2.2**, and this initial photolysis would provide an entry into a catalytic sequence of dehydrogenation and decarbonylation based on **4.1** and **2.2**. In fact, **2.2** is also an active catalyst for photochemical (but not thermal) alcohol decarbonylation and surprisingly, more active than **4.1** (Table 4.1, entry 18). In contrast to the rhodium complexes, the iridium analogue, $To^MIr(CO)_2$,[27] is not an effective catalyst under these conditions for alcohol decarbonylation (Table 4.1, entry 20). We speculated that the bidentate dicarbonyl complexes could catalyze

the decarbonylation. The $(acac)Rh(CO)_2$ and $Bp^*Rh(CO)_2$ complexes as well as the cationic $[\{N\text{-}Me\text{-}To^M\}Rh(CO)_2]OTf$ (**2.5**) were tested, yet these complexes fail to convert the alcohol to the alkane (Table 4.1, entries 21–23).

We then investigated the reaction using **2.2** as the catalyst for the decarbonylation of a sereis of primary alcohols (Table 4.2). The overall yield ranges from 81% to 99 %.

Table 4.2. Substrate scope of the photolytic alcohol decarbonylation.[a]

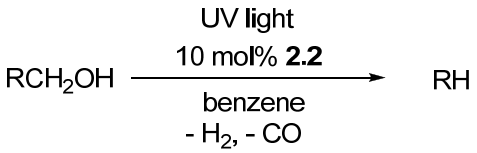

Entry	R	Time (h)	Yield (%)[b]
1	Cyp	24	93
2[c]	Cy	24	94
3[c]	Ph	24	92
4	4-MeC_6H_4	24	92
5	4-$MeOC_6H_4$	24	88
6	4-*t*-BuC_6H_4	24	90
7[d]	4-XC_6H_4	24	0
8	4-FC_6H_4	36	95
9	$PhCH_2$	24	99
10	$PhCH_2CH_2$	24	94
11	2-Naphthalyl	72	84
12	4-PhC_6H_4	72	81
13	Me_3SiCH_2	36	90

[a] Reaction conditions: Reaction conditions: 0.09 mmol of alcohols, 0.009 mmol of **2.2**, 0.7 mL of benzene, 450 W medium pressure Hg lamp. [b] GC yield. [c] Use toluene as the solvent. [d] X = CO_2Me, NO_2, Cl.

The alkyl alcohols (Table 4.2, entries 1 and 2) including silicon substituted 2,2-dimethyl butanol (Table 4.2, entry 13) were converted in excellent yields.

The benzyl alcohol derivatives were also decarbonylated to give arenes. Some of these functionalized substrates contain ether linkage or fluorine substituted phenyl rings (Table 4.2, entries 3–6 and 8). In contrast, this catalyst system do not tolerate ester, nitro and chloro functional groups, presumably due to deactivation of the reactive $To^{M}Rh(CO)$ intermediate by these moieties (Table 4.2, entry 7). Other alkyl/ aryl-tethered alcohols are also successfully decarbonylated (Table 4.2, entries 9 and 10). The biphenyl and naphthalyl methanol provide a slightly lower yield and longer reaction time probably due to the steric effect (Table 4.2, entries 11 and 12).

A dehydrogenation process of an alcohol must occur to generate an aldehyde as observed by GC-MS, and we suspected that amines could also undergo a dehydrogenation process whereas it has been documented that even a double dehydrogenation would proceed to form a nitrile.[28] Subsequently, we carried out the reaction under the same alcohol decarbonylation condition, using isobutylamine as the substrate instead. We discovered that the isobutylamine was indeed dehydrogenated, followed by coupling of another starting amine reagent to give the condensation product, *N*-*iso*-butylidene-*iso*-propylamine along with ammonia formation.

The results of the imine synthesis *via* amine coupling are summarized in Table 4.3. The dehydrogenation/coupling process of various amines was examined by using **2.2** as the catalyst. Linear aliphatic amines provide the corresponding imines in good yield (Table 4.3, entries 1 and 2) while cyclic/branched aliphatic amines were coupled in slightly better yield

than the linear ones (Table 4.3, entries 3 and 4). Benzylamine and the related *para* or *ortho* substituted derivatives were also investigated and the coupled imine products were obtained

Table 4.3. Oxidant-free imine synthesis from various primary amines.[a]

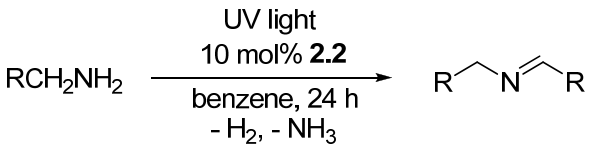

Entry	RCH_2NH_2	$RCH_2N{=}CHR$	Yield(%)[b]
1	*n*-$C_6H_{13}NH_2$	*n*-$C_6H_{13}N{=}CH(C_5H_{11})$	79
2	*n*-$C_7H_{15}NH_2$	*n*-$C_7H_{15}N{=}CH(C_6H_{13})$	77
3	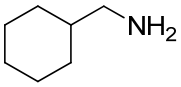	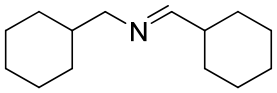	85
4	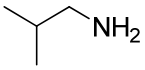	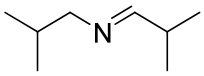	86
5	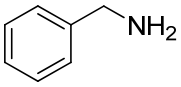	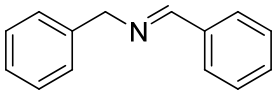	92
6	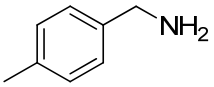	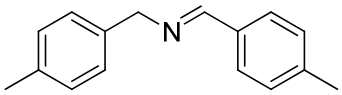	90
7	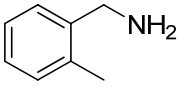	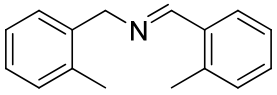	85
8	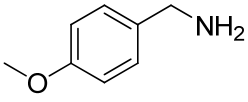	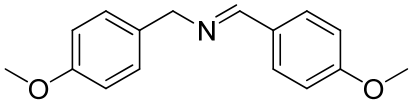	88
9	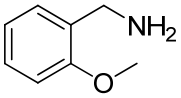	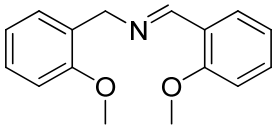	86
10	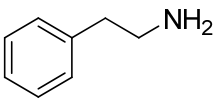	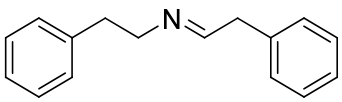	79

[a] Reaction conditions: Reaction conditions: 0.09 mmol of alcohols, 0.009 mmol of **2.2**, 0.7 mL of benzene, 450 W medium pressure Hg lamp. [b] GC yield.

at high yields (Table 4.3, entries 5–9). Phenylethylamine process proceeds under the same condition (Table 4.3, entry 10).

Catalytic reaction mechanism

To study the reaction mechanism, we attempted to determine a rate law for the photocatalytic decarbonylation of $CyCH_2OH$. It was unsuccessful, probably due to the catalyst decomposition over the reaction course. However, plots of $ln[C_6H_{13}CH_2OH]$ vs. time are linear for 2 half-lives (10 mol% of **2.2**, 4.5 h), suggesting that the substrate is present in the transition-state for the turnover-limiting step. As mentioned earlier, the dehydrogenation process to give an aldehyde is likely involved. We were curious about the interaction of an aldehyde with either **4.1** or **2.2**. Thermolysis of **4.1** or **2.2** with CyCHO gives decomposition results under both stoichiometric and catalytic conditions without conversion to CyH. Nevertheless, photolysis of CyCHO with either **4.1** or **2.2** under catalytic conditions converts the aldehyde to the decarbonylated product, CyH and the reaction yields reach 58% and 62% respectively within 30 min in benzene-d_6 (eq. 4.8).

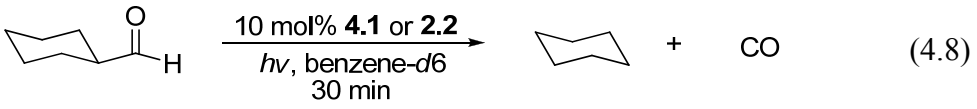

(4.8)

Obviously, the decarbonylation of an aldehyde is faster than the dehydrogenation/decarbonylation of an alcohol under the same photolytic and catalytic conditions.

We attempted to decipher the overall mechanism and study which steps proceed thermally and which require light. The photo-dissociation of CO ligand to produce carbonyl-

free intermediate is a possible step in the catalytic cycle. The reaction between carbonyl-free **4.4** and CyCHO gives **4.1** and CyH in toluene-d_8 at 110 ºC for 1.5 h (eq 4.9), which is in contrast to the photochemical reaction between carbonyl-containing **4.1** and CyCHO

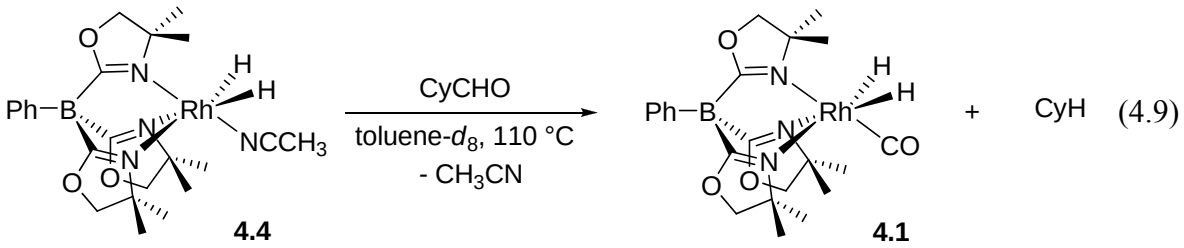

(4.9)

Compound **4.4** could also react with an alcohol under thermal conditions. For example, **4.4** reacts with $CyCH_2OH$ to give the complex **4.1**, CyH and H_2 in toluene-d_8 at 110 ºC (eq 4.10).

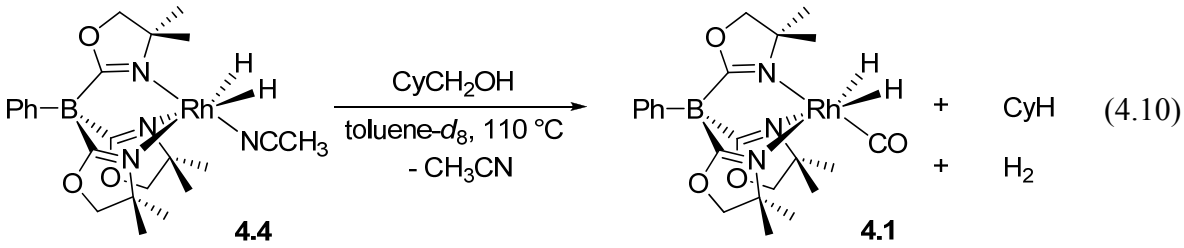

(4.10)

These two equations imply that **4.4** mediates sequential dehydrogenation and decarbonylation processes under thermal conditions. Comparing these two equations and the reactions of **4.1** with $CyCH_2OH$ or CyCHO under photolytic conditions, the results indicate that the carbonyl group in **4.1** and **2.2** hampers both alcohol and aldehyde thermal decarbonylations.

Moreover, complex **4.2** could also be another possible intermediate during the decarbonylation process. It is important to investigate the interactions between this

compound and other substrates. **4.2** reacts with PhCHO at room temperature in the dark to give **2.2** and two equivalents of benzene (eq 4.11).

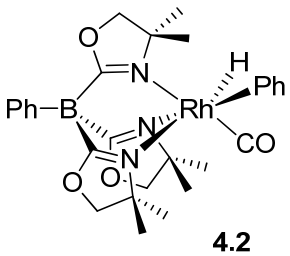

4.2

PhCHO, benzene-d_6, rt → $To^{M}Rh(CO)_2$ + 2 PhH (4.11)

2.2

It is worth noting that treating **3.1** with two equivalents of PhCHO also provides the complex **2.2** *via* the observable intermediate **4.2**. Meanwhile, **4.2** reacts with an alcohol as well. For instance, the reaction between **4.2** and $PhCH_2OH$ at room temperature affords **4.1**, one equivalent of PhH and one equivalent of PhCHO (eq 4.12).

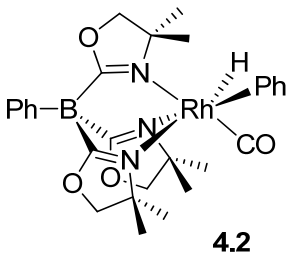

4.2

$PhCH_2OH$, benzene-d_6, rt → $To^{M}Rh(H)_2CO$ + PhH + PhCHO (4.12)

4.1

Finally, both **4.2** and **4.3** react with H_2 to give **4.1** and one equivalent of hydrocarbon in benzene-d_6 at room temperature (eq 4.13).

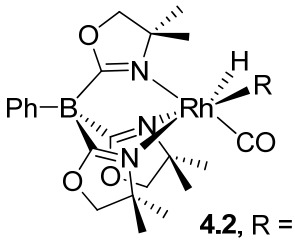

4.2, R = Ph
4.3, R = C_4H_3O

H_2, benzene-d_6, rt → $To^{M}Rh(H)_2CO$ + RH (4.13)

4.1

Combining these pieces of information of stochiometric reactivities, we could draw a catalytic cycle where several thermal and photolytic pathways are involved (Scheme 4.2). Complex **4.1** and **4.2** act as key joints for the three main cycles. The two sub-level cycles of an aldehyde decarbonylation under photolytic conditions are also crucial and indispensable for the overall mechanism.

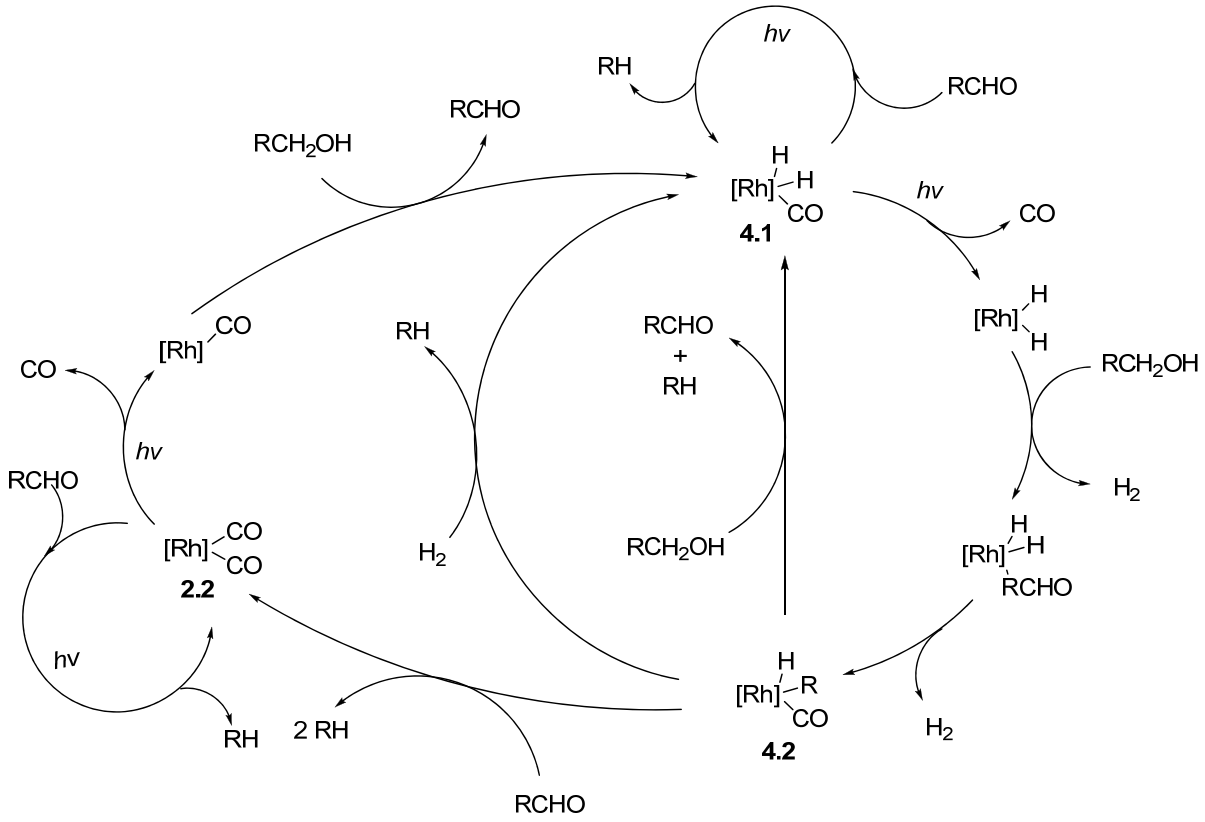

Scheme 4.2. Catalytic cycles involved in To^{M}Rh-mediated photocatalytic decarbonylation of primary alcohols with benzyl alcohol as the example substrate.

Conclusion

We have demonstrated acceptorless photolytic alcohol decarbonylation and amine coupling catalysis. The catalyst screening, substrate scope and reaction mechanism of alcohol decarbonylations are described here in this chapter. Although the mechanism of amine

coupling has yet not been entirely studied, it is presumably related to the alcohol decarbonylation mechanism. The catalysis cycle is complicated by several possible intermediates and a more detailed mechanism investigation is hindered by kinetics experiments due to the catalyst decomposition.

However, a sequential dehydrogenation/decarbonylation mechanism of an alcohol is established that we discovered the aldehyde decarbonylation is in fact faster than the alcohol decarbonylation. In addition, an aldehyde decarbonylation occurs at approximately the same rate with **4.1** as with **2.2**, but **2.2** is more efficient for alcohol decarbonylation than **4.1**. This also suggests that the photon-assisted ligand dissociation is not the turnover-limiting step. One could rationalize the enhanced reactivity of using **2.2** as supposed to **4.1** as the pre-catalyst for an alcohol decarbonylation by considering the ligand-dissociated intermediate [$To^{M}RhCO$] versus [$To^{M}Rh(H)_2$], which are generated by CO dissociation of **2.2** and **4.1** respectively. The other justification is that **2.2** is not accessible when **4.1** is used as the pre-catalyst while **4.1** is when **2.2** is used as the pre-catalyst. This would reduce the catalytic efficiency that both **4.1** and **2.2** are proved to catalyze sequential alcohol dehydrogenation/decarbonylation processes as well as aldehyde decarbonylations.

To this end, we illustrate a proof of concept of the dehydrogenative decarbonylation/coupling methodologies. We are currently searching more efficient photocatalytic systems as well as thermally accessible methods under more ambient anaerobic conditions.

Experimental

General. All manipulations were performed under an inert atmosphere using standard Schlenk techniques or in a glovebox. Pentane, benzene, toluene, diethyl ether and thf were degassed by sparging with N_2 and then dried with activated Al_2O_3 on an IT Solvent Purification System. Ethanol and methanol were dried over Na and distilled. Benzene-d_6 and toluene-d_8 were stirred over NaK alloy and then vacuum transferred. All other reagents were purchased from Sigma-Aldrich and used as received. $To^MRh(CO)_2$ (**2.2**),[29a] $To^PRh(CO)_2$ (**2.3**),[29a] [{*N*-Me-κ^2-To^M}Rh(CO)$_2$]OTf (**2.5**),[29a] $To^MRhH(\eta^3\text{-}C_8H_{13})$ (**3.1**),[29b] $To^MIr(CO)_2$,[29c] $[Rh(dppp)_2Cl]$,[30a] $[Rh(dppp)Cl(CO)]_2$,[30b] [Rh(dppe)ClCO],[30b] $[Rh(dppe)_2Cl]$,[30c] $Cp^*Rh(CO)_2$,[31a] $Cp^*Ir(CO)_2$,[31b] $Tp^*Rh(CO)_2$,[32] $(acac)Rh(CO)_2$,[33] $Bp^*Rh(CO)_2$,[34] were synthesized according to the literature procedures. All NMR spectra were obtained at room temperature using Bruker DRX-400 and Avance II-700 spectrometers. ^{15}N NMR chemical shifts were determined by ^1H-^{15}N HMBC experiments recorded on an Avance II-700 spectrometer; the chemical shift values are reported relative to CH_3NO_2. ^{11}B NMR spectra chemical shifts are reported relative to $BF_3{\cdot}Et_2O$. NMR yields were determined using *tetrakis*(trimethylsilyl)silane as the internal standard. Elemental analyses were obtained at the Iowa State Chemical Instrumentation Facility using a Perkin-Elmer 2400 Series II CHN/S. GC-MS was conducted with Agilent 6890 GC system equipped with Agilent DB-5 column. Mass detection is processed by Micromass GCT. Photolysis experiments were performed with ACE Inc. Hanovia 450 W medium pressure mercury lamp equipped with a water-jacketed quartz well cooled to 0 °C.

$To^MRh(H)_2CO$ (4.1). A solution of $To^MRhH(\eta^3\text{-}C_8H_{13})$ (**3.1**, 0.196 g, 0.329 mmol) and dry ethanol (5 mL) was stirred in benzene (20 mL) at 60 °C for 3 h. The solution was allowed to

cool to room temperature, and the reaction mixture was evaporated to dryness. The residue was extracted with benzene (20 mL), the extracts were reduced under vacuum, and the solid residue was then extracted with ether (15 mL). Evaporation of the ether gave a solid residue, which was finally extracted with pentane (2× 15 mL).The pentane solution was cooled at −35 °C. The pale brown precipitate was isolated by filtration and dried under vacuum to give To^{M}Rh(H)$_2$CO (0.088 g, 0.171 mmol, 52.0%). ^{1}HNMR (benzene-d_6, 400 MHz): δ 8.40 (d,2 H, $^{3}J_{HH}$ = 7.6 Hz, *ortho*-C_6H_5), 7.57 (t, 2 H, $^{3}J_{HH}$ = 7.6 Hz, *meta*-C_6H_5), 7.37 (t, 1 H, $^{3}J_{HH}$ = 7.2 Hz, *para*-C_6H_5), 3.53 (m, 6 H, CNCMe$_2$C*H*$_2$O), 1.03 (s, 6 H, CNC*Me*$_2$CH$_2$O), 0.99 (s, 6 H, CNC*Me*$_2$CH$_2$O), 0.98 (s, 6 H, CNC*Me*$_2$CH$_2$O), −13.33 (d, 2 H, $^{1}J_{RhH}$ = 18.4 Hz, Rh*H*).^{13}C{^{1}H} NMR (benzene-d_6, 175 MHz): δ 192.05 (d, CO, $^{1}J_{RhC}$ = 68.3 Hz), 136.46 (*ortho*-C_6H_5), 127.24 (*meta*-C_6H_5), 126.25 (*para*-C_6H_5), 80.40 (CNCMe$_2$*C*H$_2$O), 66.79 (CN*C*Me$_2$CH$_2$O), 65.67 (CN*C*Me$_2$CH$_2$O), 28.60 (CNC*Me*$_2$CH$_2$O), 28.49 (CNC*Me*$_2$CH$_2$O), 28.11 (CNC*Me*$_2$CH$_2$O). ^{11}B NMR (benzene-d_6, 128 MHz): δ −18.0. ^{15}N{^{1}H} NMR (benzene-d_6, 71 MHz): δ −166.6 (*trans* to RhH), −176.8 (*trans* to CO). IR (KBr, cm^{-1}): ν 2970 (m), 2926 (m), 2895 (m), 2019 (s, ν_{CO}), 1606 (m, ν_{CN}), 1459 (m), 1365 (m), 1354 (w), 1277 (m), 1196 (m), 1159 (m), 963 (m). Anal. Calcd. for $C_{22}H_{31}BN_3O_4Rh$: C, 51.29; H, 6.06; N, 8.16. Found: C, 51.45; H, 5.99; N, 7.99. Mp: 186–189 °C, dec.

To^{M}RhD(C$_6$D$_5$)CO (4.2-*d*$_6$). Method A: Photolysis of To^{M}Rh(CO)$_2$ in benzene-*d*$_6$. A light-green solution of To^{M}Rh(CO)$_2$ (**2.2**, 0.012 g, 0.023 mmol) dissolved in benzene-d_6 was degassed with freeze-pump-thaw cycles (2×) and then irradiated using a 450 W mercury lamp. After 15 min. of irradiation, the solution was again degassed and irradiated for an additional 15 min. to give a brown solution. The yield was 54% based on ^{1}H NMR

integration relative to a $Si(SiMe_3)_4$ standard. No other soluble To^MRh-containing species were detected by ^1H NMR spectroscopy. Attempts to isolate **4.2** by evaporation of the volatile materials or by crystallization gave an intractable black material that did not redissolve in benzene, so the compound was generated in situ for further reactivity studies.

Method B: Reaction of $To^MRhH(\eta^3\text{-}C_8H_{13})$ and benzaldehyde. A solution of $To^MRhH(\eta^3\text{-}C_8H_{13})$ (**3.1**, 0.015 g, 0.025 mmol) dissolved in benzene-$d_6$and benzaldehyde (0.003 g, 0.025 mmol) were mixed at room temperature. The mixture was allowed to react for 6 h to give the product. The yield was 72% based on integration relative to a $Si(SiMe_3)_4$ standard. ^{1}HNMR (benzene-d_6, 400 MHz):□ δ□8.35 (d,2 H, $^3J_{HH}$ = 6.8 Hz, *ortho*-C_6H_5), 7.56 (t, 2 H, $^3J_{HH}$ = 7.2 Hz, *meta*-C_6H_5), 7.37 (t, 1 H, $^3J_{HH}$ = 7.2 Hz, *para*-C_6H_5), 3.58 (d, 1 H, $^2J_{HH}$ = 8.4 Hz, $CNCMe_2CH_2O$), 3.54 (d, 2 H, $^2J_{HH}$ = 8.4 Hz, $CNCMe_2CH_2O$), 3.45 (d, 1 H, $^2J_{HH}$ = 8.4 Hz, $CNCMe_2CH_2O$), 3.42 (d, 1 H, $^2J_{HH}$ = 8.4 Hz, $CNCMe_2CH_2O$), 3.32 (d, 1 H, $^2J_{HH}$ = 8.4 Hz, $CNCMe_2CH_2O$), 0.98 (s, 3 H, $CNCMe_2CH_2O$), 0.96 (s, 3 H, $CNCMe_2CH_2O$), 0.90 (s, 3 H, $CNCMe_2CH_2O$), 0.88 (s, 3 H, $CNCMe_2CH_2O$), 0.82 (s, 3 H, $CNCMe_2CH_2O$), 0.46 (s, 3 H, $CNCMe_2CH_2O$). $^{13}C\{^1H\}$ NMR (benzene-d_6, 175 MHz): δ 192.71 (d, $^1J_{RhC}$ = 65.8 Hz, CO), 143.07 (d, $^1J_{RhC}$ = 25.7 Hz, *ipso*-RhC_6D_5), 136.45 (RhC_6D_5), 136.33 (*ortho*-BC_6H_5), 127.24 (RhC_6D_5), 127.13 (*meta*-BC_6D_5), 126.26 (*para*-BC_6H_5), 80.92 ($CNCMe_2CH_2O$), 80.07 ($CNCMe_2CH_2O$), 79.71 ($CNCMe_2CH_2O$), 69.30 ($CNCMe_2CH_2O$), 69.06 ($CNCMe_2CH_2O$), 66.40 ($CNCMe_2CH_2O$), 29.05 ($CNCMe_2CH_2O$), 28.97 ($CNCMe_2CH_2O$), 28.57 ($CNCMe_2CH_2O$), 28.52 ($CNCMe_2CH_2O$), 27.33 ($CNCMe_2CH_2O$), 26.13 ($CNCMe_2CH_2O$). ^{11}B NMR (benzene-d_6, 128 MHz): δ −17.5. $^{15}N\{^1H\}$ NMR (benzene-d_6, 71 MHz): δ −164.0,

−168.0, −174.2. IR (KBr, cm^{-1}): ν 2982 (w), 2884 (w), 2030 (s,ν_{CO}), 1645 (s, ν_{CN}), 1459 (m), 1366 (w), 1277 (m), 1197 (m), 970 (m).

$To^{M}RhH(C_4H_3O)CO$ (4.3). A solution of $To^{M}RhH(\eta^3\text{-}C_8H_{13})$ (**3.1**, 0.018 g, 0.030 mmol) in benzene-$d_6$was allowed to react with furfural (0.029 g, 0.030 mmol) at room temperature. The mixture turned light brown over 20 min. at room temperature (83%, NMR yield). Evaporation of the volatile materials provided a black solid that did not redissolve in benzene, so the compound was used without isolation. ^{1}HNMR (benzene-d_6, 400 MHz): δ 8.33 (d, 2 H, $^3J_{HH}$ = 6.8 Hz, *ortho*-C_6H_5), 7.59 (dd, 1 H, $^3J_{HH}$ = 2.0 Hz, $^4J_{HH}$ = 0.8 Hz, *5*-C_4H_3O), 7.55 (t, 2 H, $^3J_{HH}$ = 7.6 Hz, *meta*-C_6H_5), 7.37 (t, 1 H, $^3J_{HH}$ = 7.2 Hz, *para*-C_6H_5), 6.41 (dd, 1 H, $^3J_{HH}$ = 2.0 Hz, $^3J_{HH}$ = 2.8 Hz, *4*-C_4H_3O), 6.32 (dd, 1 H, $^3J_{HH}$ = 2.8 Hz, $^4J_{HH}$ = 0.4 Hz, *3*-C_4H_3O), 3.51 (m, 6 H, $CNCMe_2CH_2O$), 0.95 (s, 3 H, $CNCMe_2CH_2O$), 0.93 (s, 3 H, $CNCMe_2CH_2O$), 0.90 (s, 3 H, $CNCMe_2CH_2O$), 0.89 (s, 3 H, $CNCMe_2CH_2O$), 0.86 (s, 3 H, $CNCMe_2CH_2O$), 0.67 (s, 3 H, $CNCMe_2CH_2O$), −12.08 (d, 1 H, $^1J_{RhH}$ = 18.8 Hz, RhH). $^{13}C\{^1H\}$ NMR (benzene-d_6, 175 MHz): δ 190.65 (d, $^1J_{RhC}$ = 61.8 Hz, CO), 150.71 (d, $^1J_{RhC}$ = 32.0 Hz, *2*-C_4H_3O), 143.05 (*5*-C_4H_3O), 136.49 (*ortho*-C_6H_5), 127.23 (*meta*-C_6H_5), 126.29 (*para*-C_6H_5), 119.72 (d, $^2J_{RhC}$ = 4.4 Hz, *3*-C_4H_3O), 112.06 (*4*-C_4H_3O), 80.84 ($CNCMe_2CH_2O$), 80.37 ($CNCMe_2CH_2O$), 80.12 ($CNCMe_2CH_2O$), 68.32 ($CNCMe_2CH_2O$), 68.02 ($CNCMe_2CH_2O$), 66.45 ($CNCMe_2CH_2O$), 29.02 ($CNCMe_2CH_2O$), 28.93 ($CNCMe_2CH_2O$), 28.45 ($CNCMe_2CH_2O$), 28.26 ($CNCMe_2CH_2O$), 25.80 ($CNCMe_2CH_2O$), 24.24 ($CNCMe_2CH_2O$). ^{11}B NMR (benzene-d_6, 128 MHz): δ −17.9. $^{15}N\{^1H\}$ NMR (benzene-d_6, 71 MHz): δ −167.6 (trans to RhH), −173.6, −179.5. IR (KBr, cm^{-1}): ν 2916 (m), 2849 (m), 2280 (s,ν_{RhH}), 2045 (m, ν_{CO}), 1576 (m, ν_{CN}), 1453 (m), 1330 (m), 1161 (m), 812 (m).

To^{M}Rh(H)$_2$NCCH$_3$ (4.4). A solution of To^{M}RhH(η^3-C_8H_{13}) (**3.1**, 0.150 g, 0.252 mmol) in CH_3CN (25 mL) was degassed by two freeze-pump-thaw cycles and then charged with 1 atm H_2. The solution was allowed to stir for 3 h at room temperature and was then filtered. The filtrate was evaporated to dryness, and the residue was extracted with benzene. Benzene was removed under vacuum and the residue was washed with pentane (3 mL) and toluene (1.5 mL) to give a brown solid (0.056g, 0.105 mmol, 42%). ^{1}HNMR (benzene-d_6, 400 MHz): δ 8.58 (d,2 H, $^3J_{HH}$ = 7.2 Hz, *ortho*-C_6H_5), 7.62 (t, 2 H, $^3J_{HH}$ = 7.6 Hz, *meta*-C_6H_5), 7.40 (t, 1 H, $^3J_{HH}$ = 7.6 Hz, *para*-C_6H_5), 3.75 (d, 2 H, $^2J_{HH}$ = 8.4 Hz, CNCMe$_2$C*H*$_2$O), 3.71 (d, 2 H, $^2J_{HH}$ = 8.4 Hz, CNCMe$_2$C*H*$_2$O),3.58 (s, 2 H,CNCMe$_2$C*H*$_2$O),1.39 (s, 6 H, CNC*Me*$_2$CH$_2$O), 1.17 (s, 6 H, CNC*Me*$_2$CH$_2$O), 1.11 (s, 6 H, CNC*Me*$_2$CH$_2$O), 0.61 (s, 3 H, NC*Me*), −16.20 (d, 2 H, $^1J_{RhH}$ = 18.4 Hz, RhH). ^{13}C{^{1}H} NMR (benzene-d_6, 175 MHz): δ 136.79 (*ortho*-C_6H_5), 128.92 (N*C*CH$_3$), 127.08 (*meta*-C_6H_5), 125.80 (*para*-C_6H_5), 80.29 (CNCMe$_2$*C*H$_2$O), 79.62 (CNCMe$_2$*C*H$_2$O), 67.72 (CN*C*Me$_2$CH$_2$O), 66.16 (CN*C*Me$_2$CH$_2$O), 29.07 (CNC*Me*$_2$CH$_2$O), 28.65 (CNC*Me*$_2$CH$_2$O), 28.27 (CNC*Me*$_2$CH$_2$O), 2.06 (CN*Me*). ^{11}B NMR (benzene-d_6, 128 MHz): δ −18.0. ^{15}N{^{1}H} NMR (benzene-d_6, 71 MHz): δ −159.8 (*trans* to RhH), −192.5(*trans* to NCCH$_3$), −198.7 (*N*CMe). IR (KBr, cm^{-1}): ν 2961 (m), 2924 (m), 2878 (m), 2282 (w, ν_{NC}), 2054 (m, ν_{RhH}), 2034 (m, ν_{RhH}), 1603 (s, ν_{CN}), 1463 (m), 1363 (m), 1273 (m), 1200 (m), 970 (m). Anal. Calcd. for $C_{23}H_{34}BN_4O_3Rh$: C, 52.29; H, 6.49; N, 10.61 Found: C, 51.96; H, 6.33; N, 10.13. Mp: 214–217 °C, dec.

Representative example of catalytic decarbonylation and amine coupling conditions. A mixture of cyclohexanemethanol (0.09 mmol), catalyst (0.009 mmol), cyclooctane (0.09 mmol) as an internal standard and benzene (0.7 mL) was loaded into a J-Young style NMR

tube. The tube was positioned adjacent to the jacket outer wall of a Hanovia lamp (c.a. 1 cm) and subjected to irradiation with 450 W medium pressure mercury lamp. After the photolysis, the solution was diluted with CH_2Cl_2 and the yield of cyclohexane was determined by GC-MS from a calibration curve.

References

(1) Dobereiner, G. E.; Crabtree, R. H. *Chem. Rev.* **2010**, *110*, 681-703.

(2) Bond energy references: (a) Sanderson, R. T. *Polar covalence*; Academic Press: New York, 1983. (b) Sanderson, R. T. *Chemical bonds and bond energy*, 2nd ed.; Academic Press: New York, 1976.

(3) (a) Huber, G. W.; Iborra, S.; Corma, A. *Chem. Rev.* **2006**, *106*, 4044-4098. (b) Huber, G. W.; Chheda, J. N.; Barrett, C. J.; Dumesic, J. A. Science **2005**, *308*, 1446-1450.

(4) (a) de Lasa, H.; Salaices, E.; Mazumder, J.; Lucky, R.; *Chem. Rev.* **2011**, *111*, 5404-5433. (b) Matson, T. D.; Barta, K.; Iretskii, A. V.; Ford, P. C. *J. Am. Chem. Soc.* **2011**, *133*, 14090-14097.

(5) (a) Murahashi, S.-I.; *Angew. Chem. Int. Ed. Engl.* **1995**, *24*, 2443-2465. (b) Adams, J. P. *J. Chem. Soc., Perkin Trans. 1* **2000**, 125-139.

(6) Vaska, L.; DiLuzio, J. W. *J. Am. Chem. Soc.***1961**, *83*, 2784-2785.

(7) Klei, S. R.; Golden, J. T.; Tilley, T. D.; Bergman, R. G. *J. Am. Chem. Soc.* **2002**, *124*, 2092-2093.

(8) (a) Morales-Morales, D.; Redón, R.; Wang, Z.; Lee, D. W.; Yung, C.; Magnuson, K.; Jensen, C. M. *Can. J. Chem.* **2001**, *79*, 823-829. (b) Kloek, S. M.; Heinekey, D. M.;

Goldberg, K. I. Organometallics **2006**, *25*, 3007-3011. (c) Melnick, J. G.; Radosevich, A. T.; Villagrán, D.; Nocera, D. G. *Chem. Commun.* **2010**, *46*, 79-81.

(9) Boaretto, R.; Paolucci, G.; Sostero, S.; Traverso, O. *J. Mol. Catal. A: Chem.* **2003**, *204-205*, 253-258.

(10) Chen, Y.-Z.; Chan, W. C.; Lau, C. P.; Chu, H. S.; Lee, H. L.; Jia, G. *Organometallics* **1997**, *16*, 1241-1246.

(11) Chaudret, B. N.; Cole-Hamilton, D. J.; Nohr, R. S.; Wilkinson, G. *J. Chem. Soc., Dalton Trans.* **1977**, 1546-1557.

(12) (a) Coalter, J. N.; Huffman, J. C.; Caulton, K. G. *Organometallics* **2000**, *19*, 3569-3578. (b) Dinger, M. B.; Mol, J. C. *Organometallics* **2003**, *22*, 1089-1095. (c) Bolton, P. D.; Grellier, M.; Vautravers, N.; Vendier, L.; Sabo-Etienne, S. *Organometallics* **2008**, *27*, 5088-5093.

(13) Park, J. H.; Cho, Y.; Chung, Y. K. *Angew. Chem. Int. Ed.* **2010**, *49*, 5138-5141.

(14) (a) Kawai, T.; Sakata, T.; *J. Chem. Soc., Chem. Commun*. **1980**, 694-695. (b) Delgado-Lieta, E.; Luke, M. A.; Jones, R. F.; Cole-Hamilton, D. J. *Polyhedron*, **1982**, *1*, 839-840. (c) Morton, D.; Cole-Hamilton, D. J. *J. Chem. Soc., Chem. Commun.* **1987**, 248-249. (d) Morton, D.; Cole-Hamilton, D. J.; Utuk, I. D.; Paneque-Sosa, M.; Lopez-Poveda, M. *J. Chem. Soc., Dalton Trans.* **1989**, 489-495.

(15) Lang, X.; Ji, H.; Chen, C.; Ma, W.; Zhao, J. *Angew. Chem. Int. Ed.* **2011**, *50*, 3934-3937.

(16) Furukawa, S.; Ohno, Y.; Shishido, T.; Teramura, K.; Tanaka, T. *ACS Catal.* **2011**, *1*, 1150-1153.

(17) Su, F.; Mathew, S. C.; Möhlmann, L.; Antonietti, M.; Wang, X.; Blechert, S. *Angew. Chem. Int. Ed.* **2011**, *50*, 657-660.

(18) Ghosh, C. K.; Graham, W. A. G. *J. Am. Chem. Soc.* **1987**, *109*, 4726-4727.

(19) Chosen as a convenient substrate for product detection by ^{1}H NMR spectroscopy.

(20) (a) Liu, F. C.; Pak, E. B.; Singh, B.; Jensen, C. M.; Goldman, A. S. *J. Am. Chem. Soc.* **1999**, *121*, 4086-4087. (b) Ray, A.; Zhu, K. M.; Kissin, Y. V.; Cherian, A. E.; Coates, G. W.; Goldman, A. S. *Chem. Commun.* **2005**, 3388-3390. (c) Ray, A. L.; Kissin, Y. V.; Zhu, K. M.; Goldman, A. S.; Cherian, A. E.; Coates, G. W. *J. Mol. Catal. A: Chem.* **2006**, *256*, 200-207.

(21) (a) Luh, T.-Y. *Coord. Chem. Rev.* **1984**, *60*, 255–276. (b) Dasgupta, B.; Donaldson, W. A. *Tetrahedron Lett.* **1998**, *39*, 343–346. (c) Pearson, A. J.; Kwak, Y. *Tetrahedron Lett.* **2005**, *46*, 5417–5419.

(23) Under photolytic conditions in benzene-d_6, the reaction proceeds *via* H/D exchange.

(22) (a) Wrighton, M. *Chem. Rev.* **1974**, *74*, 401. (b) Geoffroy, G. L. *J. Chem. Educ.* **1983**, *60*, 861-866.

(24) Monrad, R. N.; Madsen, R. *J. Org. Chem.* **2007**, *72*, 9782-9785.

(25) (a) Hoyano, J. K.; Graham, W. A. G. *J. Am. Chem. Soc.* **1982**, *104*, 3723-3725. (b) Rest, A. J.; Whitwell, I.; Graham, W. A. G.; Hoyano, J. K.; McMaster, A. D. *J. Chem. Soc., Chem. Commun.* **1984**, 624-626. (c) Bengali, A. A.; Schultz, R. H.; Moore, C. B.; Bergman, R. G. *J. Am. Chem. Soc.* **1994**, *116*, 9585-9589.

(26) (a) Bromberg, S. E.; Yang, H.; Asplund, M. C.; Lian, T.; McNamara, B. K.; Kotz, K. T.; Yeston, J. S.; Wilkens, M.; Frei, H.; Bergman, R. G.; Harris, C. B. Science **1997**, *278*, 260-263. (b) Purwoko, A. A.; Lees, A. J. *Inorg. Chem.* **1996**, *35*, 675-682. (c) Purwoko, A. A.; Tibensky, S. D.; Lees, A. J. *Inorg. Chem.* **1996**, *35*, 7049-7055. (d) Yeston, J. S.; McNamara, B. K.; Bergman, R. G.; Moore, C. B. *Organometallics* **2000**, *19*, 3442-3446.

(27) Pawlikowski, A. V.; Gray, T. S.; Schoendorff, G.; Baird, B.; Ellern, A.; Windus, T. L.; Sadow, A. D. *Inorg. Chim. Acta* **2009**, *362*, 4517-4525.

(28) Bernskoetter, W. H.; Brookhart, M. *Organometallics* **2008**, *27*, 2036.

(29) (a) Ho, H.-A.; Dunne, J. F.; Ellern, A.; Sadow, A. D. *Organometallics* **2010**, *29*, 4105-4114.(b) Ho, H.-A.; Gray, T. S.; Baird, B.; Ellern, A.; Sadow, A. D. Dalton Trans. **2011**, *40*, 6500-6541. (c) Pawlikowski, A. V.; Gray, T. S.; Schoendorff, G.; Baird, B.; Ellern, A.; Windus, T. L.; Sadow, A. D. *Inorg. Chim. Acta* **2009**, *362*, 4517-4525.

(30) (a) James, B. R.; Mahajan, D. *Can . J. Chem.* **1979**, *57*, 180-187. (b) Sanger, A. R. *J. Chem. Soc., Dalton Trans.* **1997**, 120-129. (c) Sacco, A.; Ugo, R. *J. Chem. Soc.* **1964**, 3274-3278.

(31) (a) Kang, J. W.; Maitlis, P. M. *J. Organomet. Chem.* **1971**, *26*, 393-399. (b) Kang, J. W.; Moseley, K.; Maitlis, P. M. *J. Am. Chem. Soc.***1969**, *91*, 5970-5977.

(32) (a) Ghosh, C. K.; Graham, W. A. G. *J. Am. Chem. Soc.* **1987**, *109*, 4726-4727. (b) Purwoko, A. A.; Lees, A. J. *Inorg. Chem.* **1996**, *35*, 675-682.

(33) Hernandez-Gruel, M. A. F.; Pérez-Torrente, J. J.; Ciriano, M. A.; Oro, L. A. *Inorg. Synth.* **2004**, *34*, 128-129.

(34) Bonati, F.; Minghetti, G.; Banditelli, G. *J. Organomet. Chem.* **1974**, *87*, 365.

Chapter 5. Synthesis and characterization of cationic rhodium ethylene complexes supported by tris(pyrazolyl)methane

Modified from a paper to be submitted to *Journal of Organometallic Chemistry*

Hung-An Ho,[‡] Arkady Ellern, Aaron D. Sadow[*]

Abstract

New types of rhodium complexes supported by tris(pyrazolyl)methane (Tpm) have been synthesized. The structure, bonding properties and equilibrium behaviors in the solution state as well as in the solid state by X–ray crystallography have been investigated by using ^{1}H and $^{1}H–^{15}N$ HMBC spectroscopy. Two Tpm supported rhodium bis(ethylene) compounds $[TpmRh(C_2H_4)_2][PF_6]$ (**5.1**) and $[TpmRh(C_2H_4)_2][BAr^F{}_4]$ (**5.2**) ($BArF_4$ = tetrakis[3,5-bis(trifluoromethyl)phenyl]borate) are synthesized *via* salt metathesis. Treatment of **5.1** with π-acidic ligands CO and CN(*t*-Bu) gives the bridging dinuclear complex $[(TpmRh)_2(\mu\text{-}CO)_3][PF_6]_2$ (**5.3**) and disubstituted species $[TpmRh(CNt\text{-}Bu)_2][PF_6]$ (**5.5**) respectively. The breakup of bridging dimer **5.3** to react with C_2H_4 (1 atm) to form monomeric $[TpmRh(CO)(C_2H_4)][PF_6]$ (**5.4**). On the other hand, mono-substituted complexes $[TpmRh(C_2H_4)L][PF_6]$ (**5.6**, L = $NCCH_3$; **5.7**, L = tht (tht = tetrahydrothiophene); **5.8**, L = PMe_3) are generated by treating first compound with ligands. Exposure of **5.8** to a H_2 atmosphere affords the rhodium dihydride complex $[TpmRh(H)_2PMe_3][PF_6]$ (**5.9**). The hapticity of the compounds listed above are tridentate in solution except **5.5**, which exhibits a

---

[‡] Primary researcher and author

[*] Author for correspondence

κ^2-κ^3 equilibrium behavior. The hapticity of these compounds in the solid state are also determined by crystallography.

Introduction

Tris(pyrazolyl)borate (Tp) tridentate, monoanionic ligands have been well studied since their first report by Trofimenko in 1966.[1] The tridentate coordinate anionic Tp ligands are considered as five electron donors in the covalent model, and therefore may view as isoelectronic Cp analogues. The synthesis and catalysis applications of Tp-supported metal complexes have also been extensively reported.[2] For example, rhodium and iridium complexes bearing Tp ligands have been shown to activate inert C–H bonds of alkanes and alkenes.[3] $Tp^*Rh(PPh_3)_2$ and $Tp^*Rh(COD)$ are catalytic active in hydrophosphinylation.[4] Also, the combination of $[Rh(COD)Cl]_2$ with Tp gives a regioselective quinoline hydrogenation catalysis in one-pot system.[5]

On the other hand, tris(pyrazolyl)methane (Tpm) and its derivatives are neutral analogues of tridentate Tp spectator ligands, yet have drawn less attention.[6] A series of Tpm rhodium diene complexes were first[7] disclosed by Elguero and his co-workers.[7a] Several other iridium derivatives were also synthesized, and these show the reactivity toward alcohol activations.[7b] More recently, the substitution chemistry of the cationic carbonyl $Tpm^*Rh(I)(CO)_2$[8] (Tpm^* = 3,5-dimethyltris(pyrazolyl)methane) and the diene complexes $Tpm^*M(I)(diene)$[9] (M = Rh, Ir; diene = norbornadiene, COD, 2,3-dimethylbuta-1,3-diene) have been structurally explored and studied. Besides, the cationic iridium bis(ethylene) complex, $[TpmIr(C_2H_4)_2][BF_4]$, and its phosphine-substituted compound were compared with the Tp analogue.[10] The cationic Tpm^* analogue, $[Tpm^*Ir(C_2H_4)_2][PF_6]$, has been prepared and studied for reactivity as well.[11]

Nevertheless, the related rhodium cationic compounds containing bis(ethylene) ligands have remained unexplored. Here we report the synthesis and characterization of the complex $[TpmRh(C_2H_4)_2][X]$ (**5.1**, X = PF_6; **5.2**, X= $BAr^F{}_4$) and ethylene substitution reactions by various nucleophiles. Furthermore, the coordination of *fac*-tris chelating ligands of the group 9 transition metals has always been complicated that these complexes often form equilibrium of two different bonding modes (κ^2 and κ^3). The bonding mode of this type of complex in a solution phase does not necessarily correspond to its bonding mode in the solid state and (*vice versa*).[3] To solve the difficulties, the coordination mode and fluxionality are investigated by ^1H and $^1H–^{15}N$ NMR spectroscopy.

Results and Discussion

Synthesis and characterization of rhodium bis(ethylene) complexes

Reaction of the solid mixture of Tpm, $[Rh(\mu\text{-}Cl)(C_2H_4)_2]_2$ and $TlPF_6$ in methylene chloride at room temperature affords the complex $[TpmRh(C_2H_4)_2][PF_6]$ (**5.1**) within 5 h (eq 5.1). The signals of the ethylene appeared as a singlet at δ 2.74 in the ^1H NMR spectrum. The three pyrazoles are equivalent which showed three signals at 8.22, 7.96 and 6.50 ppm respectively. The ^{13}C NMR signal of ethylene group was observed at 51.56 ppm ($^1J_{RhC}$ = 12.3 Hz) in the $^{13}C\{^1H\}$ NMR spectrum. The solid state structure of the complex adopted TBP (TBP = trigonal bipyramidal) geometry, and all the pyrazole nitrogens are coordinated to the rhodium center (Fig 5.1).

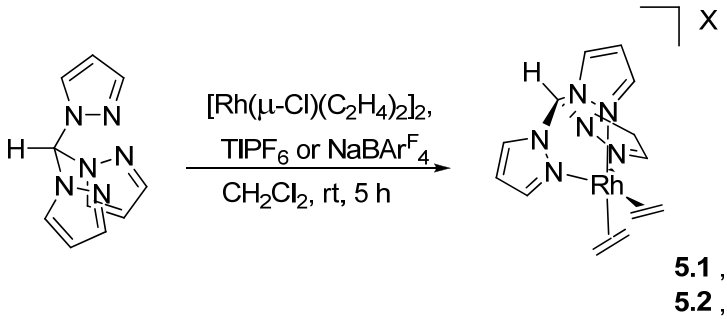

(5.1)

The distance of the two carbons of the ethylene ligand at the equatorial site (C11–C12, 1.461(6) Å) is, significantly, longer than the one at the axial position (C13–C14, 1.251(7) Å). Additionally, the average distance between the rhodium and ethylene carbon is shorter for the equatorial C_2H_4 (Rh1–C11, 2.081(3); Rh1–C12, 2.086(3); Rh1–C13, 2.167(4); Rh1–C13, 2.153(4) Å). These data are consistent with π back-donation of the rhodium equatorial ligand than to the axial one. In contrast, the two coordinated equatorial pyrazoles have a longer Rh–N distance (Rh1–N1, 2.220(2); Rh1–N6, 2.255(3) Å) compared to the axial Rh–N (Rh1–N4, 2.100(2) Å). However, since the TBP geometry should generate two sets of pyrazole signals in 2:1 ratio (2 for the equatorial pyrazoles and 1 for the axial one) and only one set of signal was observed for **5.1** in the solution ^{1}H NMR spectrum. Clearly, the compound is fluxional in the solution and a large portion of the equilibrium is established presumably due to inter-conversion between equatorial and axial positions of both pyrazoles and ethylene ligands rather than κ^2-κ^3 equilibrium of the coordination and uncoordination of the third pyrazole arm (more details related to fluxionality determination will be discussed below).

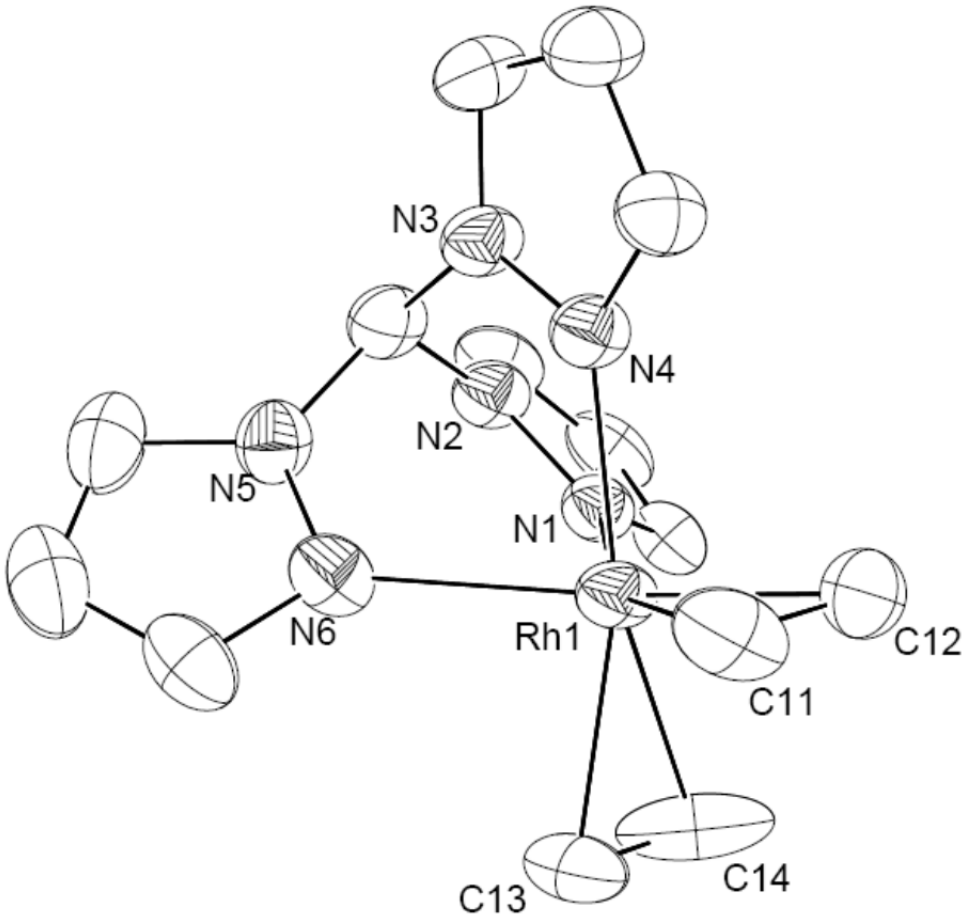

Figure 5.1. ORTEP diagram of [TpmRh(C_2H_4)$_2$][PF_6] (**5.1**) drawn at 50% probability. Hydrogen atoms and PF_6 are omitted for clarity. The crystal was obtained by slow vapor diffusion of Et_2O to CH_2Cl_2 solution at room temperature. Selected bond angles (°): C11–Rh1–C13, 88.0(2); C12–Rh1–C14, 85.3(2); N4–Rh1–N1, 83.27(9); N4–Rh1–N6, 81.35(9).

In comparison, an cationic iridium analogue, [Tpm*Ir(C_2H_4)$_2$][PF_6] (Tpm* = 3,5-dimethyltris(pyrazolyl)methane) has also been reported as a highly fluxional complex in solution ($CDCl_3$, 20 ºC) although no direct evidence was reported for the solid state structure.[11] So far, to the best of our knowledge, **5.1** serves as the first example of explicitly

determined solid state coordination geometry, evidenced by X–ray structure, among all the cationic $Tpm^{R}M(C_2H_4)_2^{+}$ (Tpm^{R} = Tpm, Tpm^{*}, M = Rh, Ir) derivatives.

$[TpmRh(C_2H_4)_2][BAr^{F}_4]$ (**5.2**; eq. 5.1) was also synthesized following a similar procedure with $Na[BAr^{F}_4]$ instead of $TlPF_6$. As expected, the characteristic rhodium-bound ethylene exhibited a singlet peak (2.79 ppm) in the ^{1}H NMR spectrum. Unsurprisingly, in the ^{1}H NMR spectrum, the three pyrazoles gave only a single set of peaks again. The chemical shift of C_2H_4 was assigned to the doublet at δ 52.56 ($^1J_{RhC}$ = 12.3 Hz) in the ^{13}C NMR spectrum, which is slightly more downfield than C_2H_4 in **5.1**. Besides, as to the $[BAr^{F}_4]$ counter ion, the carbon connected to the boron was observed at 162.34 ppm (q, $^1J_{BC}$ = 49.0 Hz) whereas the CF_3 was detected at 125.19 ppm (q, $^1J_{FC}$ = 271.3 Hz) in the ^{13}C NMR spectrum. Both ^{11}B (–6.5 ppm) and ^{19}F (–64.8 ppm) NMR spectrum supported the existence of single species as only one singlet was observed individually in both nuclei NMR spectrum.

Substitution reactions of 5.1 with π-acidic nucleophiles

Reaction of **5.1** with CO in methylene chloride is under sparging condition, three bridging COs are substituted for both ethylene ligands to afford $[(TpmRh)_2(\mu\text{-}CO)_3][PF_6]_2$ (**5.3**; eq 5.2). The binuclear compound **5.3** gave only one set of pyrazole signal in the ^{1}H NMR spectrum. The CO resonance was detected at δ 185.13 as a doublet coupled by the rhodium ($^1J_{RhC}$ = 71.0 Hz). The corresponding CO absorption in the IR spectrum exhibited exclusively intense absorption at 1863 cm^{-1}. Notably, this particularly low and single IR absorption frequency of CO is inconsistent with a monomeric dicarbonyl complex, $[TpmRh(CO)_2][PF_6]$ and suggests the existence of the bridging CO. This cation has been

previously reported as the perchlorate salt to give the structure $[(TpmRh)_2(\mu\text{-}CO)_3][ClO_4]_2$, that species gives a CO absorption band at 1865 cm^{-1}.[7b] The Tp analogue produces a related dinuclear complex[12,13] under the reaction condition whereas Tp^* analogue gives $Tp^*Rh(CO)(C_2H_4)$ as the only product.[13,14] In addition, this compound is poorly soluble in methylene chloride. Compound **5.3** was independently synthesized by reaction of Tpm, $[Rh(\mu\text{-}Cl)(CO)_2]_2$ and $TlPF_6$ in methylene chloride to give **5.3** as the major species.

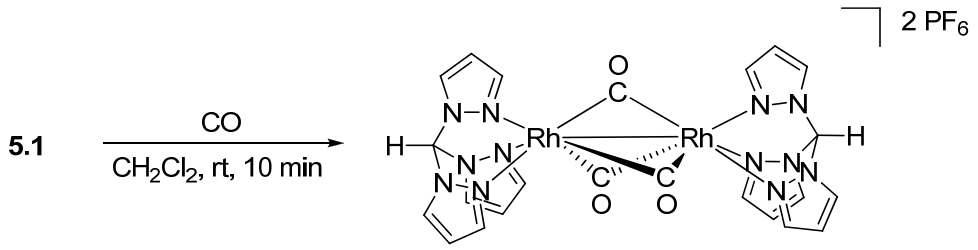

5.3 (5.2)

Meanwhile, complex **5.3** was further transformed into mono-substituted carbonyl-ethylene species by reacting with ethylene to give $[TpmRh(CO)(C_2H_4)][PF_6]$ (**5.4**) at room temperature in methylene chloride (eq 5.3). As before, the ^1H NMR spectrum of **5.4** contained only one set of pyrazole peaks. The ethylene ligand appeared as two broad peaks at δ2.96 and 2.72, integrating to 2 H each in the ^1H NMR spectrum. The two doublet peaks at 186.98 (d, $^1J_{RhC}$ = 67.0 Hz) and 33.43 ppm (d, $^1J_{RhC}$ = 15.0 Hz) represent *C*O and C_2H_4 respectively. The CO absorption in the IR spectrum appeared at 2046 cm^{-1}. The related substitution chemistry of the compound $[Tpm^*Ir(C_2H_4)_2][PF_6]$ has been reported that mono-substituted $[Ir](CO)(C_2H_4)$ is the kinetic product while the dicarbonyl $[Ir](CO)_2$ is the thermodynamic product.[11]

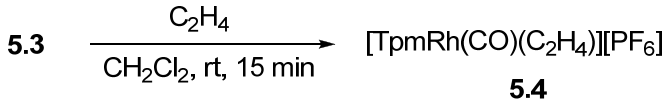

(5.3)

The reaction of **5.1** with *tert*-butyl isocyanide gives the bis(isocyanide) complex [TpmRh(CN*t*-Bu)$_2$][PF$_6$] (**5.5**) at room temperature in methylene chloride in excellent yield (eq 5.4). In the ^{1}H NMR spectrum, the two *tert*-butyl groups appeared at 1.52 ppm, integrating to 18 protons and the three pyrazoles once more contain only one set of three signals. The X-ray quality crystals were grown by slow diffusion of ether into methylene chloride solution at −30 ºC. Compound **5.5** is coordinated with a bidentate Tpm in the X-ray structure. The solid phase IR spectrum of **5.5** showed two isocyanide bands at 2168 and 2129 cm^{-1}. In contrast, treatment of TpRh(C$_2$H$_4$)$_2$ with CNRs (R = C$_6$H$_{11}$ or *t*-Bu) generates the bridging binuclear complex [TpRh]$_2$(μ-CNR)$_3$ exhibiting CN absorption band at 1735 cm^{-1} in the IR spectrum while the reactions of Tp*Rh(C$_2$H$_4$)$_2$ and the isocyanides gives the mono-substituted product Tp*(C$_2$H$_4$)(CNR).[13]

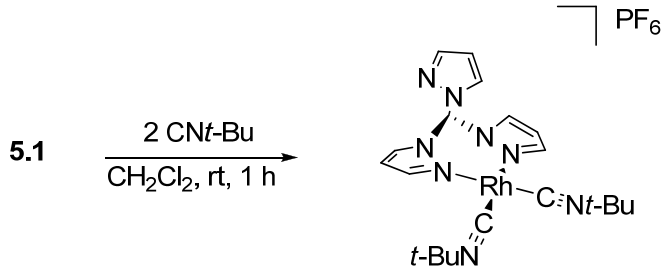

5.5

(5.4)

This indicates that complex **5.5** renders κ^2-κ^3 equilibrium *via* rapid exchange of coordinated and uncoordinated pyrazole rings in the solution phase.[15]

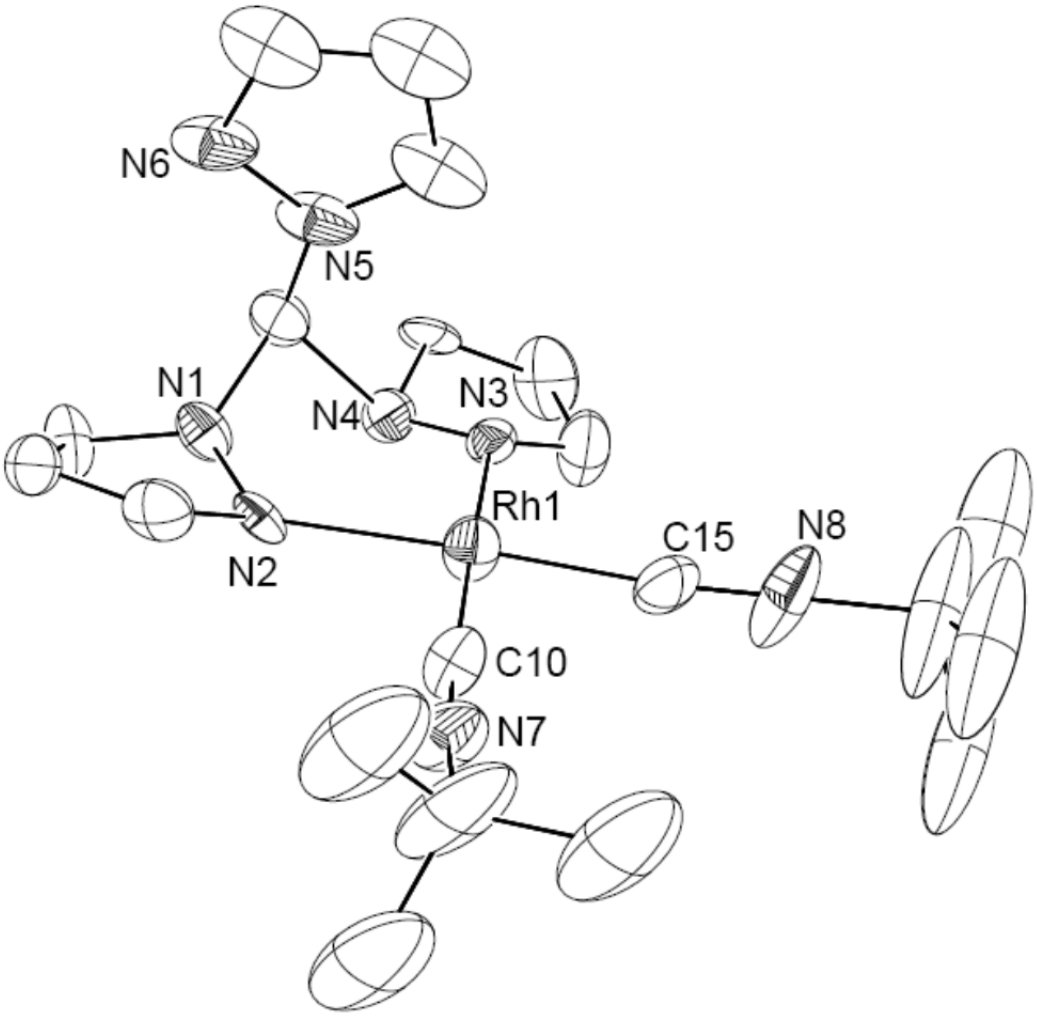

Figure 5.2. ORTEP drawing of **5.5**. Ellipsoids are shown at 50% probability. Hydrogens and PF_6 are omitted for clarity. Selected bond distances (Å): Rh1–C15, 1.909(9); Rh1–C10, 1.916(8); Rh1–N3, 2.066(5); Rh1-N2, 2.071(5). Selected bond angles (°): C15–Rh1–N2, 176.5(8); C10–Rh1–N3, 178.0(8).

The two bound pyrazoles and the two isocyanide ligands together with the rhodium center display a SP (SP = square planar) geometry (Fig 5.2). This SP geometry is only slightly distorted that the bond angels of C15–Rh1–C10 and N3–Rh1–N2 are 88.1(3)° and 88.1(4)° respectively. Additionally, the six-membered ring formed by the two bound pyrazoles and the rhodium center adopts an envelope conformation rather than a boat one

that the unbound pyrazole ring is more upright toward the square plane when compared to the unbound pyrazole of the $Tp^*Rh(CNR)_2$ (R = *t*-Bu, neopentyl, 2,6-xylyl) analogues whose is roughly parallel with the square plane.[15]

Substitution reactions of 5.1 with hard and soft Lewis basic donor

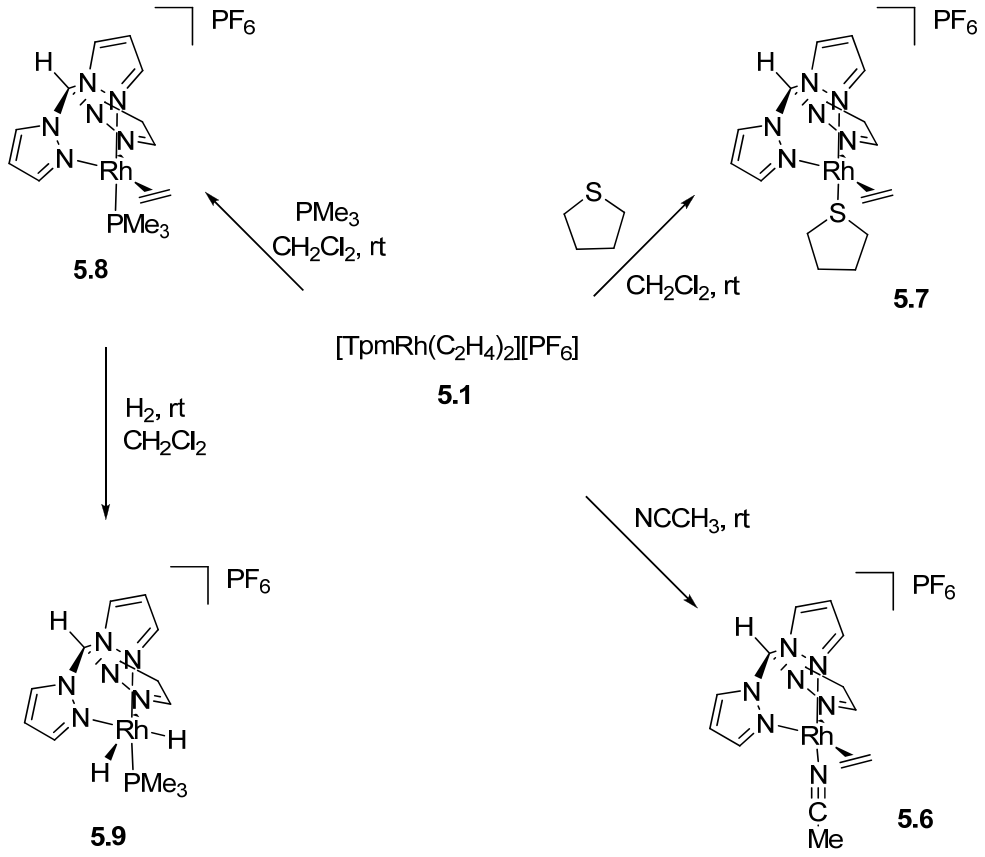

Scheme 5.1. Substitution reactions of **5.1** toward various hard and soft σ donors under mild conditions.

Dissolution of complex **5.1** in CH_3CN at room temperature gives $[TpmRh(C_2H_4)(NCCH_3)][PF_6]$ (**5.6**) in quantitative yield (Scheme 5.1). The whole complex

is C_s symmetric that the pyrazole peaks are composed of two sets of resonances in 2:1 ratio in the ^{1}H NMR spectrum, representing the two equatorial pyrazole rings and one axial ring respectively. Other notable resonances in the ^{1}H NMR spectrum include the four ethylene protons appearing as two doublets at δ 2.57 and 2.24 ($^2J_{RhH}$ = 8.4 Hz for both) as well as a singlet resonance at 2.26 ppm assigned to CH_3CN. The corresponding coordinated ethylene and acetonitrile (CH_3CN) peaks in the ^{13}C NMR spectrum were observed at δ 123.40 ($^2J_{RhC}$ = 8.8Hz) and 28.20 ($^1J_{RhC}$ = 17.5 Hz). IR spectrum was also found to be consistent with the formation of complex **5.6**, showing the nitrile absorption band at 2129 cm^{-1}.

The solid state structure of **5.6** adopts TBP geometry in which the equatorial ethylene ligand and axial acetonitrile ligand are clearly depicted (Fig 5.3). Like the structure of **5.1**, the bond distance of the rhodium and the two equatorial pyrazole nitrogens is longer than the axial one (Rh1–N5, 2.213(2); Rh1–N3, 2.226(3); Rh1–N1, 2.033(2) Å). The C–C bond length of the ethylene is 1.507(8) Å, which is longer than both equatorial and axial ethylenes of **5.1,** while the average bond length of the equatorial ethylene-rhodium of **5.6** (Rh1–C14, 2.058(4); Rh1–C13, 2.065(4) Å) is slightly shorter (compared to equatorial ethylene of **5.1**). Nonetheless, both the solution phase and solid phase structure of **5.6** are undoubtedly demonstrated to have κ^3 connectivity based on these NMR spectroscopic and X-ray diffraction studies.

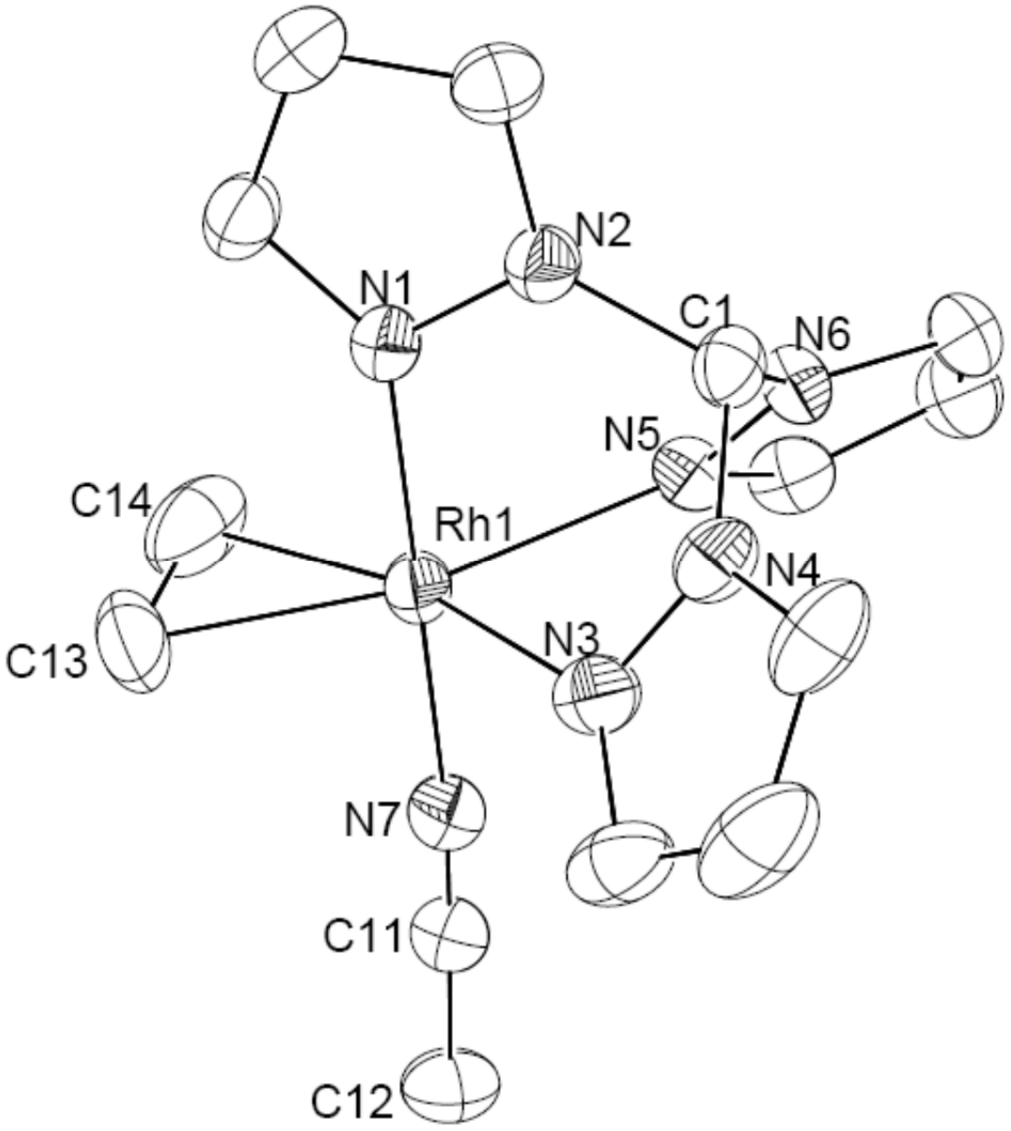

Figure 5.3. ORTEP diagram of **5.6** drawn at 50% probability. Hydrogens and PF_6 are omitted for clarity. The crystal was obtained by slow evaporation of Et_2O into CH_2Cl_2 solution at room temperature. Selected bond distance (Å): Rh1–N7, 1.987(3). Selected bond angles (°): N1–Rh1–N7, 179.5(7); C13–Rh1–N5: 162.3(1); C14–Rh1–N3, 160.3(8).

Interestingly, the reaction of $Tp^*Rh(C_2H_4)_2$ with $NCCH_3$ affords $Tp^*Rh(C_2H_5)(CH{=}CH_2)(NCCH_3)$ as the kinetic product whereas the thermodynamic product $Tp^*Rh(C_2H_4)(NCCH_3)$ is obtained at elevated temperature (60 ºC) *via* a reversible

pathway.[14,16] In the current system, multiple unidentified products were observed when heating **5.6** in tetrahydrofuran-d_8 solution at 60 ºC overnight, and no detectable metal hydride(s) appeared in the ^{1}H NMR spectrum.

Given the reaction of **5.1** with acetonitrile as a hard donor, we then investigated the interaction of **5.1** with soft donors such as tht and PMe_3. The interaction of these two ligands with **5.1** give [TpmRh(C_2H_4)(tht)][PF_6] (**5.7**) and [TpmRh(C_2H_4)(PMe_3)][PF_6] (**5.8**) respectively (Scheme 5.1). In the ^{1}H NMR spectra of **5.7** and **5.8**, the resonances attributed to ethylene were detected at 1.96 and 1.97 ppm respectively. **5.8** also shows the characteristic metal-phosphine bond at δ 13.36 ($^1J_{RhP}$ = 153.9 Hz) as a doublet in the ^{31}P NMR spectrum. In addition, unlike the Tp$M(C_2H_4)_2$ (M = Rh, Ir) analogues, **5.1** could not react with a bulkier phosphine such as PPh_3 even at higher temperature (condition: tetrahydrofuran-d_8, 70 ºC, overnight).[17.96]

The X-ray crystal structures of both **5.7** (Fig 5.4) and **5.8** (Fig 5.5) show TBP geometry with ethylene bound at equatorial plane and heteroatom-containing ligand coordinated into axial site. The equatorial ethylene ligand of **5.7** and **5.8** shows the bond length of 1.432(2) Å and 1.471(7) respectively. Compared to **5.1** and **5.6**, the bond length of the equatorial ethylenes decrease in the order of **5.6** > **5.8** > **5.1** > **5.7**. Thus, we are able to conclude that the electron donating ability of the axial ligands decrease in the order of $NCCH_3$ > PMe_3 > C_2H_4 > tht in the corresponding complexes series.

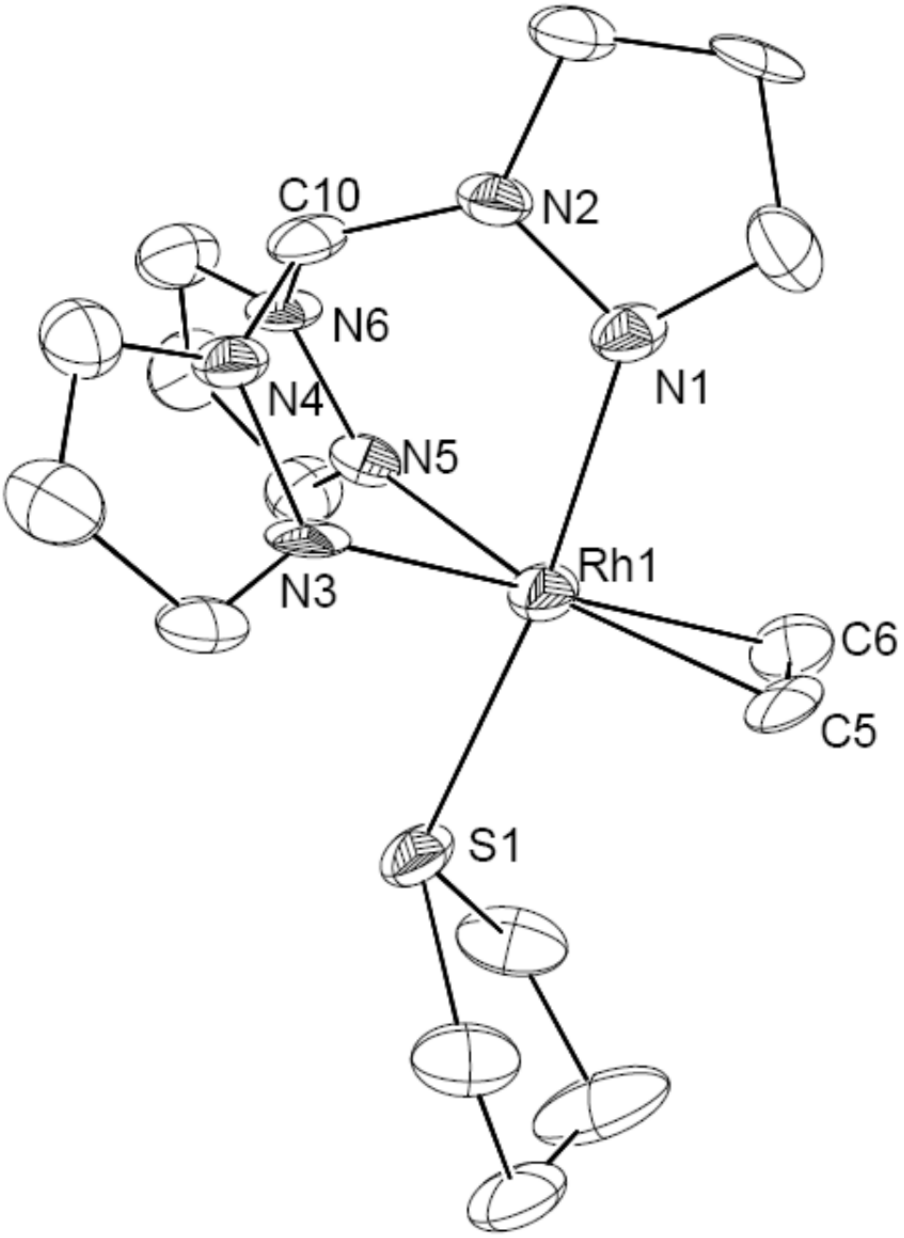

Figure 5.4. ORTEP diagram of **5.7** drawn at 50% probability. Hydrogens and PF_6 are omitted for clarity. The crystal was obtained by slow evaporation of Et_2O into thf solution at −30 ºC. Selected bond distance (Å): Rh1−C5: 2.059(1); Rh1−C6, 2.029(1); Rh1−N1, 2.070(8); Rh1−N3, 2.219(8); Rh1−N5, 2.198(8); Rh1−S1, 2.285(3). Selected bond angles (°): C6−Rh1−N3, 160.0(4); C5−Rh1−N5, 159.0(4); N1−Rh1−S1, 172.8(2).

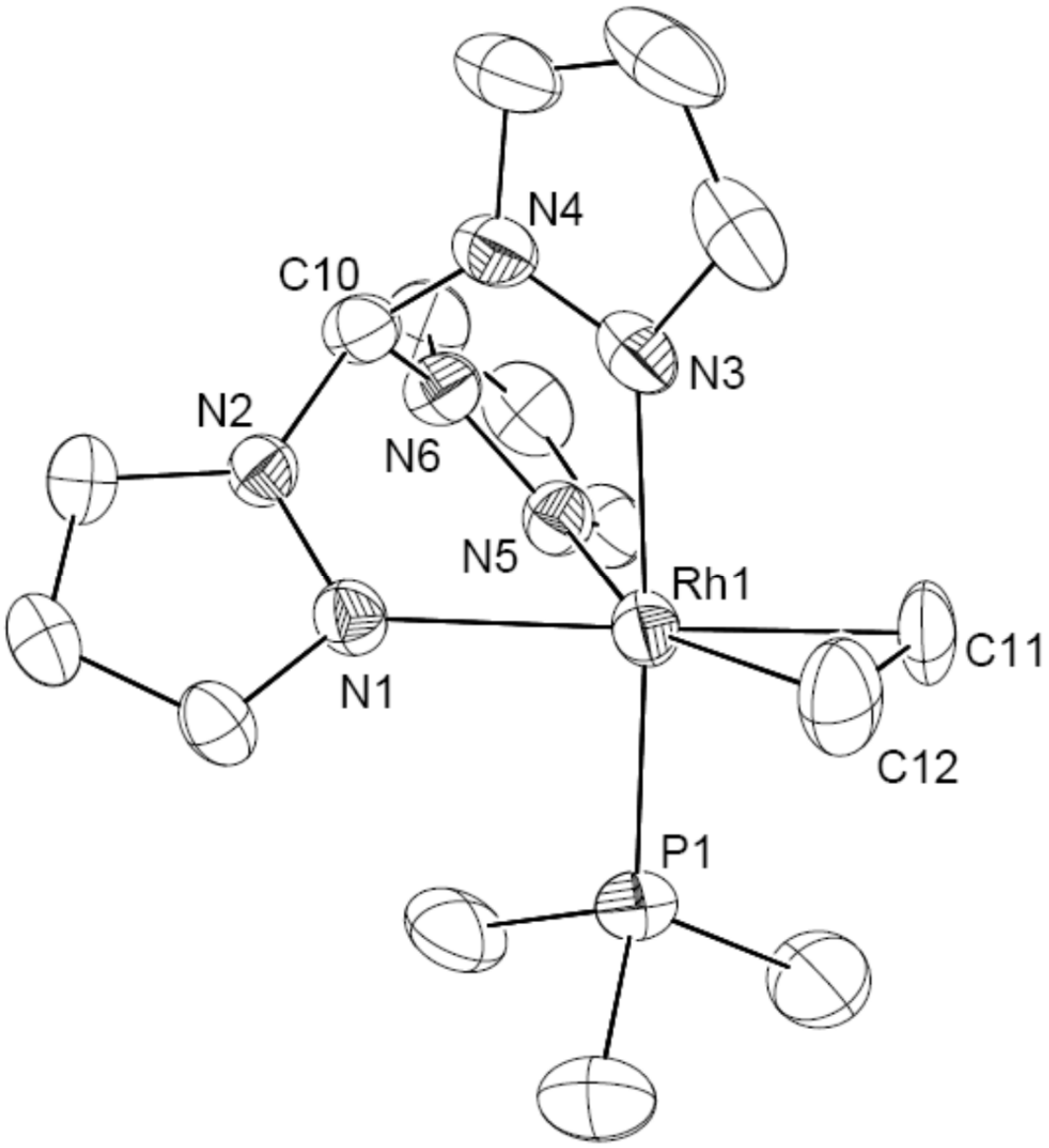

Figure 5.5. ORTEP diagram of **5.8** drawn at 50% probability. Hydrogens and PF_6 are omitted for clarity. The crystal was grown by slow evaporation of Et_2O into CH_2Cl_2 solution at room temperature. Selected bond distance (Å): Rh1−C11, 2.087(4); Rh1−C12, 2.074(4); Rh1−P1, 2.225(1); Rh1−N1, 2.219(3); Rh1−N3, 2.132(3); Rh1−N5, 2.221(3). Selected bond angles (°): N3−Rh1−P1, 176.1(6); C11−Rh1−N1, 161.3(4); C12−Rh1−N5, 155.5(8).

Lastly, numerous examples showing a route for the synthesis of the formula $Tp^RM(H)_2$(phosphine) (M= Rh, Ir) complexes have been reported .

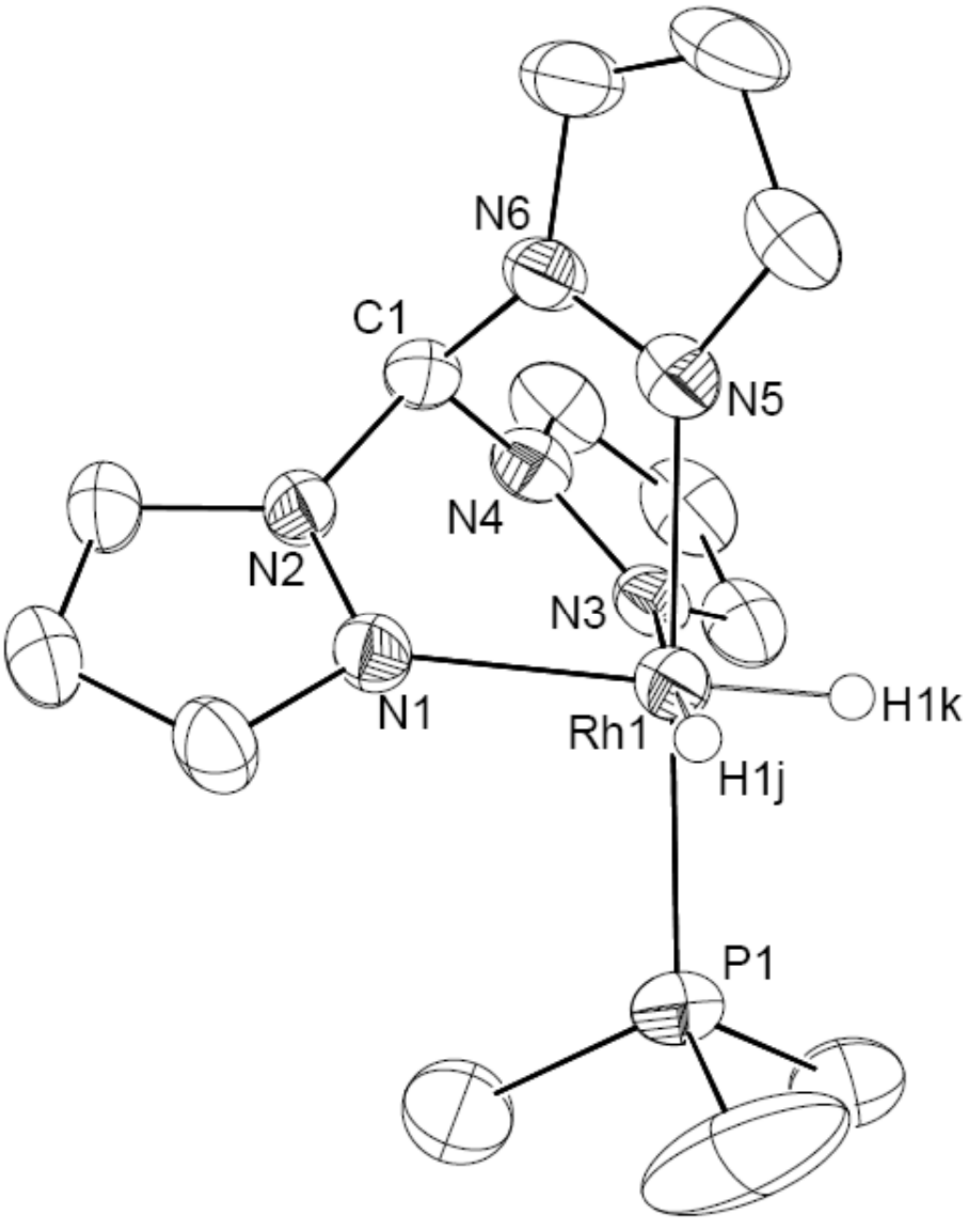

Figure 5.6. ORTEP diagram of **5.9**. Ellipsoids are drawn at 50% probability. Hydrogens (except hydrides) and PF_6 are omitted for clarity. The crystal was obtained by vapor diffusion of Et_2O into CH_2Cl_2 solution at room temperature. Selected bond distance (Å): Rh1–N1, 2.064(4); Rh1–N5, 2.113(4); Rh1–N3, 2.227(4); Rh1–P1, 2.239(3); Rh1–H1K, 1.241(1); Rh1–H1J, 1.56(6). Selected bond angles (°): N3–Rh1–H1J, 177.2(0); N1–Rh1–H1K, 176.3(0); N5–Rh1–P1, 177.1(8).

The preparation method typically involves hydrogenation of $Tp^RM(C_2H_4)$(phosphine) under mild conditions.[13,17,18] Similarly, treatment of **5.8** with 1 atm of H_2 in methylene chloride solution gives $[TpmRh(H)_2PMe_3][PF_6]$ (**5.9**) as the only product in quantitative yield (Scheme 5.1). The ^{1}H NMR spectrum contains a doublet of doublet at –17.44 ppm ($^2J_{PH}$ = 34.4 Hz, $^1J_{RhH}$ = 23.2 Hz) in assigned to the RhH_2. A doublet at 10.86 ppm ($^1J_{RhP}$ = 118.3 Hz) in the ^{31}P NMR spectrum was observed. An absorption band in the IR spectrum was detected at 2058 cm^{-1}, supporting the presence of the Rh–H bond. The geometry of rhodium (III) center was confirmed by X-ray crystallography that **5.9** adopts octahedral structure. Two of the metal hydrides are located on the equatorial plane *trans* to the two pyrazoles and the third pyrazole is visually aligned with the phosphorus atom through the rhodium center on the axial axes (Fig 5.6). The solid state of **5.9** reveals the κ^3 coordination nature of the d^6 rhodium center without exception, comparing to the reported examples.

NMR study for hapticity, fluxionality and ligand (C_2H_4) rigidity of the complexes

Tp^RMLL'(M = Rh, Ir) have been known to show different coordinating modes, that is, either a bidentate with one arm dissociating or a tridentate that gives 18 electron species. Even an equilibrium behavior could co-exist for both modes, depending on the coordinating Tp^R analogues, the metal center and the L ligands. Even when the solid state coordination mode could be demonstrated by X-ray crystallography easily, the solution phase coordination mode is always more complicated that a static SP (κ^2) geometry or a TBP (κ^3) geometry could appear solely or as an dynamic equilibrium. Besides, a fluxional ligand interconversion with a TBP κ^3 coordination mode could be involved as an alternative mechanism for dynamic behavior (Scheme 5.2).

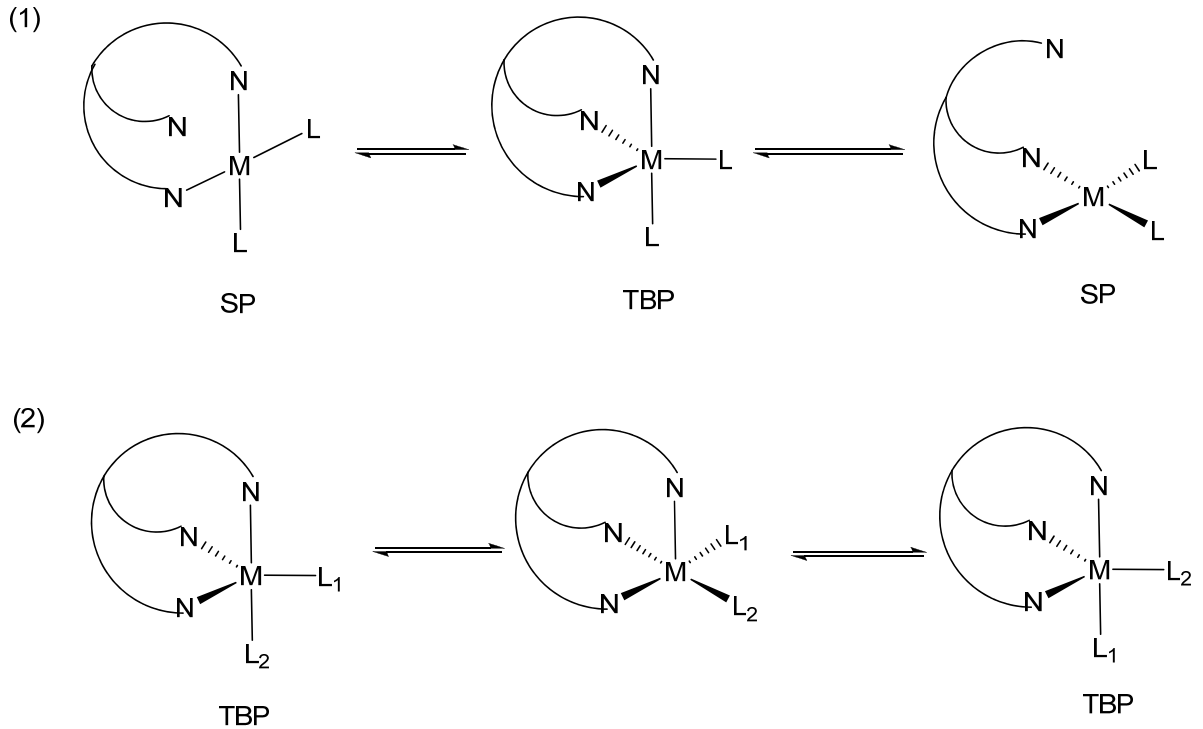

Scheme 5.2. (1) SP (κ^2)-TBP (κ^3) dynamic equilibrium. (2) Fluxional ligand interconversion equilibrium of TBP structure with κ^3 coordination mode.

To address this issue, in addition to ^{1}H NMR spectroscopy, ^{15}N NMR spectroscopy method serves as one of the important tools for determining the geometry and structure for these metal compounds. For example, Venanzi and co-workers employed ^{15}N NMR spectroscopy to determine the hapticity and fluxional behavior of the tris(pyrazolyl)borate metal complexes. The study concluded that the ^{15}N chemical shift value of the coordinated $N_{2\text{-}Pz}$ (N^2) would appear at a more upfield region of the spectrum (−75 to −138 ppm). The average calculated value (N^2) for dynamic κ^2-κ^3 equilibrium would be close to −117 ppm for the κ^2 form. Increasing portions of the κ^3-form of the complex would give a more upfield chemical shift.[19]

In our system (Table 5.1), **5.1** could not be a static (either SP or TBP) structure in the solution because the ^{1}H NMR spectrum contained only one set of pyrazole resonance. Comparing **5.1**–**5.3**, the ^{15}N chemical shift of N^2 of **5.1** (−131.6 ppm) is close to that of **5.3** (−135.6 ppm) and **5.3** has been confirmed as a κ^3 structure. Thus, we could conclude that the ground state of **5.1** shows a κ^3 coordination mode with ligand interconversion (Scheme 5.2, (1)), which is similar to the $Tp^{R}Rh(C_2H_4)_2$ analogues.[13] By applying this principle, **5.2** (−128.8 ppm) and **5.4** (−136.6 ppm) are assigned to have the same coordination behavior in the solution. In contrast, the ^{15}N signal of the N^2 of **5.5** exhibited at −123.7 ppm. This value is somewhat close to the reported value (−117 ppm) comparing to **5.1**–**5.4**, which clearly indicates the tendency of giving the κ^2 form. Considering the combination ^{1}H and ^{15}N NMR spectroscopy of **5.5**, we determine that the connectivity of **5.5** adopts dynamic κ^2-κ^3 equilibrium (Scheme 5.2, (2)). For complexes **5.6**–**5.8**, although the ^{15}N chemical shift value of N^2 at axial site is more downfield and close to the value for the κ^2 form, one should be aware that it is the average of both equatorial and axial N^2 chemical shifts that validate the hapticity assignments. Thus, the average ^{15}N chemical shifts of the N^2 for **5.6**–**5.8** have the range of −128.2 to −142.8 ppm, which represents the κ^3 mode. However, ligand fluxionality does not exist for **5.6**–**5.8** due to two sets of pyrazole peaks (2:1 ratio) showing in the ^{1}H NMR spectra. Therefore, **5.6**–**5.8** are assigned to give static κ^3 coordination mode in the solution phase. **5.9** is the only Rh(III) species among all the complexes reported in the context and Rh(III) has been generally considered to show κ^3 octahedral structure in both solution and solid phases. Without exception, this assignment of **5.9** is in good agreement of both ^{1}H and ^{15}N spectra data.

Table 5.1. ^{1}H pattern, ^{15}N chemical shift value and hapticity of **5.1**–**5.9**

Compound[a]	^{15}N of $N_{1\text{-Pz}}$ (N^1)[b]	^{15}N of $N_{2\text{-Pz}}$ (N^2)	^{1}H of Pz (set(s))	^{1}H of C_2H_4 (set(s))	Hapticity (solution)	Hapticity (solid)
5.1, $Rh(C_2H_4)_2$	-175.2	-131.6	1	1	κ^3	κ^3
5.2, $Rh(C_2H_4)_2$	-169.3	-128.8	1	1	κ^3	κ^3
5.3, $Rh_2(CO)_3$	-174.5	-135.6	1	n.a.[c]	κ^3	κ^3
5.4, $Rh(CO)(C_2H_4)$	-174.7	-136.6	1	2	κ^3	n.a.[d]
5.5, $Rh(CN$*t*$\text{-Bu})_2$	-175.3	-123.7	1	n.a.[c]	κ^2-κ^3	κ^2
5.6, $Rh(C_2H_4)(NCCH_3)$	-172.5 (eq) -173.4 (ax)	-166.6 (eq) -119.0 (ax)	2 (2: 1 ratio)	2	κ^3	κ^3
5.7, $Rh(C_2H_4)$(tht)	-172.9 (eq) -173.3 (ax)	-156.6 (eq) -120.0 (ax)	2 (2: 1 ratio)	1	κ^3	κ^3
5.8, $Rh(C_2H_4)(PMe_3)$	-172.6 (eq) -174.6 (ax)	-134.3 (eq) -122.1 (ax)	2 (2: 1 ratio)	1	κ^3	κ^3
5.9, $Rh(H)_2PMe_3$	-173.0 (eq) -175.1 (ax)	-131.8 (eq) -134.3 (ax)	2 (2: 1 ratio)	n.a.[c]	κ^3	κ^3

[a]Tpm and PF_6 are omitted for clarity. [b]Pz = pyrazole, ax = axial, eq = equatorial. [c]No ethylene ligands. [d]Could not be determined.

The solid state structure could not be obtained for **5.2**–**5.4**. Aside from the identical cation structure between **5.2** and **5.1** as well as the reported complex with different counter ion and **5.3**,[7b] **5.4** is the only one remained uncertain for the hapticity determination in the solid state.

Additionally, for **5.1**, **5.2**, **5.4** and **5.6**–**5.8** containing ethylene ligand, it is noteworthy that **5.4** and **5.6** showed two sets of ethylene signals in the ^{1}H NMR spectra while the others contained only one set. This implies the rigidity of the ethylene coordinated to the rhodium center without rotation of the Rh–C_2H_4 bonds for **5.4** and **5.6**.[17,20] Comparing **5.1**, **5.2**, **5.4**, **5.6** and **5.8** to the Tp*[Rh] analogues, complex **5.1**, **5.2** and **5.6** are in accordance with the corresponding analogues showing either one set or two sets of ethylene signals whereas **5.4** and **5.8** are contrary to what have been observed.[13,21]

Conclusion

The cationic bis(ethylene) rhodium compounds [TpmRh(C_2H_4)$_2$][X] (**5.1**, X = PF_6; **5.2**, X = BAr^F_4) have been synthesized and characterized. The solid state of **5.1** was obtained and confirmed to be a TBP structure with a tridentate-coordinated Tpm ligand. This compound represents the first example of bis(ethylene) rhodium complexes supported by tris(pyrazolyl)methane ligand. The reactivity of **5.1** was examined by reacting with π-acidic nucleophiles as well as hard and soft Lewis basic donors. The electron donating ability is compared among **5.1** and **5.6**–**5.8**, which shows that this ability decrease in the order of $NCCH_3$ > PMe_3 > C_2H_4 > tht, which is supported by the solid state evidence of the equatorial ethylene bond length. The hapticity, fluxionality and ligand rigidity were also studied by conducting ^{1}H and ^{15}N NMR spectroscopy. All the complexes reported herein appear to have κ^3 connectivity in the solution phase except **5.5** which is proved to behave κ^2-κ^3 equlibrium. The solid state hapticity is clearly described by either the X-ray structures or by comparison with the closely related analogues. Fluxional ligand interconversion phenomenon is also observed for some of the complexes (**5.1**, **5.2** and **5.4**). The rigidity determination of

Rh–C_2H_4 bond was further supported by the pattern of the ethylene group in the ^{1}H NMR spectra.

Experimental

General. All manipulations were performed under an inert atmosphere using standard Schlenk techniques or in a glovebox. All solvents were dried and degassed unless otherwise indicated. Methylene chloride, diethyl ether and thf were degassed by sparging with N_2 and then dried with activated Al_2O_3 on an IT Solvent Purification System. Acetonitrile was degassed and distilled. Methylene chloride-d_2 was refluxed over CaH_2 powder and then vacuum transferred. All other reagents were purchased from Sigma-Aldrich and used as received. Tpm,[22] $[Rh(\mu\text{-Cl})(C_2H_4)_2]_2$[23] and $Na[BAr^F{}_4]$[24] were synthesized according to the literature procedures. All NMR spectra were obtained at room temperature using Bruker DRX-400 and Avance II-700 spectrometers. ^{15}N NMR chemical shifts were determined by ^{1}H-^{15}N HMBC experiments recorded on an Avance II-700 spectrometer; the chemical shift values are reported relative to CH_3NO_2. ^{11}B NMR spectra chemical shifts are reported relative to $BF_3{\cdot}Et_2O$. NMR yields were determined using a *tetrakis*(trimethylsilyl)silane as the internal standard. Elemental analyses were obtained at the Iowa State Chemical Instrumentation Facility using a Perkin-Elmer 2400 Series II CHN/S.

$[TpmRh(C_2H_4)_2][PF_6]$ (5.1) A mixture of Tpm (0.287 g, 1.34 mmol), $[Rh(\mu\text{-Cl})(C_2H_4)_2]_2$ (0.261 g, 0.67 mmol) and $TlPF_6$ (0.492 g, 1.41 mmol) was suspended in CH_2Cl_2 (30 mL). The mixture was vigorously stirred at room temperature for 5 h and then filtered. The filtrate was evaporated to dryness to give a pale orange solid (0.64 g, 1.24 mmol, 92%). ^{1}H NMR (methylene chloride-d_2, 400 MHz): δ 8.88 (s, 1 H, *H*CPz$_3$), 8.22 (d, 3 H, $^3J_{HH}$ = 2.4 Hz, *3*-Pz),

7.96 (d, 3 H, $^{3}J_{HH}$ = 2.4 Hz, *5*-Pz), 6.50 (t, 3 H, $^{3}J_{HH}$ = 2.4 Hz, *4*-Pz), 2.74 (s, 8 H, C_2H_4). $^{13}C\{^{1}H\}$ NMR (methylene chloride-d_2, 175 MHz): δ 142.78 (5-Pz), 133.85 (3-Pz), 108.58 (4-Pz), 76.19 (H*C*Pz$_3$), 51.56 (d, $^{1}J_{RhC}$ = 12.3 Hz, C_2H_4). $^{15}N\{^{1}H\}$ NMR (methylene-d_2, 71 MHz): δ –131.6 (N, *2*-Pz), –175.2 (N, *1*-Pz). ^{31}P NMR (methylene chloride-d_2, 162 MHz): δ –142.6 (sept, $^{1}J_{PF}$ = 712.8 Hz, PF_6). IR (KBr, cm^{-1}): ν 3142 (m), 3024 (w), 1520 (w), 1445(m), 1411 (m), 1290 (s), 1253 (m), 1226 (w), 1096 (m), 1061 (m), 983 (w). Anal. Calcd. for $C_{14}H_{18}N_6PF_6Rh$: C, 32.45; H, 3.50; N, 16.22 Found: C, 32.55; H, 3.82; N, 16.33. Mp: above 300 ^{o}C, dec.

[TpmRh(C$_2$H$_4$)$_2$][BAr$^{F}_4$] (5.2) A mixture of Tpm (0.109 g, 0.51 mmol), [Rh(μ-Cl)(C_2H_4)$_2$]$_2$ (0.099 g, 0.25 mmol) and Na[BAr$^{F}_4$] (0.473 g, 0.53 mmol) was suspended and stirred in CH_2Cl_2 (10 mL) for 5 h. The reaction mixture was filtered and evaporated to dryness to give a light brown solid (0.59 g, 0.47 mmol, 93%). ^{1}H NMR (methylene chloride-d_2, 400 MHz): δ 8.01 (d, 3 H, $^{3}J_{HH}$ = 1.6 Hz, *3*-Pz), 7.98 (s, 1 H, *H*CPz$_3$), 7.92 (d, 3 H, $^{3}J_{HH}$ = 2.4 Hz, *5*-Pz), 7.72 (s, 8 H, *ortho*-BAr$^{F}_4$), 7.55 (s, 4 H, *para*-BAr$^{F}_4$), 6.56 (t, 3 H, $^{3}J_{HH}$ = 2.4 Hz, *4*-Pz), 2.79 (s, 8 H, C_2H_4). $^{13}C\{^{1}H\}$ NMR (methylene chloride-d_2, 175 MHz): δ 162.34 (q, $^{1}J_{BC}$ = 49.0 Hz, *ipso*-BAr$^{F}_4$), 143.73 (*3*-Pz), 135.40 (*ortho*-BAr$^{F}_4$), 132.61 (*5*-Pz), 129.47 (q, $^{2}J_{FC}$ = 31.5 Hz, *meta*-BAr$^{F}_4$), 125.19 (q, $^{1}J_{FC}$ = 271.3 Hz, *C*F$_3$), 118.10 (*para*-BAr$^{F}_4$), 109.32 (*3*-Pz), 77.50 (H*C*Pz$_3$), 52.56 (d, $^{1}J_{RhC}$ = 12.3 Hz, C_2H_4). $^{15}N\{^{1}H\}$ NMR (methylene chloride-d_2, 71 MHz): δ –128.8 (N, *2*-Pz), –169.3 (N, *1*-Pz). ^{11}B NMR (methylene chloride-d_2, 128 MHz): δ –6.5. ^{19}F NMR (methylene chloride-d_2, 375 MHz): δ –64.8. IR (KBr, cm^{-1}): ν 3154 (m), 3022 (w), 2963 (w), 2085 (m), 1611 (m), 1523 (m), 1442 (s), 1404 (s), 1355 (s), 1270

(s), 1252 (s), 1225 (m), 1104 (s), 1057 (s), 986 (m). Anal. Calcd. for $C_{46}H_{30}N_6BF_{24}Rh$: C, 44.68; H, 2.45; N, 6.80 Found: C, 45.00; H, 2.57; N, 6.55. Mp: 140–143 ^{o}C, dec.

[(TpmRh)$_2$(μ-CO)$_3$][PF$_6$]$_2$ (5.3) In a 50 mL Schlenk flask, the solution of **5.1** (0081 g, 0.156 mmol) in CH_2Cl_2 (20 mL) was bubbled through with CO for 10 min. The solution was then evaporated to dryness, and the solid residue was washed with Et_2O (5 mL) to yield a pale yellow solid (0.069 g, 0.069 mmol, 88%). ^{1}H NMR (methylene chloride-d_2, 400 MHz): δ 9.04 (s, 1 H, *H*CPz$_3$), 8.24 (d, 3 H, $^3J_{HH}$ = 2.8 Hz, *3*-Pz), 7.91 (d, 3 H, $^3J_{HH}$ = 2.4 Hz, *5*-Pz), 6.54 (t, 3 H, $^3J_{HH}$ = 2.4 Hz, *4*-Pz). ^{13}C{^{1}H} NMR (methylene chloride-d_2, 175 MHz): δ 185.13 (d, $^1J_{RhC}$ = 71.0 Hz, CO), 146.17 (*5*-Pz), 134.41 (*3*-Pz), 109.13 (*4*-Pz), 77.46 (H*C*Pz$_3$). ^{15}N{^{1}H} NMR (methylene chloride-d_2, 71 MHz): δ –135.6 (N, *2*-Pz), –174.5 (N, *1*-Pz). ^{31}P NMR (methylene chloride-d_2, 162 MHz): δ –143.8 (sept, $^1J_{PF}$ = 712.8 Hz, PF_6). IR (KBr, cm^{-1}): ν 3167 (w), 3137 (m), 1863 (s, ν_{CO}), 1445 (m), 1412 (m), 1295 (s), 1256 (m), 1225 (w), 1099 (m), 1062 (m), 991 (w). Anal. Calcd. for $C_{23}H_{20}N_{12}O_3P_2F_{12}Rh_2$: C, 27.40; H, 2.00; N, 16.67 Found: C, 27.80 H, 2.10; N, 16.94. Mp: above 300 ^{o}C, dec.

[TpmRh(CO)(C$_2$H$_4$)][PF$_6$] (5.4) In a 100 mL Schlenk flask, C_2H_4 was bubbled through a partially suspended **5.3** (0.055 g, 0.106 mmol) in CH_2Cl_2 (20 mL) for 15 min. Solvents were evaporated, and the solid residue was washed with Et_2O (5 mL) to afford an off-white solid (0.049g, 0.096 mmol, 90%). ^{1}H NMR (methylene chloride-d_2, 400 MHz): δ 9.04 (s, 1 H, *H*CPz$_3$), 8.29 (d, 3 H, $^3J_{HH}$ = 2.8 Hz, *3*-Pz), 7.85 (d, 3 H, $^3J_{HH}$ = 2.0 Hz, *5*-Pz), 6.51 (t, 3 H, $^3J_{HH}$ = 2.4 Hz, *4*-Pz), 2.96 (br, 2 H, C_2H_4), 2.72 (br, 2 H, C_2H_4). ^{13}C{^{1}H} NMR (methylene chloride-d_2, 175 MHz): δ 186.98 (d, $^1J_{RhC}$ = 67.0 Hz, CO), 143.84 (*5*-Pz), 134.03 (*3*-Pz), 108.77 (*4*-Pz), 76.46 (H*C*Pz$_3$), 33.43 (d, $^1J_{RhC}$ = 15.0 Hz, C_2H_4). ^{15}N{^{1}H} NMR (methylene

chloride-d_2, 71 MHz): δ –136.6 (N, *2*-Pz), –174.7 (N, *1*-Pz). ^{31}P NMR (methylene chloride-d_2, 162 MHz): δ –143.8 (sept, $^1J_{PF}$ = 712.8 Hz, PF_6). IR (KBr, cm^{-1}): ν 3161 (m), 3141 (m), 3023 (w), 2046 (s, ν_{CO}), 1520 (w), 1444 (m), 1411 (m), 1289 (m), 1255 (m), 1227 (w), 1099 (m), 1063 (m), 980 (w). Anal. Calcd. for $C_{13}H_{14}N_6OPF_6Rh$: C, 30.13; H, 2.72; N, 16.22 Found: C, 30.37; H, 3.00; N, 16.21. Mp: above 300 ^oC, dec.

[TpmRh(CN*t*-Bu)$_2$][PF$_6$] (5.5) In a glovebox, CN*t*-Bu (0.032 g, 0.386 mmol) was added to a solution of **5.1** (0.100 g, 0.193 mmol) in CH_2Cl_2 (10 mL) in a vial (20 mL) was added at room temperature. The mixture was allowed to stir for 2 h. Solvents were evaporated and the residue was washed with Et_2O (3 mL) to yield a yellow solid (0.103 g, 0.164 mmol, 85%). ^{1}H NMR (methylene chloride-d_2, 400 MHz): δ 8.76 (s, 1 H, *H*CPz$_3$), 8.04 (d, 3 H, $^3J_{HH}$ = 4.0 Hz, *3*-Pz), 7.76 (d, 3 H, $^3J_{HH}$ = 4.0 Hz, *5*-Pz), 6.51, (t, 3 H, $^3J_{HH}$ = 4.0Hz, *4*-Pz), 1.52 (s, 18 H, CNC*Me*$_3$). ^{13}C{^{1}H} NMR (methylene chloride-d_2, 175 MHz): δ 145.68 (*5*-Pz), 134.00 (*3*-Pz), 108.55 (*4*-Pz), 80.58 (H*C*Pz$_3$), 31.07 (C(*Me*)$_3$), 30.66 (*C*(Me)$_3$). ^{15}N{^{1}H} NMR (methylene chloride-d_2, 71 MHz): δ –123.7 (N, *2*-Pz), –175.3 (N, *1*-Pz), –191.5 (N, C*Nt*-Bu). ^{31}P NMR (methylene chloride-d_2, 162 MHz): δ –142.2 (sept, $^1J_{PF}$ = 712.8 Hz, PF_6). IR (KBr, cm^{-1}): ν 3135 (m), 2987 (m), 2168 (s, ν_{CN}), 2129 (s, ν_{CN}), 1460 (m), 1431 (w), 1407 (m), 1392 (m), 1374 (m), 1360 (w), 1307 (m), 1284 (m), 1260 (w), 1234 (w), 1198 (m). Anal. Calcd. for $C_{20}H_{28}N_8PF_6Rh$: C, 38.23; H, 4.49; N, 17.83 Found: C, 38.66; H, 5.12; N, 17.55. Mp: above 300 ^oC, dec.

[TpmRh(C$_2$H$_4$)(NCCH$_3$)][PF$_6$] (5.6) In a glove box, **5.1** (0.120 g, 0.232 mmol) was dissolved in CH_3CN (10 mL) in a 20 mL scintillation vial. The solution was stirred at room temperature for 10 min and evaporated to dryness to give a light brown solid quantitatively.

^{1}H NMR (methylene chloride-d_2, 400 MHz): δ 8.87 (s, 1 H, *H*CPz$_3$), 8.24 (d, 2 H, $^{3}J_{HH}$ = 2.8 Hz, *3*-Pz$_{eq}$), 8.15 (d, 1 H, $^{3}J_{HH}$ = 2.8 Hz, *3*-Pz$_{ax}$), 8.06 (d, 2 H, $^{3}J_{HH}$ = 2.4 Hz, *5*-Pz$_{eq}$), 7.01 (d, 1 H, $^{3}J_{HH}$ = 1.6 Hz, *5*-Pz$_{ax}$), 6.49 (t, 2 H, $^{3}J_{HH}$ = 2.4 Hz, *4*-Pz$_{eq}$), 6.28 (t, 1 H, $^{3}J_{HH}$ = 2.8 Hz, *4*-Pz$_{ax}$), 2.57 (d, 2 H, $^{2}J_{RhH}$ = 8.4 Hz, C$_2$*H*$_4$), 2.26 (s, 3 H, C*H*$_3$CN), 2.24 (d, 2 H, $^{2}J_{RhH}$ = 8.4 Hz, C$_2$*H*$_4$). ^{13}C{^{1}H} NMR (methylene chloride-d_2, 175 MHz): δ 144.03 (*5*-Pz$_{eq}$), 140.54 (*5*-Pz$_{ax}$), 134.80 (*3*-Pz$_{ax}$), 132.65 (*3*-Pz$_{eq}$), 123.40 (d, $^{2}J_{RhC}$ = 8.8Hz, CH$_3$*C*N), 108.36 (*4*-Pz$_{eq,ax}$), 76.83 (H*C*Pz$_3$), 28.20 (d, $^{1}J_{RhC}$ = 17.5 Hz, *C*$_2$H$_4$), 4.50 (*C*H$_3$CN). ^{15}N{^{1}H} NMR (methylene chloride-d_2, 71 MHz): δ –119.0 (N, *2*-Pz$_{ax}$), –166.6 (N, *2*-Pz$_{eq}$), –173.4 (N, *1*-Pz$_{ax}$), –172.5 (N, *1*-Pz$_{eq}$), –209.4 (CH$_3$C*N*) ^{31}P NMR (methylene chloride-d_2, 162 MHz): δ –143.8 (sept, $^{1}J_{PF}$ = 712.8 Hz, PF$_6$). IR (KBr, cm^{-1}): ν 3140 (m), 2033 (m), 2980 (w), 2251 (w, ν_{NC}), 1518 (m), 1442 (s), 1402 (s), 1291 (s), 1252 (m), 1227 (w), 1091 (s), 1054 (m). Anal. Calcd. for C$_{14}$H$_{17}$F$_6$N$_7$PRh: C, 31.65; H, 3.23; N, 18.46 Found: C, 31.50; H, 2.97; N, 17.98. Mp: above 300 ^{o}C, dec.

[TpmRh(C$_2$H$_4$)(tht)][PF$_6$] (5.7) In a glovebox, tetrahydrothiophene (0.014 g, 0.154 mmol) was added to a solution of **5.1** (0.080 g, 0.154 mmol) in CH$_2$Cl$_2$ (10 mL) in a vial (20 mL) at room temperature and allowed to stir at this temperature for 1 h. The solution was evaporated to dryness and the solid residue was washed with Et$_2$O (3 mL) to give a light brown solid (0.083 g, 0.144 mmol, 93%). ^{1}H NMR (methylene chloride-d_2, 400 MHz): δ 8.90 (s, 1 H, *H*CPz$_3$), 8.29 (d, 2 H, $^{3}J_{HH}$ = 2.4 Hz, *3*-Pz$_{eq}$), 8.16 (d, 1 H, $^{3}J_{HH}$ = 2.4 Hz, *3*-Pz$_{ax}$), 8.02 (d, 2 H, $^{3}J_{HH}$ = 1.2 Hz, *5*-Pz$_{eq}$), 7.11 (s, 1 H, *5*-Pz$_{ax}$), 6.52 (t, 2 H, $^{3}J_{HH}$ = 2.4 Hz, *4*-Pz$_{eq}$), 6.32 (s, 1 H, *4*-Pz$_{ax}$), 2.73 (m, 4 H, S(C$_2$*H*$_4$)(C$_2$H$_4$)), 2.20 (d, 4 H, $^{2}J_{RhH}$ = 5.2 Hz, C$_2$*H*$_4$), 1.96 (m, 4 H, S(C$_2$H$_4$)(C$_2$*H*$_4$)). ^{13}C{^{1}H} NMR (methylene chloride-d_2, 175 MHz): δ 144.53 (*5*-Pz$_{eq}$), 139.67

(*5*-Pz$_{ax}$), 134.39 (*3*-Pz$_{ax}$), 133.28 (*3*-Pz$_{eq}$), 108.50 (*4*-Pz$_{eq}$), 108.32 (*4*-Pz$_{ax}$), 76.72 (H*C*Pz$_3$), 36.22 (S(C_2H_4)(C_2H_4)), 30.19 (S(C_2H_4)(C_2H_4)), 26.89 (d, $^1J_{RhC}$ = 8.75 Hz, C_2H_4). $^{15}N\{^1H\}$ NMR (methylene chloride-d_2, 71 MHz): δ –120.0 (N, *2*-Pz$_{ax}$), –156.6 (N, *2*-Pz$_{eq}$), –172.9 (N, *1*-Pz$_{eq}$), –173.3 (N, *1*-Pz$_{ax}$). ^{31}P NMR (methylene chloride-d_2, 162 MHz): δ –143.8 (sept, $^1J_{PF}$ = 712.8 Hz, PF_6). IR (KBr, cm^{-1}): ν 3141 (m), 3033 (m), 2955 (m), 1521 (m), 1440 (s), 1402 (s), 1290 (s) 1250 (s), 1222 (m), 1137 (w), 1095 (s), 1073 (m), 1056 (m), 991 (w). Anal. Calcd. for $C_{16}H_{22}N_6PF_6SRh$: C, 33.23; H, 3.83; N, 14.53 Found: C, 32.77; H, 3.56; N, 14.33. Mp: above 300 °C, dec.

[TpmRh(C_2H_4)(PMe_3)][PF_6] (5.8) In a glovebox, PMe_3 (0.013 g, 0.166 mmol) was added to a solution of **5.1** (0.086 g, 0.166 mmol) in CH_2Cl_2 (10 mL) in a vial (20 mL) at room temperature. The solution was stirred for 15 min and evaporated to dryness to yield a pale yellow solid (0.089 g, 0.156 mmol, 94%). ^{1}H NMR (methylene chloride-d_2, 400 MHz): δ 8.90 (s, 1 H, *H*CPz$_3$), 8.29 (d, 2 H, $^3J_{HH}$ = 2.8 Hz, *3*-Pz$_{eq}$), 8.15 (s, 1 H, *3*-Pz$_{ax}$), 7.95 (d, 2 H, $^3J_{HH}$ = 1.2 Hz, *5*-Pz$_{eq}$), 7.25 (s, 1 H, *5*-Pz$_{ax}$), 6.49 (t, 2 H, $^3J_{HH}$ = 2.4 Hz, *4*-Pz$_{eq}$), 6.34 (s, 1 H, *4*-Pz$_{ax}$), 1.97 (m, 4 H, C_2H_4), 1.30 (dd, 9 H, $^2J_{PH}$ = 10.0Hz, $^3J_{RhH}$ = 0.4 Hz, P*Me*$_3$). $^{13}C\{^1H\}$ NMR (methylene chloride-d_2, 175 MHz): δ 145.20 (*5*-Pz$_{eq}$), 138.93 (*5*-Pz$_{ax}$), 133.76 (*3*-Pz$_{ax}$), 133.41 (*3*-Pz$_{eq}$), 108.39 (*4*-Pz$_{eq}$), 108.05 (*4*-Pz$_{ax}$), 76.73 (H*C*Pz$_3$), 25.58 (dd, $^1J_{RhC}$ = 19.3Hz, $^2J_{PC}$ = 3.5 Hz, C_2H_4), 15.86 (dd, $^1J_{PC}$ = 31.5 Hz, $^2J_{RhC}$= 1.0 Hz, P*Me*$_3$). $^{15}N\{^1H\}$ NMR (methylene chloride-d_2, 71 MHz): δ –122.1 (N, *2*-Pz$_{ax}$), –134.3 (N, *2*-Pz$_{eq}$), –172.6 (N, *1*-Pz$_{eq}$), –174.6 (N, *1*-Pz$_{ax}$). ^{31}P NMR (methylene chloride-d_2, 162 MHz): δ 13.36 (d, $^1J_{RhP}$ = 153.9 Hz, PMe_3), –143.8 (sept, $^1J_{PF}$ = 712.8 Hz, PF_6). IR (KBr, cm^{-1}): ν 3139 (m), 3029 (w), 1521 (w), 1444 (m), 1410 (m), 1291 (s), 1253 (m), 1225 (w), 1098 (m), 1061 (s), 962 (m).

Anal. Calcd. for $C_{15}H_{23}N_6F_6P_2Rh$: C, 31.82; H, 4.09; N, 14.84 Found: C, 31.77; H, 3.83; N, 15.01. Mp: above 300 ^oC, dec.

[TpmRh(H)$_2$(PMe$_3$)][PF$_6$] (5.9) In a 100 mL Schlenk tube, the solution of **5.8** (0.089 g, 0.156 mmol) in CH_2Cl_2 (15 mL) was treated with freeze-pump-thaw process and charged with 1 atm H_2. The solution was stirred at room temperature for 30 min. The volatile components were evaporated, and the solid residue was washed with Et_2O (3 mL) to give a pale yellow solid (0.078 g, 0.145 mmol, 93%). ^{1}H NMR (methylene chloride-d_2, 400 MHz): δ 8.97 (s, 1 H, *H*CPz$_3$), 8.29 (d, 2 H, $^3J_{HH}$ = 2.8 Hz, *3*-Pz, *trans* to RhH), 8.17 (d, 1 H, 2.8 Hz, *3*-Pz, *trans* to PMe$_3$), 7.79 (d, 2 H, $^3J_{HH}$ = 2.0 Hz, *5*-Pz, *trans* to RhH), 7.77 (s, 1 H, *5*-Pz, *trans* to PMe$_3$), 6.46 (t, 2 H, $^3J_{HH}$ = 2.4 Hz, 4-Pz, *trans* to RhH), 6.36 (s, 1 H, 4-Pz, trans to PMe$_3$), 1.59 (dd, 9 H, $^2J_{PH}$ = 10.4Hz, $^3J_{RhH}$ = 1.2 Hz, P*Me*$_3$), –17.44 (dd, 2 H, $^2J_{PH}$ = 34.4 Hz, $^1J_{RhH}$ = 23.2 Hz, Rh*H*). ^{13}C{^{1}H} NMR (methylene chloride-d_2, 175 MHz): δ 145.90 (*5*-Pz, *trans* to PMe$_3$), 142.08 (*5*-Pz, *trans* to RhH), 134.23 (3-Pz, *trans* to PMe$_3$), 133.63 (3-Pz, *trans* to RhH), 108.46 (4-Pz, trans to RhH), 107.69 (4-Pz, *trans* to PMe$_3$), 76.87 (H*C*Pz$_3$), 21.16 (d, $^1J_{PC}$ = 36.4 Hz, P*Me*$_3$). ^{15}N{^{1}H} NMR (methylene chloride-d_2, 71 MHz): δ –131.8 (N, *1*-Pz, *trans* to RhH), –134.3 (N, *1*-Pz, *trans* to PMe$_3$), –173.0 (N, *2*-Pz, *trans* to RhH), –175.1 (N, *2*-Pz, *trans* to PMe$_3$). ^{31}P NMR (methylene chloride-d_2, 162 MHz): δ 10.86 (d, $^1J_{RhP}$ = 118.3 Hz, PMe$_3$), –143.8 (sept, $^1J_{PF}$ = 712.8 Hz, PF$_6$). IR (KBr, cm^{-1}): ν 3199(m), 3030 (w), 2976 (w), 2058 (m, ν_{RhH}), 1521(m), 1443(m), 1407(m), 1293(s), 1249(m), 1095(m), 1057(m), 960(m).

Anal. Calcd. for $C_{13}H_{21}N_6F_6P_2Rh$: C, 28.90; H, 3.92; N, 15.56 Found: C, 29.10; H, 3.75; N, 15.22. Mp: above 300 ^oC, dec.

References

(1) (a) Trofimenko S. *Chem. Rev.* **1993**, *93*, 943-980. (b) Trofimenko, S. *J. Am. Chem. Soc.* **1966**, *88*, 1842-1844.

(2) Trofimenko, S. *Scorpionates: The coordination chemistry of polypyrazolylborate ligands*; Imperial College Press: London, 1999.

(3) Slugovc, C.; Padilla-Martínez, I.; Sirol, S.; Carmona, E. *Coord. Chem. Rev.* **2001**, *213*, 129-157.

(4) (a) Cao, C.; Fraser, L. R.; Love, J. A. *J. Am. Chem. Soc.* **2005**, *127*, 17614-17615. (b) Cao, C.; Wang, T,; Patrick, B. O.; Love, J. A. *Organometallics* **2006**, *25*, 1321-1324. (c) Rooy, S. V.; Cao, C.; Patrick, B. O.; Lam, A.; Love, J. A. *Inrog. Chim. Acta* **2006**, *359*, 2918-2923.

(5) Alvarado, Y.; Busolo, M.; López-Linares, F. *J. Mol. Catal. A-Chem.* **1999**, *142*, 163-167.

(6) Pettinari, C.; Pettinari, R. *Coord. Chem. Rev.* **2005**, *249*, 525-543.

(7) Esteruelas, M. A.; Oro, L. A.; Apreda, M. C.; Foces-Foces, C.; Cano, F. H.; Claramunt, R. M.; Lopez, C.; Elguero, J.; Begtrup, M. *J. Organomet. Chem.* **1988**, *344*, 93-108. (b) Esteruelas, M. A.; Oro, L. A.; Claramunt, R. M.; Lopez, C.; Lavandera, J. L.; Elguero, J. *J. Organomet. Chem.* **1989**, *366*, 245-255.

(8) Adams, C. J.; Connelly, N. G.; Emslie, D. J. H.; Hayward, O. D.; Manson, T.; Orpen, A. G.; Rieger, P. H. *Dalton Trans.* **2003**, 2835-2845.

(9) Hallett, A. J.; Anderson, K. M.; Connelly, N. G.; Haddow, M. F. *Dalton Trans.* **2009**, 4181-4189.

(10) Heinekey, D. M.; Oldham, Jr., W. J.; Wiley, J. S. *J. Am. Chem. Soc.* **1996**, *118*, 12842-12843.

(11) Padilla-Martínez, I. I.; Poveda, M. L.; Carmona, E. *Organometallics* **2002**, *21*, 93-104.

(12) Cocivera, M.; Desmond, T. J.; Ferguson, G.; Kaltner, B.; Lalor, F. J.; O'Sullivan, D. J. *Orgnometallics* **1982**, *1*, 1125-1132.

(13) Nicasio, M. C.; Paneque, M.; Pérez, P. J.; Pizzano, A.; Poveda, M. L.; Rey, L.; Sirol, S.; Taboada, S.; Trujillo, M.; Monge, A.; Ruiz, C.; Carmona, E. *Inorg. Chem.* **2000**, *39*, 180-188.

(14) Pérez, P. J.; Poveda, M. L.; Carmona, E. *Angew. Chem. Int. Ed. Engl.* **1995**, *34*, 231-233.

(15) (a) Jones, W. D.; Hessell, E. T. *Inorg. Chem.* **1991**, *30*, 778-783. (b) Northcutt, T. O.; Lachicotte, R. J.; Jones, W. D. *Organometallics* **1998**, *17*, 5148-5152.

(16) Paneque, M.; Pérez, P. J.; Pizzano, A.; Poveda, M. L.; Taboada, S.; Trujillo, M.; Carmona, E. *Organometallics* **1999**, *18*, 4304-4310.

(17) (a) Oldham, Jr., W. J.; Hinkle, A. S.; Heinekey, D. M. *J. Am. Chem. Soc.* **1997**, *119*, 11028-11036. (b) Oldham, Jr., W. J.; Heinekey, D. M. *Organometallics* **1997**, *16*, 467-474.

(18) (a) Gutiérrez-Puebla, E.; Monge, Á.; Nicasio, M. C.; Pérez, P. J.; Poveda, M. L.; Rey, L.; Ruíz, C.; Carmona, E. *Inorg. Chem.* **1998**, *37*, 4538-4546. (b) Alvarado, Y.; Boutry, O.; Gutiérrez, E.; Monge, A.; Nicasio, M. C.; Poveda, M. L.; Pérez, P. J; Ruíz, C.; Bianchini, C.; Carmona, E. *Chem.–Eur. J.* **1997**, *3*, 860-873.

(19) (a) Del Ministro, E.; Renn, O.; Rügger, H.; Venanzi, L. M.; Burckhardt, U.; Gramlich, V. *Inorg. Chim. Acta* **1995**, *240*, 631-639. (b) Bucher, U. E.; Currano, A.; Nesper, R.; Rügger, H.; Venanzi, L. M. *Inorg. Chem.* **1995**, *34*, 66-74. (c) Bucher, U. E.; Fässler, T. F.; Hunziker, M.; Nesper, R.; Rügger, H.; Venanzi, L. M. *Gazz. Chim. Ital.* **1995**, *125*, 181-188.

(20) Nagaraja, C. M.; Nethaji, M.; Jagirdar, B. R. *Organometallics* **2007**, *26*, 6307-6311.

(21) Ghosh, C. K.; Hoyano, J. K.; Krentz, R.; Graham, W. A. G. *J. Am. Chem. Soc.* **1989**, *111*, 5480-5481.

(22) Jameson, D. L.; Castellano, R. K. *Inorg. Synth.* **1998**, *32*, 59-61.

(23) Cramer, R. *Inorg. Synth.* **1974**, *15*, 14-16.

(24) Reger, D. L.; Little, C. A.; Lamba, J. J. S.; Brown, K. J. *Inorg. Synth.* **2004**, *34*, 5-8.

Chapter 6. Conclusion

The importance of fundamental study of synthetic chemistry has never faded away. Functional group transformation relies on the process of bond formation. However, one always designs a tedious synthesis route to bring two or more synthons together to produce a molecule and multiple steps to remove a functional group. The initial bond activation mediated by transition metals in the overall synthesis could provide a shortcut to achieve this goal. Rhodium complexes have proved to be an outstanding transition metal catalyst in every aspect, extending from academic area to industrial world. The sustainable development of a more efficient catalyst is beneficial and valuable in terms of synthesis efficiency, atom economy and greener chemistry in this field.

We have introduced C–X, C–H, O–H, N–H and H–H bond activation chemistry by using tris(oxazolinyl)phenylborate and tris(pyrazolyl)methane supported rhodium complexes. We have demonstrated the possibility of combining the study of regioselectivity and stereoselectivity in a single system. The regioselectivity depends on the species of the electrophiles, in that the strong electrophiles bonds to the pedant arm of the ancillary ligand and the weak electrophiles undergo oxidative addition on the rhodium metal center. The highly diastereoselective result in the case of using chiral ancillary ligand could be further expanded to possible applications in asymmetric catalysis. We also described a new concept of allylic C–H activation and functionalization synthesis strategy. Several allylic C–H activation complexes were synthesized and characterized. The stepwise azide insertion followed by reductive elimination to give the stoichiometric functionalized product still leaves a huge space for improvement and evolved to a catalytic version.

Meanwhile, the photon-sensitive dicarbonyl complex used in the investigation of C–X activation and thermally susceptible allyl hydride compound studied in the exploration of allylic C–H activation converge on the same target to show decarbonylation reactivity toward various primary alcohols under both stoichiometric and catalytic conditions. Aldehydes are observed during the course of the reaction and mechanistic study partially suggests that primary alcohols undergo dehydrogenation followed by decarbonylation in the overall mechanism. This dehydrogenative strategy occurring at the initial stage was also applied to primary amines. The homo-coupling of several primary amines proceed under the same photolytic condition to give the imines as the product presumably *via* dehydrogenation and subsequent coupling reaction pathway. Lastly, we serendipitously discovered Tpm-supported cationic rhodium complex as the first example of crystallographically characterized complexes among all the cationic $Tpm^{R}M(C_2H_4)_2^{+}$ (M = Rh, Ir) derivatives. The substitution chemistry of this cationic complex was investigated, in which the trimethylphosphine-substituted ethylene complex activates dihydrogen molecule to give the dihydride complex. The solution behavior (hapticity, fluxionality and ligand rigidity) as well as the solid state connectivity were also studied and compared by means of $^{1}H–^{15}N$ HMBC spectroscopy and X-ray crystallography.

To^{M} has been proved as a superior ancillary ligand for the rhodium-mediated bond activations. To^{P} was also verified as a highly diastereoselective-directing chiral auxiliary that the C–X, C–H and H–H bond activation examples could be possibly and potentially expanded to asymmetric synthesis and catalysis. For the O–H and N–H (bond activation) corresponded alcohol decarbonylation and amine coupling transformation, the development

of a visible light-promoted or thermally accessible dehydrogenation method will be critical for a more practical use. A rational design of cooperative ligand-metal set is of a key importance of developing a catalyst with high performance for such a purpose. One of the improving methods is to exploit a bifunctional ancillary ligand with a suitable electron-donating ability since the elevated electron density on the metal center might impede the subsequent decarbonylation step. Therefore, in this regard, a high oxidation-state transition metal center or an electron deficient cationic structure should also be considered. On the other hand, a recoverable catalyst would meet the requirement of environmental sustainability. In this respect, the solid-supported catalyst with high surface area could enhance the efficiency for the reactions in heterogeneous catalysis. These future directions are expected to continue to discover new types of reactive catalysts for a more general substrate scope under milder and environmentally friendly conditions.